rf design

engineering principles and practices

1978 1988 10th ANNIVERSARY

November 1988

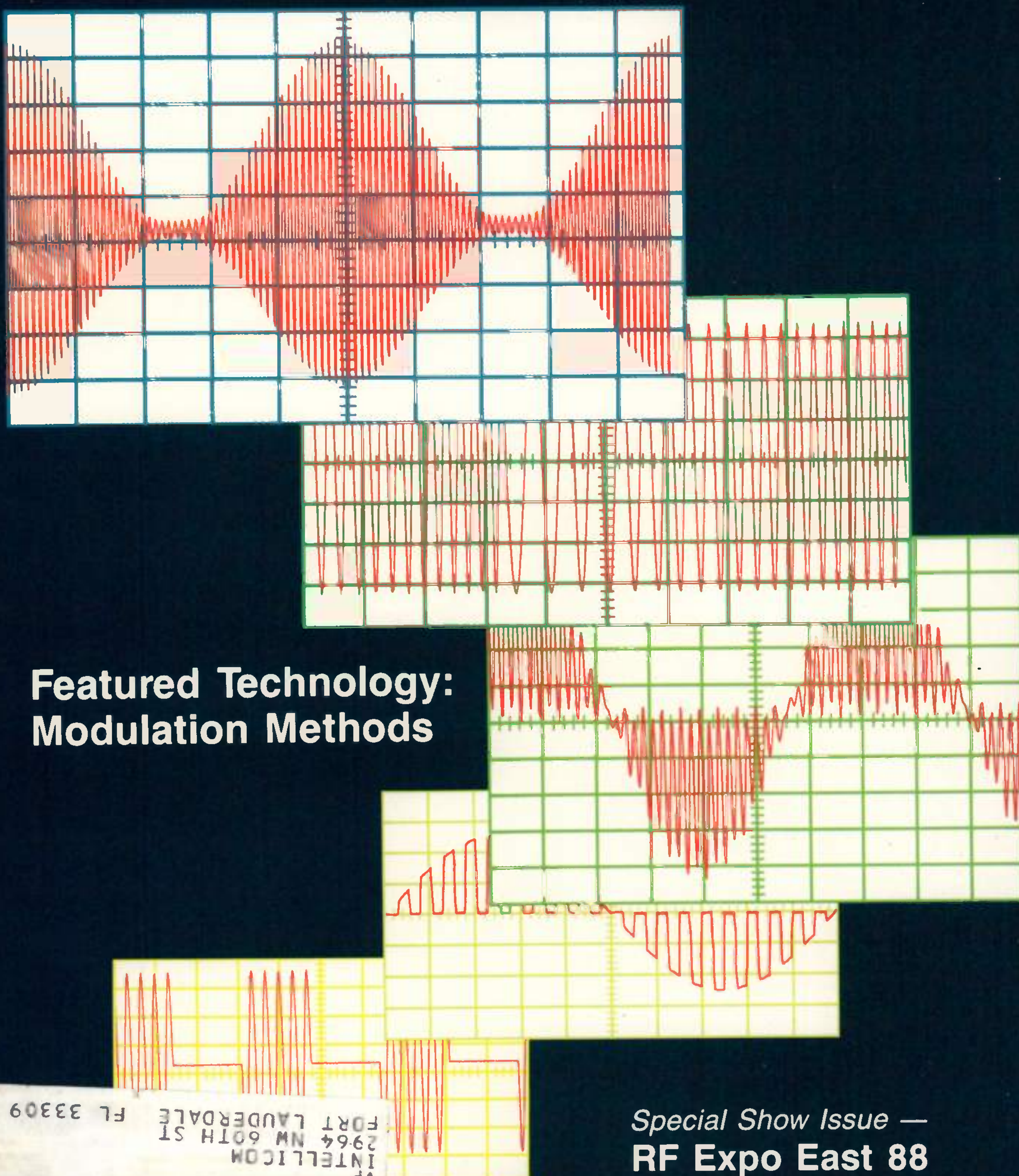

Featured Technology: Modulation Methods

Special Show Issue —

RF Expo East 88

OUR STARS HAVE EARNED OUR STRIPES.

Acrian is America's foremost manufacturer of application specific semiconductor power transistors.

That's why it's no accident that Acrian is also the largest supplier of VHF and UHF FETs to the U.S. Military.

The Army's SINCGARS manpack radio utilizes Acrian FETs for long-range/short-range vehicular communications
Photo courtesy of ITT Aerospace/Optical Division.

They know that when gain and stability are the major concern for broadband performance, Acrian FETs have proven themselves under even the most extreme conditions to offer greater gain and stability than the equivalent bipolar.

And because Acrian FETs offer greater gain/bandwidth capabilities, they lend themselves to more applications, as well as significantly reducing design cycle time.

Take for instance the Acrian UMIL40FT, a 40 Watt broadband UHF FET, capable of providing 12dB of gain across a 100 to 500 MHz band.

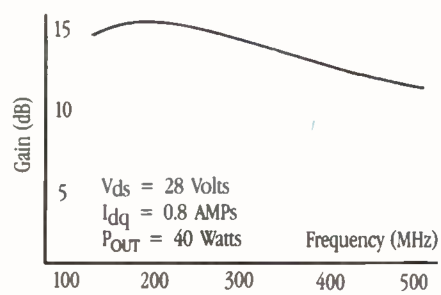

The UMIL40FT produces a remarkably small, well defined stability circle, enabling the wideband amplifier designer to easily identify and avoid areas of potential instability.

At Acrian we have an ongoing commitment to technical leadership, quality control and in-depth service and support.

Which means we can offer our customers a larger number of power solutions.

We find they appreciate that.

For information on Acrian products call (408) 294-4200.

ACRIAN
POWER SOLUTIONS

490 Race Street
San Jose, California, U.S.A. 95126

INFO/CARD 1

DAICO RF/IF SWITCHES AND ATTENUATORS

SURFACE MOUNT

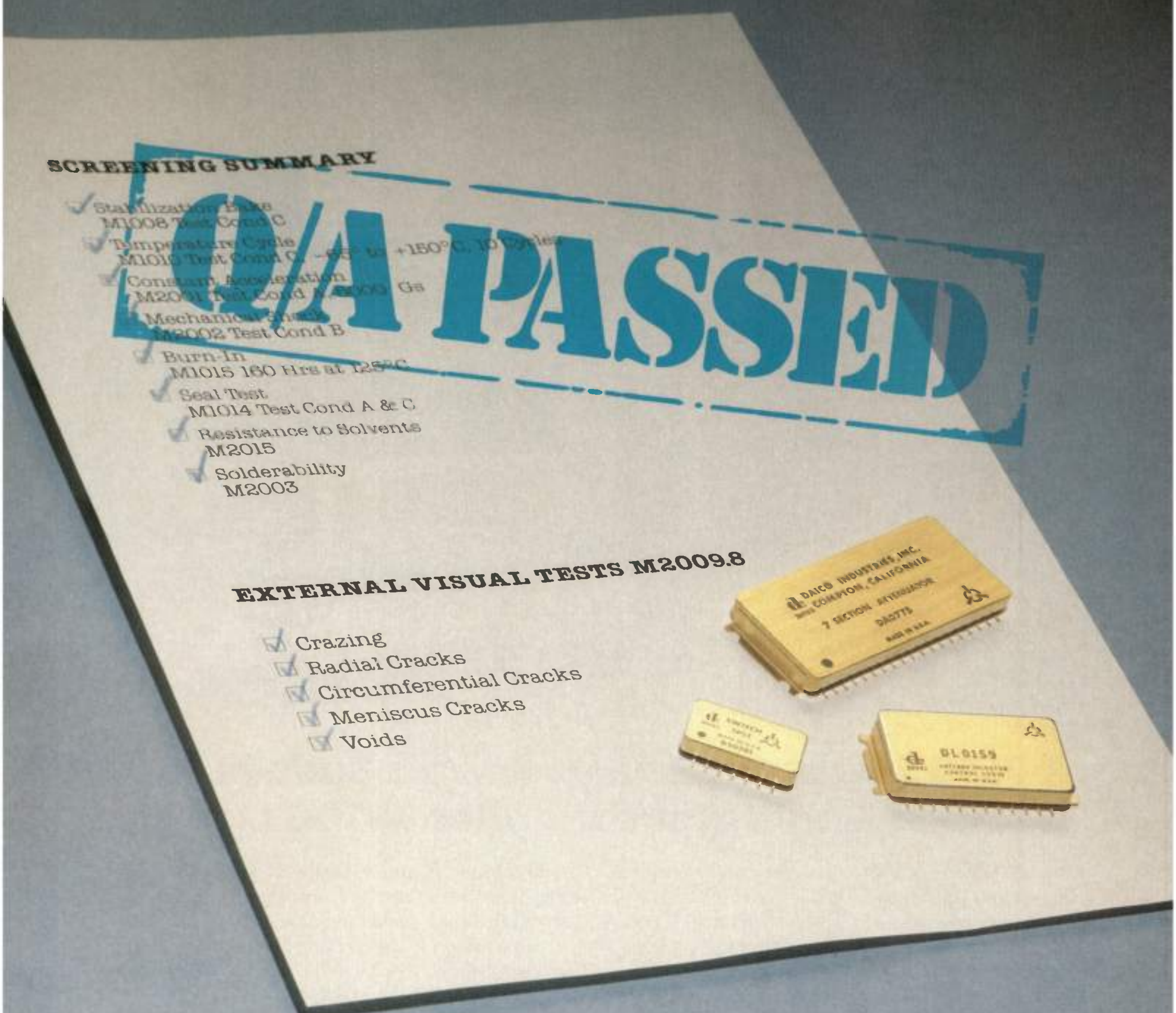

- ☐ **Pre-formed leads**
- ☐ **No special soldering techniques required**
- ☐ **Visible solder joints easily inspected**
- ☐ **Low stress design protects glass seals.**

DAICO surface mount packages with their unique, proven design will meet your demanding military requirements. A full line of surface mount switches and attenuators is now in production. Call or write for details.

DAICO INDUSTRIES, INC.
2139 East Del Amo Blvd., Compton, CA 90220
Telephone (213) 631-1143 FAX (213) 631-8078

INFO/CARD 3

rf design

November 1988

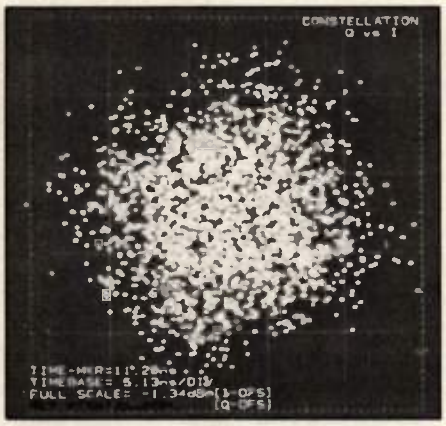

Page 44 — Complex Waveform Generator

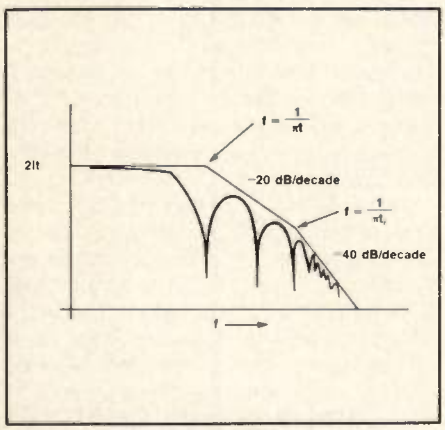

Page 65 — Electrostatic Discharge

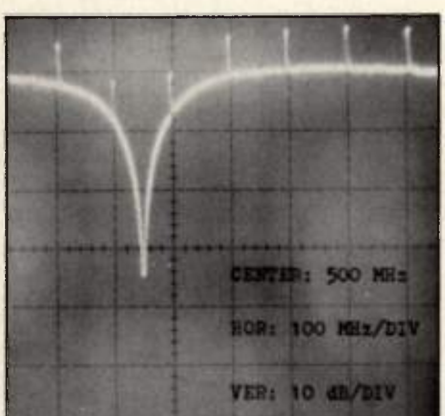

Page 72 — Improving Notch Filters

Cover Story

Featured Technology

Departments

R.F. DESIGN (ISSN: 0163-321X USPS: 453-490) is published monthly plus one extra issue in September. November 1988, Vol. 11, No. 11. Copyright 1988 by Cardiff Publishing Company, a subsidiary of Argus Press Holdings, Inc., 6300 S. Syracuse Way, Suite 650, Englewood, CO 80111 (303) 220-0600. Contents may not be reproduced in any form without written permission. Second-Class Postage paid at Englewood, CO and at additional mailing offices. Subscription office: 1 East First Street, Duluth, MN 55802, (218-723-9355). Domestic subscriptions are sent free to qualified individuals responsible for the design and development of communications equipment. Other subscriptions are: $33 per year in the United States; $43 per year in Canada and Mexico; $47 (surface mail) per year for foreign countries. Additional cost for first class mailing. Payment must be made in U.S. funds and accompany request. If available, single copies and back issues are $4.00 each (in the U.S.). This publication is available on microfilm/fiche from University Microfilms International, 300 N. Zeeb Road, Ann Arbor, MI 48106 USA (313) 761-4700.
POSTMASTER & SUBSCRIBERS: Please send address changes to: R.F. Design, P.O. Box 6317, Duluth, MN 55806.

Making Room for HDTV

By Gary A. Breed
Editor

The first time I saw a demonstration of high definition television (HDTV), I was ready to go out and buy an HDTV set, if there were any available. If you haven't seen it, imagine television with the quality of 35 mm film. With this kind of picture quality, HDTV is unquestionably the next step in the delivery of television programming. The problem, however, is that it requires more bandwidth than current methods, and requires government (FCC) policy decisions.

With their recent "tentative decision" on HDTV, the FCC has given the U.S. television industry some tough technical and political challenges. The technical challenges will have a profound effect on many *RF Design* readers who work on video, broadcast, satellite, or cable TV equipment. The political decisions will affect us all as consumers.

The shortest summary of the FCC decision is this: the eventual HDTV system implemented in the U.S. must be downwardly compatible with the current NTSC method, and must be capable of broadcast on terrestrial TV stations, within the spectrum now allocated for TV. One result of this decision is that the original system developed by the Japanese cannot be used in the U.S. — it's not compatible. Another aspect is that the economic interests of broadcasters are served, consistent with recent government policy.

It is easy to see the technical problems. Getting the most information in a given bandwidth is an ongoing problem for RF engineers. Transmitting four times as much data in a channel only 1½ or two times as wide is real challenge. Accommodating existing services is another tough requirement in the HDTV equation.

The situation is now somewhat chaotic. There are at least 17 proposed methods of broadcasting HDTV in the U.S. Some make more efficient use of the 6 MHz channels currently allocated for TV stations, some use those channels plus another 3 MHz for additional picture information, and others use a second 6 MHz channel for the additional bandwidth. The FCC will have the difficult task of deciding which system will be the U.S. standard.

As an industry observer, I am concerned that a good technical choice will be made by the FCC, given their awkward handling of AM and TV stereo standards. I worry that the compatibility requirement might exclude the best methods. As a consumer, I'm concerned that "marketplace" considerations might keep me from getting all the quality that HDTV offers. My TV set is 14 years old. Will it last until I can get that HDTV set I've been wanting?

Major improvements in technology don't come along all that often, and when they do, we need to be ready. Unless something happens quickly, the U.S. will be the last place HDTV is implemented. Japan already has it developed, and Europe appears to be well on the way. Before long, consumers will demand HDTV, just like they demanded VCRs and CDs. If the U.S. doesn't have the standards and the products to support them, the rest of the world will be waiting with theirs.

Gary A. Breed

Silicon MMICs Any Way You Want!

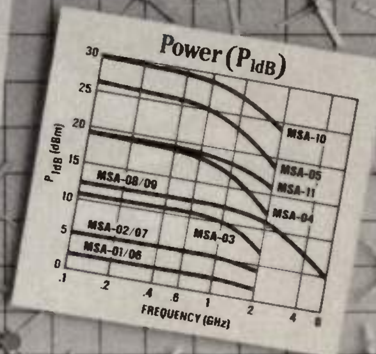

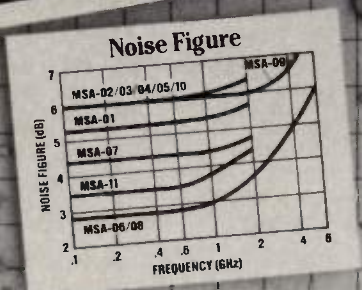

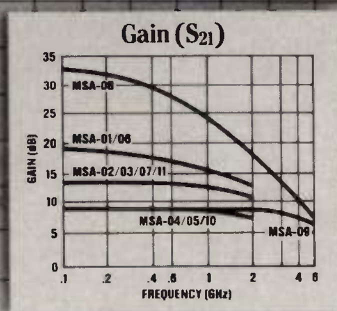

Avantek Offers the Widest Selection of Wideband Silicon MMIC Amplifiers

Now the trade off between performance, package and price is easier. Avantek has a package/die combination that offers the ideal solution to your overall system performance and cost goals. Our MODAMP™ series, DC to 6 GHz silicon MMIC wideband amplifiers, includes eleven different amplifier die types and nine package options. A total of more than 70 different models. These MMIC amplifiers are available with a wide spectrum of performance options to satisfy nearly every design need.... Minimum noise figures as low as 2.8 dB, gains as high as 33 dB, and P_{1dB} as high as 29 dBm.

Packages — Low Cost to High Rel

The MMIC performance you need is available in a range of packages to fit your overall system design and cost needs. Avantek's new Package "86" (85 mil surface mount plastic package) combines premium performance with low cost. Both Package "86" and the industry standard SOT-143, are available on tape and reel, making them ideal for low cost, high volume applications. For high reliability applications, such as space or military environments, we offer MODAMP MMICs in a range of hermetic metal/ceramic packages. MODAMP packages include:

- SOT-143 Plastic
- 4-Pac Plastic
- 85-Mil Plastic
- 85-Mil Plastic Surface Mount
- micro-X Stripline
- 70 Mil Hermetic
- 100 Mil Hermetic
- 200 Mil BeO
- 230 Mil Flange

Available in Quantity for Volume Applications

Avantek presently produces more than 1,000,000 MMICs per month. So you can be assured the MMICs you need will be available to support your volume production programs. And, all MODAMP MMICs are in stock at your local Avantek distributor. For additional information, or the name and address of your local distributor, contact the regional sales office nearest you.

Regional Sales Offices

North America

Eastern:	(301) 381-2600
Central:	(214) 437-5694
Western:	(805) 373-3870
European:	(44) 276-685753

AVANTEK

3175 Bowers Avenue
Santa Clara, California 95054-3292

INFO/CARD 5

See us at RF Expo/East, Booth #411.

rf design

a Cardiff publication — Established 1978
Main Office:
6300 S. Syracuse Way, Suite 650
Englewood, CO 80111 • (303) 220-0600

Publisher
Robert A. Searle

Associate Publisher
Kathryn Walsh

Editor
Gary A. Breed

Technical Editor
Mark Gomez

Assistant Editor
Katie McCormick

Consulting Editors
Andy Przedpelski
Robert J. Zavrel, Jr.

Research Manager
Barb Binge

Advertising:
West Coast District Manager
Mary Bandfield
1341 Ocean Ave., Ste. 58
Santa Monica, CA 90401
(213) 458-6683

Midwestern States
Bill Pettit
Main Office

Eastern States
Kate Walsh
Main Office

Editorial Review Board
Alex Burwasser
Doug DeMaw
Dave Krautheimer
James W. Mize, Jr.
Robert J. Zavrel, Jr.
Ed Oxner
Andy Przedpelski
Jeff Schoenwald
Raymond Sicotte

Advertising Services
Mary Brussell

Circulation Director
Patricia Shapiro

Assistant Circulation Manager
Cindy Zimmer

Vice President — Convention Management
Kathy Kriner

Assistant Convention Manager
Linda Fortunato

Trade Show Assistant
Bonnie Ward

Exhibits Coordinator
April DeBaker

Convention Assistant
Cherry Hughes

Production Manager
Madeline Price

Associate Production Manager
Matt Park

Assistant Production Manager
Mary Barr Felker

Artists
Maurice Lydick
Mary Modeer
Paul Rivera
Bill Schmitt

Composition
Ellen Wilson

Published by
CARDIFF PUBLISHING COMPANY, INC
BPA

President
Robert A. Searle

Treasurer
Marvin Laut

Vice President — Production
Cherryl Greenman

Controller
Jenni Burger

Member of Business Publications Audit of Circulations, Inc.

Please address subscription inquiries to:
RF Design, Cardiff Publishing Company,
P.O. Box 6317, Duluth, MN 55806
Postmaster: send form 3579
to the above address.

american technical ceramics CORP.

News From ATC

Published by ATC November 1988

SPECIAL REPORT

48 Hour Shipment for 250 Capacitors or Less.

ATC is the industry leader for quality, rugged, reliable **UHF/Microwave Capacitors.** Our new **QUIK-PICK**™ System launches our commitment to be the leader in service and customer satisfaction. At American Technical Ceramics, we know the importance of your deadline.

At ATC, Deadlines Are No Joke.

☐ Call me. I have immediate requirements.
☐ I want more information. Please send me ATC's 3-Ring Binder Product Catalog.
☐ Put me on your mailing list.

NAME/TITLE ____________

COMPANY ____________

ADDRESS ____________

CITY/STATE ____________ ZIP ______

PHONE ____________

Mail to:
American Technical Ceramics, Advertising Dept.
One Norden La., Huntington Station, NY 11746-2102

RFD 11/88

INFO/CARD 7

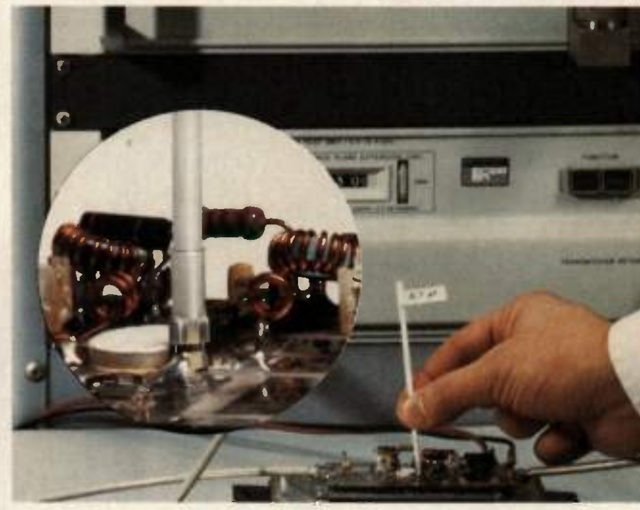

New From ATC: Tuning Sticks

Select the capacity value your circuit needs with ease.

Now during bench test or design, value selection can be achieved without soldering capacitors in.

A Tuning Stick consists of an ATC 100 Series Superchip® permanently attached to a non-conductive holder.

The Stick material is selected so that its effect on the capacitance value and Q is minimal.

Tuning Stick Kits are available off the shelf. Request **ATC TS1001.** 48 Hour **QUIK-PICK**™ Shipment.

$49.95

Tuning Stick Kits contain 20 values:

CAPACITY VALUE (pf)	TOLERANCE
0.1 0.5	B
1.0 1.2 1.5 1.8 2.2 2.7 3.3 3.9	C

CAPACITY VALUE (pf)	TOLERANCE
4.7 5.6	C
6.8 8.2 10 47 68 100	J
470 1000	K

TOLERANCE CODE: B = ±0.1 pf; C = ±0.25 pf; J = ±5%; K = ±10%

INFO/CARD 8

american technical ceramics CORP.
one norden lane, huntington station, n.y. 11746-2102 • 516-271-9600 • telexes 221201 • 825707 • fax 516-271-9615

FLUKE AND PHILIPS — THE GLOBAL

FLUKE®

Two Gigahertz.

Fluke 6062A Signal Generator.

$10,750.

Sure, for out-of-band testing, the HP 8642B is an excellent 2GHz signal generator. But for many other applications, the Fluke 6062A may fit your needs just as well. At nearly 1/3 the price.

Choosing the right 2GHz programmable RF signal generator doesn't have to be a painful decision. You have two good choices... at two very different prices.

For off-channel testing, where spectral purity is critical, the $31,500 HP 8642B is a good choice, despite the bite it takes from your budget.

But for many applications, Fluke has a painless alternative: The 6062A 2GHz Signal Generator. At nearly one-third the price, it may be the best signal generator for your application, not to mention your budget.

Where pulse modulation performance is important, the 6062A simply leaves the HP 8642B behind. With a rise/fall time of 15ns and on/off ratio of 80dB at all frequencies, the 6062A has what it takes to meet your most demanding system requirements.

And when you need both repeatability and confidence in your measurements, the 6062A holds steady with level

A L L I A N C E   I N   T E S T   &   M E A S U R E M E N T

PHILIPS

Two Gigahurts.

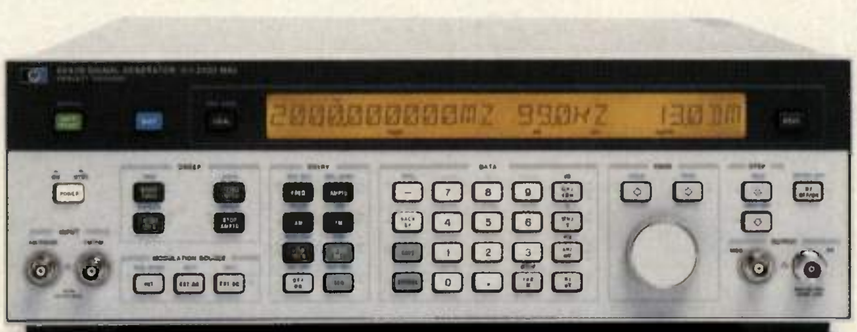

Hewlett-Packard 8642B Signal Generator.

$31,500.

accuracy and linearity performance that is simply outstanding.

Of course, the 6062A is reliable and easy to use. And we stand behind it with the best service and support in the test and measurement business.

The 6062A is just one of a family of Fluke RF signal generators, designed and built to give you the maximum value for the investment.

Challenge the 6062A's performance in your application. Call us toll-free at **1-800-44-FLUKE** and arrange for a demonstration. Then you decide. At a savings of $20,750, you'll feel no pain.

Fluke 6062A
100kHz to 2,100MHz
+16dBm maximum output level
+/− 1dB level accuracy
−60dBc spurious ≤1GHz
AM, FM ØM and pulse modulation

John Fluke Mfg. Co., Inc., P.O. Box C9090, M/S 250C, Everett, WA 98206. U.S. (206) 356-5400. Canada (416) 890-7600. Europe: (The Netherlands) 040-4580455. Other countries (206) 347-6100.

FLUKE®

INFO/CARD 9

See us at RF Expo/East, Booth #526 & 528.

A New Twist On Performance.

The Crimp Connector Challenge.

M/A-COM Omni Spectra has met the challenge to produce a solderless connector that won't twist off your semi-rigid cable assembly. The cable-to-connector joint formed by our unique OSCC Solderless Compression Crimp attachment system exceeds the torque specifications of MIL-C-17 RG 405 (.085) and RG 402 (.141) semi-rigid cable. Under stress or strain the cable will fail before the OSCC Connector-to-cable attachment.

Connector-to-cable attachment has never been so reliable –and easy. OSCC connectors meet all the electrical, mechanical and environmental requirements of solder connectors. And they can be assembled in seconds by personnel unskilled in complicated soldering techniques.

Our compression retention system has been used with confidence in military airborne, shipboard and ground based systems, anywhere vibration and temperature stability are critical. You too could be using the easiest, most reliable connector assembly system available. Call today for our latest OSCC Solderless Compression Crimp Connector System catalog.

M/A-COM

Omni Spectra

21 Continental Boulevard, Merrimack, NH 03054 (603) 424-4111
50 Milford Road, Reading, Berkshire, Great Britain RG1 8LG (0734) 580833

INFO/CARD 10

rf letters

Letters should be addressed to: Editor, *RF Design*, 6300 S. Syracuse Way, Suite 650, Englewood, CO 80111.

Oscillator Observations

Editor:

The article "Quartz Crystals and Aperiodic Oscillators in RF Systems, Part II" (September 1988, *RF Design*) claims that the Pierce oscillator circuit is more stable than the Colpitts, and that the Colpitts will oscillate at a higher frequency when using the same crystal. In fact, for equivalent circuit values, the two circuits will operate identically since both use exactly the same circuit topology.

Assuming a bipolar transistor is the active device, and ignoring bias and coupling components, each circuit consists of a capacitor from collector to emitter, another capacitor from base to emitter, and a resonator from collector to base. The output is typically coupled between collector and emitter. A Colpitts oscillator can be converted to a Pierce, and vice versa, simply by redefining the ground reference.

While it is common to include a tuned circuit at the output of a Pierce oscillator, the same could be done with a Colpitts oscillator with the same effect. The decision as to which circuit to use should be based on convenience of biasing and decoupling, not on any perceived difference in fundamental performance.

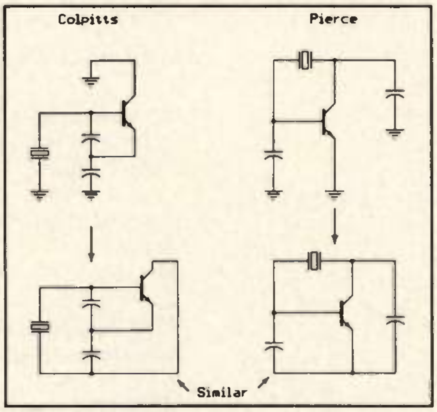

Colpitts/Pierce comparison

Alan Bloom
Hewlett Packard Company
Santa Rosa, CA

Useful Network Theorems

Editor:

I am sure many of your readers are using network theorems daily. I would like to make available a condensed, seven-page listing of up-to-date network theorems. It contains the latest versions of the Thevenin-Norton Theorem and associated theorems, as well as a "Coupled Equivalent Generator Theorem." Interested readers should send a 45-cent stamped return envelope to: SERCOLAB, Box 767, East Dennis, MA 02641.

Dr. Harry E. Stockman
SERCOLAB
East Dennis, MA

Correction

An incorrect address was given for the Bio Electromagnetics Society (BEMS) in the August 1988 *RF Design* article "EMC Organizations and Societies." The Society's correct address is: 120 W. Church Street, Frederick, MD 21701.

rf courses

UCLA Extension

Kalman Filtering II
November 28-December 2, 1988, Los Angeles, CA

Microwave Circuit Design I
November 28-December 2, 1988, Los Angeles, CA

Microwave Circuit Design II
December 5-9, 1988, Los Angeles, CA

Superconductive Electronics
February 7-9, 1989, Los Angeles, CA

Information: UCLA Extension, P.O. Box 24901, Los Angeles, CA 90024-0901. Tel: (213) 825-1047

The George Washington University

New HF Communications Technology: Advanced Techniques
December 12-16, 1988, Washington, DC

Optical Fiber Communications
December 12-16, 1988, Orlando, FL

Methods for Achieving Effective ECM Systems
January 9-13, 1989, Washington, DC

Modern Radar System Analysis
January 23-27, 1989, San Diego, CA

Intelligent Automated Target Recognition Systems
January 25-27, 1989, Washington, DC

Numerical Techniques in Electromagnetics
January 30-February 2, 1989, Washington, DC

Introduction to Electronic Warfare Receivers
February 1-3, 1989, Washington, DC

Radar Operation and Design
February 1-3, 1989, Washington, DC

Information: Misael Rodriguez, Continuing Engineering Education, George Washington University, Washington, DC 20052. Tel:(800) 424-9773; (202) 994-6106

R & B Enterprises

Real Life Solutions to EMI Problems
November 29-December 1, 1988, Philadelphia, PA

Grounding, Bonding & Shielding
November 21-22, 1988, Orlando, FL

MIL-STD 461C/462 Test Workshop
December 8-9, 1988, Philadelphia, PA

Information: Grant R. Brown, R & B Enterprises, West Conshohocken, PA 19428. Tel: (215) 825-1960

EEsof, Inc.

Nonlinear Circuit Design
November 21-22, 1988, Westlake Village, CA

Information: Sandra Scoredos, EEsof, Inc., 5795 Lindero Canyon Road, Westlake Village, CA 91362. Tel: (818) 991-7530

Interference Control Technologies, Inc.

Grounding and Shielding
December 5-9, 1988, Los Angeles, CA
January 23-27, 1989, Orlando, FL

Practical EMI Fixes
December 5-9, 1988, Las Vegas, NV
January 16-20, 1989, San Diego, CA

EMC Design and Measurement
December 12-16, 1988, Washington, DC

TEMPEST Facilities Design
January 16-20, 1989, Palo Alto, CA

Information: Penny Caran, Registrar, Interference Control Technologies, Inc., State Route 625, P.O. Box D, Gainsville, VA 22056. Tel:(703) 347-0030

Integrated Computer Systems

C Advanced Programming Techniques and Data Structures
December 13-16, 1988, San Diego, CA
December 13-16, 1988, Washington, DC

CASE: Computer-Aided Software Engineering
November 22-25, 1988, Toronto, Ontario, Canada
December 6-9, 1988, Boston, MA

Digital Control Systems: Design Techniques and Tools
December 13-16, 1988, San Diego, CA
January 10-13, 1989, Washington, DC

Digital Signal Processing: Techniques and Applications
November 29-December 2, 1988, San Diego, CA
December 13-16, 1988, Washington, DC
January 17-20, 1989, Los Angeles, CA

Fiber Optic Communication Systems
November 29-December 2, 1988, Los Angeles, CA
January 10-13, 1989, Washington, DC

Image Processing and Machine Vision
November 29-December 2, 1988, San Diego, CA
December 6-9, 1988, Washington, DC

Information: John Valenti, Integrated Computer Systems, 5800 Hannum Avenue, P.O. Box 3614, Culver City, CA 90321-3614. Tel:(800) 421-8166; (213) 417-8888

rf calendar

December 11-14, 1988
1988 IEEE International Electron Devices Meeting
San Francisco Hilton, San Francisco, CA
Information: Reedy Langevin, IEDM, 655 15th Street, Suite 300, Washington, DC 20005. Tel: (202) 639-5089

January 11-13, 1989
SC Global 89
Hyatt Regency, San Francisco, CA
Information: SCAA, 24781 Camino Villa Avenue, El Toro, CA 92630. Tel: (714) 586-8727

January 25-26, 1989
14th Annual San Diego Electronics Show
Del Mar Fairgrounds, Del Mar, CA
Information: Epic Enterprises, Show Management, 3838 Camino Del Rio North, Suite 164, San Diego, CA 92108.
Tel: (619) 284-9268

January 30-31, 1989
Electronic Warfare
The Catamaran Hotel, San Diego, CA
Information: Susan Call, Frost & Sullivan, Inc., 106 Fulton Street, New York, NY 10038-2786. Tel: (212) 233-1080

February 12-17, 1989
IEEE 1989 Aerospace Applications Conference
Breckenridge, CO
Information: Harvey Endler, 15137 Gilmore Street, Van Nuys, CA 91411.

February 14-16, 1989
RF Technology Expo 89
Santa Clara Convention Center, Santa Clara, CA
Information: Linda Fortunato, Cardiff Publishing Company, 6300 S. Syracuse Way, Suite 650, Englewood, CO 80111.
Tel: (303) 220-0600; (800) 525-9154

February 20-25, 1989
Asia Telecom 89
Westin Stamford and Plaza, Singapore
Information: Angelina Goh, Asia Telecom 89 Secretariat, Singapore Telecom, 31 Exeter Road 26-00, Comcentre, Singapore 0923. Tel: 65 730 3283

March 1-3, 1989
EMC Japan '89
Sunshine City Convention Center, Tokyo, Japan
Information: Secretariat of EMC Japan, Japan Management Association, 3-1-22, Shiba-koen, Minato-ku, Tokyo 105, Japan.

March 21-23, 1989
3rd European Frequency and Time Forum
Le Kursaal, Place Granvelle, Besancon, France
Information: A. Remond, 41bis, avenue de l'Observatoire, 25044 Besancon Cedex, France. Tel: 81.80.22.66

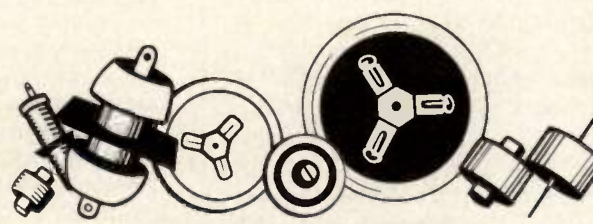

$56 Million Voice of America Contract Awarded

The United States Information Agency (USIA) has awarded the American joint venture of Marconi Electronics, Inc. (MEI) and Cincinnati Electronics Corporation (CEC) a $56,616,911 contract to further the modernization of the Voice of America (VOA). The joint venture will provide state-of-the-art 500 kW high-power shortwave transmitters, a high-power switch matrix, coaxial transmission lines, baluns, dummy loads and related equipment for VOA's new station in Morocco. Contract options will allow USIA to standardize on identical equipment, if funds become available for VOA to proceed with planned new stations in Thailand, Sri Lanka and Botswana. Over 78 percent of the goods and services provided under the initial contract will come from U.S. sources.

A National Security Council directive instructs the Voice of America to develop a stronger, more reliable signal, particularly to those areas of the world where information does not circulate freely. A special requirement was a strengthened signal into critical areas of the USSR, West and Central Europe, Eastern and Southern Africa, Central America and the Caribbean, and West Africa. This award to the MEI/CEC joint venture is a major step toward the completion of this Voice of America effort.

PST to Synchronize L.A. Traffic Signals

Precision Standard Time (PST) has been selected to provide equipment for a new program aimed at reducing traffic congestion in the busiest Los Angeles County commute corridors. Value of the agreement is expected to exceed $2 million. PST will install its Time Source controllers to synchronize traffic signals along key arteries, allowing motorists traveling at the posted speed limits to hit significantly fewer red lights. Each Time Source controller is extremely accurate, operating off the WWV radio signal broadcast by the National Institute of Standards and Technology. Since the time signal does not drift, as a clock does, traffic signals across the entire corridor will stay reliably synchronized.

Expanded Coaxial Noise Calibrations Available

Scientists at the National Institute of Standards and Technology (NIST) can now calibrate noise sources in the 8 to 12 GHz range for government and industry. The calibration is achieved using an automated radiometer and a cryogenic coaxial noise standard. With the addition, the system now routinely calibrates noise sources from 2 to 12 GHz at all frequencies and at all noise power spectral densities below 18,000 K. Measurement uncertainties typically range from one to three percent. In principle, there is no limit on the type of coaxial connector. Current connectors are precision N, APC7 and GR900, as well as various rectangular waveguide flange connectors. For more information, contact: George J. Counas, Division 723.02, NIST, Boulder, CO 80303. Tel: (303) 497-3664.

Manufacturing Research Center to Focus on Competitiveness

Work has begun in Atlanta on a new Manufacturing Research Center which will explore ways to make U.S. electronics companies more competitive. Located at the Georgia Institute of Technology, the new Center is backed by $1 million apiece from Motorola, Inc. and Digital Equipment Corporation. $15 million in funding for the Center came through the Georgia Research Consortium. Georgia Tech officials have pledged to obtain $15 million in industrial research support over five years to match the state's support. The Center's initial focus will be on assembly systems, interconnection technology, distribution systems, robotics and precision measurement.

IMI Wins $2.75 Million in Gate Array Contracts

International Microcircuits, Inc. (IMI) of Santa Clara, Calif., has been awarded $2.75 million in production contracts for military-standard applications in defense, space and other high-reliability environments. IMI is currently delivering production quantities of its MIL Standard 883-screened arrays to: Rockwell International's Collins Government Avionics Division for use in the "Navstar" Global

Positioning Satellite (GPS) program; Canadian Marconi of Montreal and SCI of Huntsville, Ala., both of which are alternate sources on the GPS program; Singer's Kearfott division in Wayne, N.J., for a NASA space station application; and Magnavox's Marine and Sensor division in Fort Wayne, Ind., as part of the government's Gator program.

Interstate Electronics Delivers Translator Units for SDI

Interstate Electronics Corporation of Anaheim, Calif., has delivered to the Air Force the first two ballistic missile translator units to be used for tracking position and velocity in the Strategic Defense Initiative (SDI) test demonstration phase of the Exo-Atmospheric Reentry Intercept System (ERIS) program. The translators, which will be installed in both the targets and the interceptors, will receive GPS signals from the NAVSTAR satellite constellation, perform a frequency shift and retransmit the signals to a ground tracking station, also being supplied by Interstate. The $4.4 million Air Force contract calls for a total of 44 units to be delivered by late 1990.

New Name for Electronic Connector Study Group

The Electronic Connector Study Group (ECSG) of Deerfield, Ill., announced that it has changed its name to the International Institute of Connector and Interconnection Technology (IICIT). The group is a professional society with 20 affiliated chapters throughout Canada, the United States and Europe with members representing all aspects of connectors and interconnection technology. The name change emphasizes the worldwide participation in the society as well as the broader range of subjects now studied. For further information on IICIT, contact its headquarters at 104 Wilmot Road, Suite 201, Deerfield, IL 60015-5195. Tel.: (312) 940-8800.

Call for Microwave Papers

The 2nd International Symposium on Recent Advances in Microwave Technology will be held August 28 -September 1, 1989 in Beijing, China. Authors are invited to submit abstracts of proposed papers for consideration. Papers on any area of microwave technology and its applications are invited, but proposals on components and circuits, antenna and radar technology, MICs and MMICs, remote sensing, biological effects and other applications, communication systems, CAD techniques, and propagation and measurements are especially encouraged. Three copies of one-page abstracts (in English only) should be submitted by November 30, 1988 to: Dr. Banmali Rawat, Dept. of Electrical Engineering/Computer Science, University of Nevada - Reno, Reno, NV 89557-0030. Tel.: (702) 784-6927; Fax: (702) 784-1300.

Fluke Endorses VXI Bus Standard and Joins Consortium

Electronic test and measurement equipment vendor John Fluke Mfg. Co., Inc. recently joined the VXI Consortium and announced its support for the development and popularization of the VXI bus standard for modular instrumentation-on-a-card architecture. The VXI Consortium was established for the purpose of developing a standard to ensure compatibility between modular instruments made by different companies. The VXI bus standard is based on VME bus open architecture and covers backplane definitions, electromagnetic compatibility, communications protocols, synchronization and clock signals, and packaging requirements.

Natel Receives Contract from Ocean Technology, Inc.

Natel Engineering Co., Inc. of Simi Valley, Calif., has received an order from Ocean Technology, Inc. (OTI) for approximately $2 million worth of synchro conversion components for use in the Navy's Mark 53 Update Combat Console Program. Included in the order are HSRD1056 16-bit hybrid Synchro(Resolver)-to-Digital converters, DSC5131 16-bit Digital-to-Synchro converters and a variety of other parts, to be packaged by OTI as improved SEM modules.

Anaren Wins DRFM Contract for ASPJ

Anaren Microwave, Inc. has received a $545,693 contract from Westinghouse Electric Corporation's Defense and Electronics Center to produce Digital RF Memories (DRFMs) for the joint ITT Avionics and Westinghouse ALQ-165 Airborne Self-Protection Jammer (ASPJ) program. The award is part of Phase I of the ALQ-165 production verification contract between the Westinghouse/ITT team and the U.S. Navy and Air Force. The order calls for three full-scale development units, with delivery scheduled to begin in May, 1989.

NIST Expands Capabilities of Anechoic Chamber

The NIST Electromagnetic Fields Division has expanded the capabilities of its electromagnetic (EM) anechoic chamber in Boulder, Colo. The facility generates standard EM fields with minimum reflections of interference. It will be used to measure a variety of antennas and probes in the frequency range from 200 MHz to 40 GHz, up from the previous 18 GHz limit. The increased range will enable NIST to calibrate hazard field probes that go up to 40 GHz. For additional information, contact: Galen Koepke, Division 723.03, NIST, Boulder, CO 80303. He can be reached by telephone at (303) 497-5766.

Wiltron Awarded Test Equipment Contract

A contract worth more than $1 million has been awarded to Wiltron Company of Morgan Hill, Calif., a manufacturer of microwave test instrumentation, by Fernmelde Technisches Zentralamt (FTZ) of West Germany. Wiltron will supply FTZ, West Germany's national telephone company, with 15 fault locator systems. These will be used to maintain ground microwave communication systems located throughout the country, and to measure the waveguide components on their antenna towers.

INFO/CARD 16

"They must have used a very high performance signal generator to get quality like this!"

The 'theatrephone' entertaining guests of a grand hotel in Paris. Late 19th century. ©The Bettmann Archive

"How could they afford it?"

To make top quality receivers, you need top-dollar signal generators. Right? Wrong. The new HP 8657A has shattered all the old ideas about the cost of high performance signal generation.

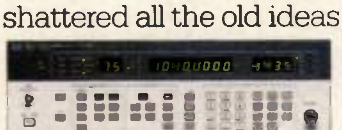

The HP 8657A Synthesized Signal Generator

For just $7900,* you can make the measurements you need to design, build and test better two-way radios, cellular phones, pagers and any other receivers.

That low price buys you great spectral purity from 100 kHZ to 1040 MHz. Phase noise is < -130 dBc/Hz @ 500 MHz, 20 kHz (< -136 dBc/Hz typically). Residual FM <2 Hz RMS (0.3 to 3 kHz) @ 500 MHz (<1 Hz RMS typically). Spurious as good as < -72 dBc.

Another breakthrough keeps our signal generator going strong, even in high-use situations. We invented an electronic attenuator. With no moving parts, it's virtually failure-free. Even after a billion cycles, operating at temperatures from $-50°$ to $+95°$C, and 99% humidity.

So now you can afford to get really competitive. For more information, call **1-800-752-0900, Ext. 744C.**

we never stop asking

"What if..."

HEWLETT PACKARD

See us at RF Expo/East, Booth #404, 406, 408 & 410.

Toko coils and filters attack RF design problems before they come to life!

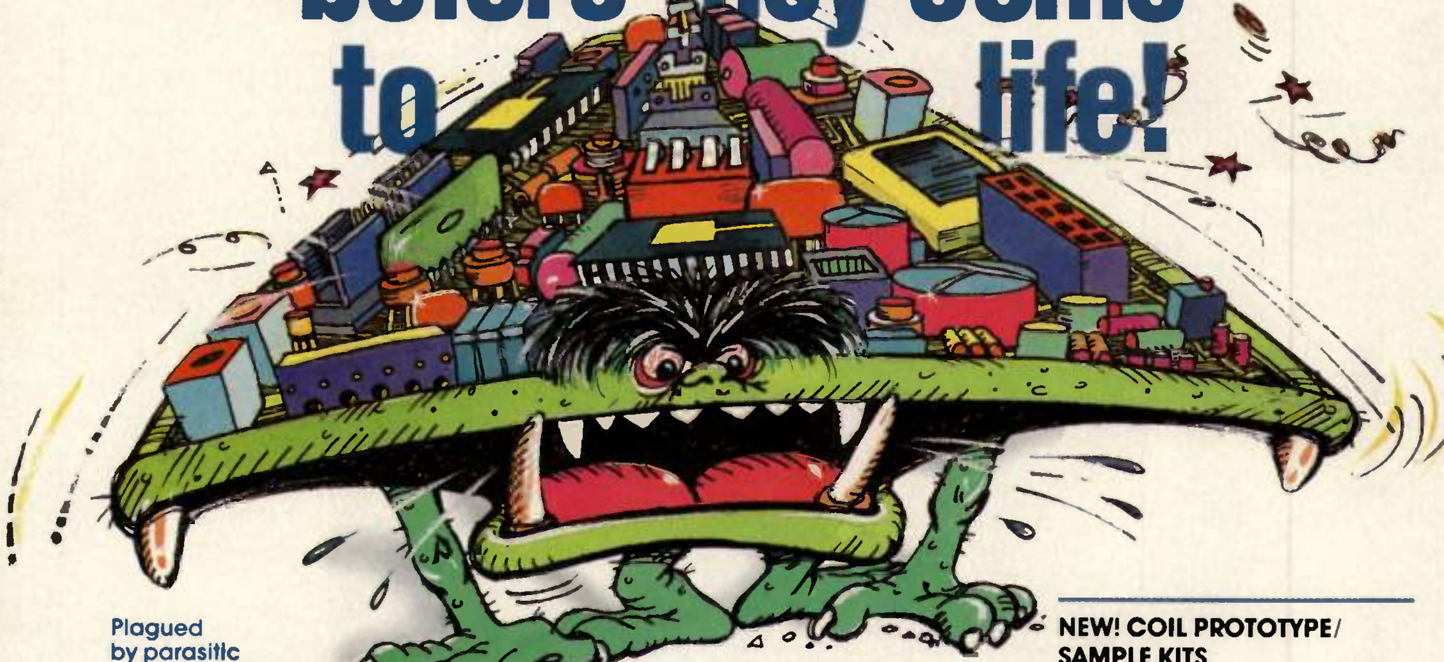

Plagued by parasitic oscillations, spurs, harmonics and feedback? The problem may not be your design, but the coils and filters you selected. Toko is the world's largest manufacturer of quality small coils and filters, with a selection so large, you're sure to find the right components to neutralize your rf design problems.

SUBMINIATURE ADJUSTABLE AND FIXED

Toko has what you need, so you won't need to compromise... subminiature adjustable coils and transformers, molded coils, radial fixed coils and fixed coils with axial leads. Toko high-Q coils are engineered in sizes from 5mm to 15mm, and inductance ranges from .02 µH to 500 mH.

CHIP AND ADJUSTABLE SMD

Need to reduce the size of your products or automate production? Toko solves these problems with a wide range of surface mountable coils and LC, ceramic and helical filters in fixed and adjustable configurations. Packaged for automatic insertion and available for reflow or solder dipping.

CUSTOM MODULES

Toko hybrid modules are a great way to simplify design and production tasks. With short lead time, Toko can develop compact custom modules utilizing a variety of components, surface mounted on a ceramic substrate. One module replaces dozens of components.

FILTERS

For i-f or tuned rf circuitry. Toko filters simplify attenuation of out-of-band signals, while cleanly passing your desired signal. Ultra-miniature ceramic and LC filters at popular i-f frequencies fit tight spaces and tight budgets. With frequencies up to 1.2 GHz Toko helical filters are the right choice for communications transceivers.

ACTIVE FILTERS

If you're advancing the state-of-the-art in digital audio or PCM products you'll appreciate Toko active filters. Especially designed for small size and low distortion, they're also very cost-effective.

NEW! COIL PROTOTYPE/SAMPLE KITS

Toko sample kits give you more choices and cost less!

- Molded Sample Kit: 82 values (123 parts) 30MHz-150MHz; 0.0393-1.173 µH
- 7mm Sample Kit: 54 values (108 parts), 70kHz-50MHz; 0.1-22.0 mH
- 10mm Sample Kit: 68 values (136 parts), 79kHz-75MHz; 0.08 µH-56 mH

INTRODUCTORY PRICED AT $49 EACH. ORDER YOURS TODAY!

Isn't it time to tame the design monsters before they bite back...call or write Toko today for a free coil and filter catalog or a quote on your needs.

Your strategic partner... for all the right reasons.

TOKO
TOKO AMERICA, INC.

(CORPORATE HEADQUARTERS)
1250 Feehanville Drive
Mt. Prospect, IL 60056
(312) 297-0070, FAX (GIII): (312) 699-7864
(Western Branch) (408) 996-7575
(Eastern Branch) (914) 694-5618
(Southeastern Branch) (205) 830-0952

For more information on:
Subminiatures, INFO/CARD 17
Chip/SMD, INFO/CARD 18
Custom Modules, INFO/CARD 19
RF & I-F Filters, INFO/CARD 20
Active Filters, INFO/CARD 21
Sample Kit, INFO/CARD 22

MIRAGE SYSTEMS

"THE TECHNICAL INNOVATION CONTINUES . . . "

FPD-002

145-170 MHz FREQUENCY & PHASE DETECTOR

FEATURES

- Combined Instantaneous Frequency Measurement and Fast Phase Detection Circuit
- Small Size, Low Power, Surface Mount Technology

LLA-003

LOGARITHMIC AMPLIFIER

FEATURES

- Wide Dynamic Range . . 60 dB
- High Linearity . . . . ±1 dB
- Wide Bandwidth . 50 to 250 MHz
- Fast Risetime . . . . . 35 nSec.
- Log Video and Limited IF Outputs
- Single +5 Volt, 130 mA
- Miniature Size, Low Cost

TFG-002

50-500 MHz TRANSMIT FEED/GAIN UNIT

FEATURES

- Broadband, High Linearity, Temperature Compensated, Active Multi-channel Signal Combining and Processing Transmitter

RFG-002

50-250 MHz RECEIVE FEED/GAIN UNIT

FEATURES

- Broadband, High Linearity, Temperature Compensated, Active Multi-channel Signal Combining and Processing Receiver

VMA-002

VECTOR MODULATOR ASSEMBLY

FEATURES

- Independent, High Resolution Control of:
  - Amplitude . . . . . . 0.07 dB
  - Phase . . . . 0.45 Deg.
- Fast Settling Time . . 150 nSec
- Wide Bandwidth . 135 to 235 MHz
- Size . . . . . 3.4W x 0.6H x 5.8H

DQD

DIGITAL QUADRATURE DETECTOR

FEATURES

- Ultra-High Accuracy:
  - Amplitude . . . . ±0.02 dB Typ.
  - Phase . . . . ±0.2 Degrees Typ.
- Wide Dynamic Range . >90 dB
- Flexible Operation . . . . CW to 200 nSec Pulses
- Sampling Rate . . . . to 300K Samples/Sec.
- Resolution, I & Q . . . . . 16 Bits
- Computer Interface . . Parallel or Multiplexed
- Temp. Stable . . . . 0 to 50°C
- Rack Mount . . . 3.5 Inch Panel

APPLICATIONS

Precision Doppler Radar Systems; RCS and Antenna Range Instrumentation; Synthetic Pulse and Imaging Radars; Communication Systems; Signal Nulling Systems; and Coherent STE Systems.

ARMS

AUTOMATED RADAR MEASUREMENT SYSTEM

FEATURES

Computer Controlled

- High Speed Data Acquisition
  - 10 K Pulses per Second
  - Pulse by Pulse Frequency Agility

Coherent I/Q Detection

- 16 Bits per Channel
- Pulse by Pulse Recording

Precision

- ±0.3∓ Phase
- ±0.05 dB Amplitude

Frequency Range

- 100 MHz to 2 GHz
- Expandable to 18 GHz

537 LAKESIDE DRIVE • SUNNYVALE, CALIFORNIA 94086 • PHONE: (408) 733-3200 FAX: (408) 738-6952

Modulation, Signals and Noise

This Month's Featured Technology is a Universal Topic for RF Engineers

Introducing the subject of modulation to RF engineers is like introducing your Mother to your Father — this is what RF is all about. Getting information onto a carrier, then recovering it at the other end of the signal path is the principal use of RF. This issue has three articles dealing with this subject.

One of the "traditional" parts of RF technology is amplitude modulation (AM). Bill Sabin of Rockwell-Collins presents an analysis of the envelope detector and noise figure in an AM system. Although it is hardly an exotic modulation method, this analysis of AM has universal value, since all signals have an amplitude component.

The second article describes new modulation technology. Greg Lowitz of Hewlett-Packard offers background on instrumentation for RF testing using complex modulation. New instruments allow the digital generation of virtually any waveform that can be mathematically defined, giving engineers a "real" signal source for simulation of unique radar, communications or data modulation.

The other presentation is instruction on the use of spreadsheet programs for system analysis. John Bordelon and Dave Hertling of Georgia Tech share the results of their work using common personal computer spreadsheets for the analysis and manipulation of a large number of variables in a system. This method of computation can be used for many things, but the example used is system noise analysis.

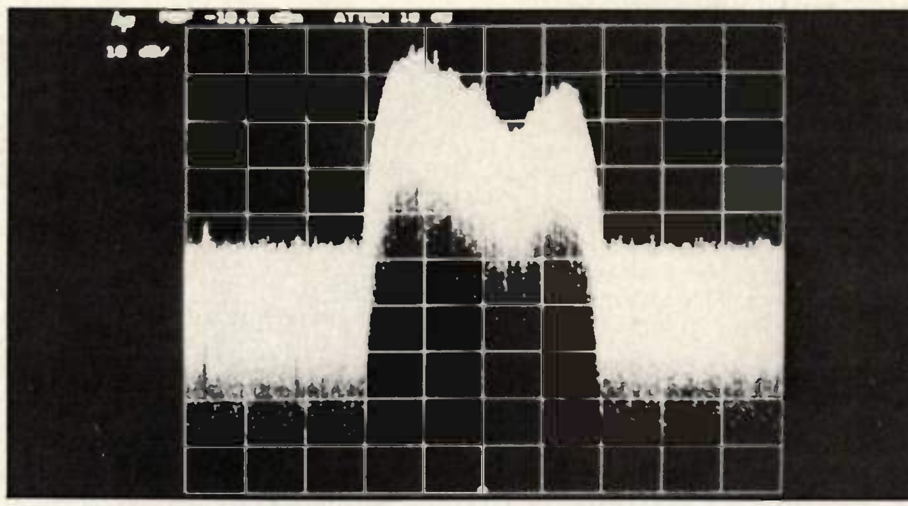

An example of complex modulation, seeing growing use.

Current Work and Future Trends

There is plenty of activity in advanced modulation methods right now. As this month's Editorial notes, high-definition television (HDTV) has entered the practical development phase. This wide-bandwidth technology requires bandwidth compression techniques to minimize the occupied spectrum, but will still have a broader transmission channel than current TV technology. Circuit designers will have to develop accurate broadband modulators, plus efficient broadband power amplifiers to broadcast the signal. Receiver designers will have a new set of standards to design to, including advanced IF or baseband signal processing.

High data rate transmission is another area of interest, with some of the same problems as HDTV, regarding maximum information in minimum bandwidth. Multiple quadrature amplitude modulation (QAM) schemes with 128 or more signal states are being put into operation. These systems offer the challenge to RF engineers to maintain accuracy in an environment where formerly minor noise and propagation characteristics now have significant effects.

Spread spectrum technology has been given a lot of attention, due to its military applications. It is a sufficient challenge just to generate and recover a signal with a rapidly changing frequency, but the spread spectrum engineer has to deal with differing signal paths, fading, and propagation times for the range of frequencies in use. Adaptive AGCs, time correlation, and error detection are all part of this advanced modulation method.

In medical electronics, magnetic resonance imaging (MRI) systems are another place where new modulation techniques are being developed. In order to detect the response of molecules to the excitation of an intense RF-generated magnetic field, that field has to be shut off and a sensitive detector activated in microsecond (or less) times. Medical researchers are seeking lower power MRI systems which will reduce the cost and increase the availability of this powerful diagnostic tool. To achieve their goals, low noise, high dynamic range pulse-modulation techniques must be refined.

Radar systems utilize chirped signals, with their associated dispersion and convolving circuitry, to improve accuracy and jamming immunity. Both analog and digital techniques are used in this area, which leads to another note about current modulation engineering efforts. Neither analog nor digital methods appear to be heading for a monopoly in complex modulation. Digital generation and analysis has significant accuracy advantages, but analog techniques are capable of operating in real time. It is interesting to note that as digital circuitry evolves to match performance previously the sole domain of analog electronics, the capabilities of analog circuitry have seen a similar improvement.

With this brief look at a few areas of current interest, we introduce the following articles covering this month's featured technology: modulation methods. rf

★ ★ ★ ★ ★ ★ Announcing ★ ★ ★ ★ ★ ★ the Fourth Annual RF Design Awards Contest

Your idea may win this Grand Prize, provided by Webb Laboratories:

CommView
Receiver simulation software. Calculates pre- and post-detection SNRs, bit error probability and AGC voltage for user-entered system cascades. Graphics support Pagemaker and Ventura desktop publishing software.

FilSolv
Webb Labs' filter synthesis package. Creates practical, buildable lowpass, highpass and band-pass filters in Butterworth, Chebyshev, Bessel and Elliptic realizations. Incorporates losses found in "real" components. Files can be saved in formats compatible with major circuit analysis packages.

SYSCAD
RF/Microwave system engineering software. Performs link, terminal and RADAR characterization, receiver architecture analysis, transmit and receive spurious analysis through an order of 2000, plus phase noise calculations.

TRANSCAD
Powerful single and coupled transmission line and waveguide synthesis package. Analyzes and synthesizes over 40 structures, including nearly every microwave geometry of interest. Applies numerical methods to the best known algorithms to eliminate common synthesis errors.

Plus, a Zenith *SupersPort* laptop computer, with an 8088/8087 pair running at 8 MHz, 640 K RAM, a 3.5 in. 720 K floppy and an internal 20 MB hard disk! Includes CGA graphics, MS-DOS 3.21 and carrying case. Perfect for running all of Webb Labs' software!

★ ★ ★ ★ Look for complete rules and additional prizes in the December issue of *RF Design.* ★ ★ ★ ★

TFL HAS YOUR OSCILLATORS

DTCXO

"The upgraded replacement for OCXO's."

Frequency Range: 5 Hz – 30 MHz
Frequency Stability: ± 0.1 PPM: (0-70°C)
Aging: < 0.2 PPM/yr
Supply Voltage: + 5 Vdc
Supply Current: < 25 mA
Warm-up Time: < 200 msec
Size: < 2″ × 2″ × 1″

OCXO

Frequency Range: to 50 MHz
Short Term Stabilities: up to 5×10^{-12} (1 sec)
Warm-Up Time: As low as 1 min
Temperature Stability: $\pm 5 \times 10^{-10}$ (0° to + 50°C)
Low Aging Rate: $< 5 \times 10^{-11}$/Day
Low Noise: < – 157 dBc@ 10 kHz Offset
Low Vibration Sensitivity: 3×10^{-10}/g
Temperature Range: – 55° to + 120°C

TCXO

Frequency Range: 0.02 Hz to 20 MHz
Frequency Stability: ± 0.8 PPM (– 40° to + 85°C)
Aging: ± 1.0 PPM/yr typ.
Supply Voltage: 2 to 15 Vdc
Supply Current: As low as 1.0 mA
Size:
Standard: 1.5″ × 1.5″ × 0.5″
As small as: 0.960″ × 0.5″ × 0.2″

CXO

Frequency Range:
TTL: 10 Hz to 100 MHz
C-MOS: 1 Hz to 5 MHz
ECL: 5 MHz to 500 MHz
Sinewave: 1 Hz-1 GHz
Frequency Stability:
Typ. ± 50 PPM (– 20° to + 70°C, Industrial)
Typ. ± 50 PPM (– 55° to + 125°C, Military)
Up to ± 10 PPM available (– 20° to + 70°C)
Aging:
± 10 PPM/yr (Industrial)
± 5 PPM/yr (Military)
Outputs: TTL, C-MOS, ECL, Sinewave
Packages: TO-5, TO-8, DIP, Hermetically Sealed Metal Case

Complete line of quartz crystals are also available.
All oscillators can be manufactured to meet MIL-O-55310, MIL-STD-202, and MIL-STD-810.

At TFL The Quality Is Crystal Clear.

Time & Frequency Ltd.
55 Charles Lindbergh Boulevard
Mitchel Field, New York 11553 • 516-794-4500
INFO/CARD 24

GaAs MMIC Amplifiers

— *from Pacific Monolithics*

20 MHz to 20 GHz

Military and Commercial Applications

- *Narrowband and Broadband*
- *Small-signal, Power and Limiting*
- *Single Supply Voltage*
- *Low-Noise*
- *Medium Power — Up to 1/2 Watt*
- *MMIC Reliability and Repeatability*
- *Easily Cascadable*
- *Off-the-shelf and Affordable*

Chips

- Frequency range: 2-20 GHz
- Low current consumption
- 9 to 14 dB gain blocks
- On-chip gain control
- Flat gain response
- Smallest die size in the industry

Packaged Components

- Frequency range: 20 MHz to 20 GHz
- Broadband, 10 dB to 35 dB gain blocks
- As low as 1.5 dB noise figure
- ±1 dB flatness for 30 dB gain blocks
- Gain control and temperature compensation as options
- Low current consumption

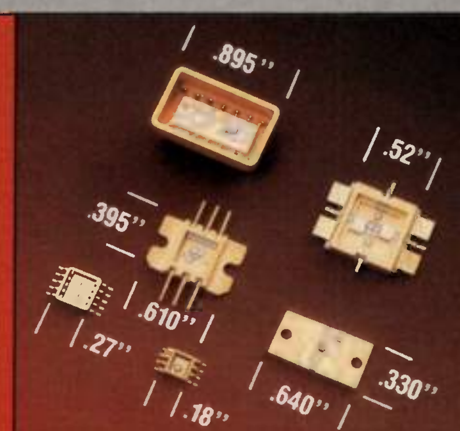

Amplifier Subsystems

- Frequency range: 20 MHz to 20 GHz
- Ultra-small packages and low power dissipation
- Multiple gain options to 70 dB
- High isolation
- P-1dB to 27 dBm
- Temperature compensation

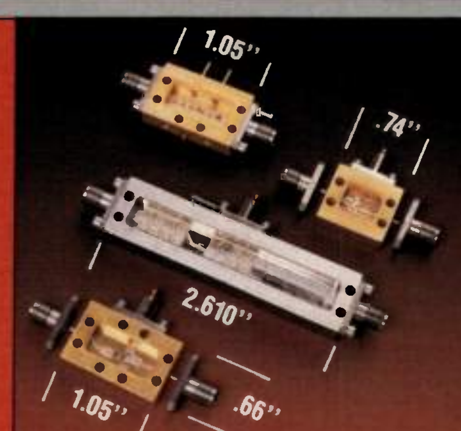

PACIFIC MONOLITHICS

245 Santa Ana Ct.
Sunnyvale, CA 94806-4512
(408) 732-8000
TWX: 510-600-3726
FAX: 408 732-3413

Pacific Monolithics' line of GaAs MMIC-based amplifiers can be combined with other PM components, such as oscillators, switches and attenuators, to form larger multifunction MIC assemblies. Call for more information.

The Proven MMIC Integrator

Shape Up!

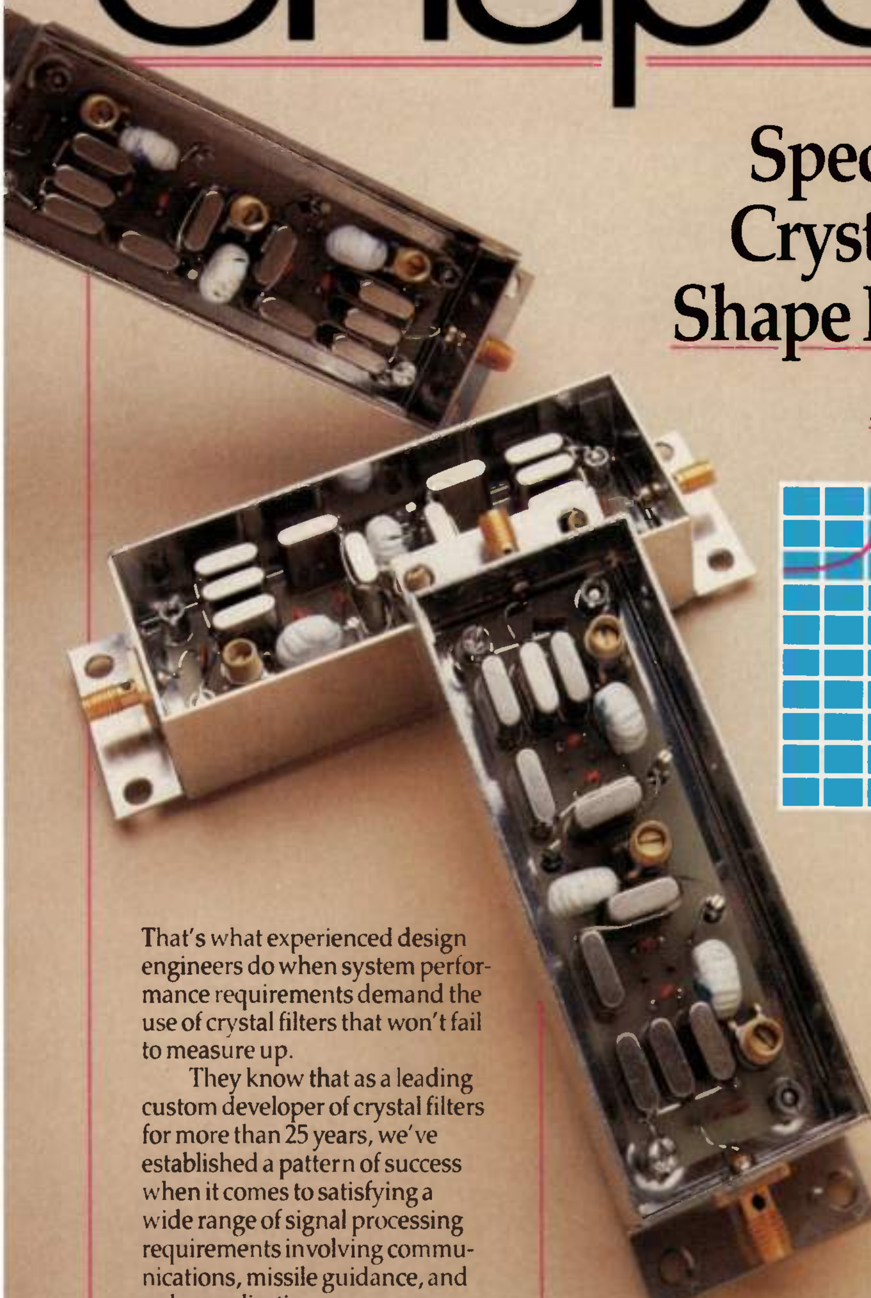

Specify DAMON Crystal Filters with Shape Factors As Steep As 1.05:1.

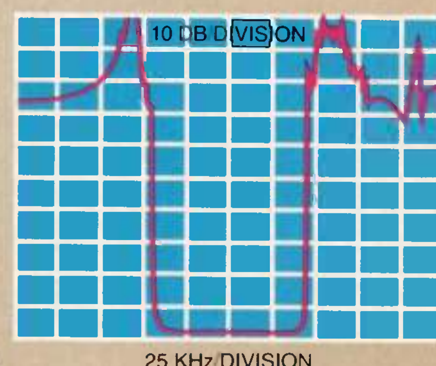

That's what experienced design engineers do when system performance requirements demand the use of crystal filters that won't fail to measure up.

They know that as a leading custom developer of crystal filters for more than 25 years, we've established a pattern of success when it comes to satisfying a wide range of signal processing requirements involving communications, missile guidance, and radar applications.

And that in the process, we've earned a reputation for meeting some rather imposing specifications in the 10KHz–150MHz range with a set of equally imposing accomplishments that include: Shape factors as steep as 1.05:1 with 80dB attenuation levels... Phase and amplitude matching within the tightest tolerances... And passbands that remain constant over a wide temperature range.

As a system designer it means that you can optimize incoming signal processing, thus assuring better selectivity at the front end.

All of which adds up to increased design flexibility in terms of both performance and packaging, as well as improved reliability at the overall system level.

Behind this claim is Damon's continuing commitment to the latest in manufacturing resources, which includes a facility that's equipped with the latest in CAD and CAE technology, as well as provisions for in-house environmental testing (MIL-Std-202), crystal fabrication (MIL-C-3098), and soldering (WS-6536E). And that's only the beginning.

For more information, call us today to discuss your application (1-800-348-0028). And send for our complete catalog.

Damon also manufactures a full line of V.C.X.O.'s, T.C.X.O.'s and S.A.W. Delay Lines.

DAMON/ELECTRONICS DIVISION

80 WILSON WAY, WESTWOOD, MASS. 02090, TEL: (617) 329-2460
FAX (617) 329-0551, TWX 710-348-6722

INFO/CARD 27

RF POWER

As You Like It.

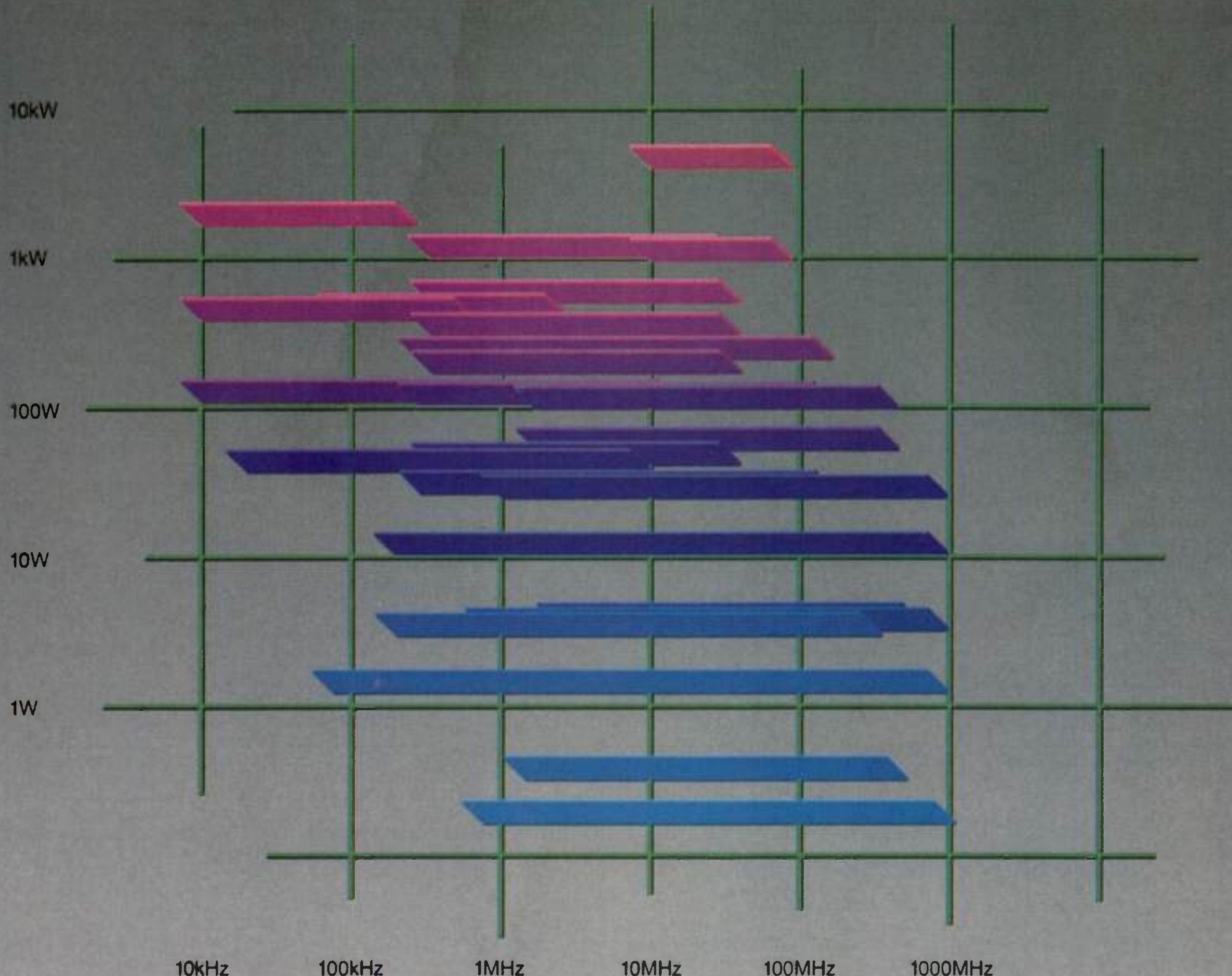

All solid state. Unconditionally stable. Compact. Tremendously versatile. Whatever your need for RF Power, ENI offers you a choice of Class A power amplifiers unsurpassed in quality. Our wide line spans a frequency spectrum from 10kHz to 1GHz with power outputs that range from 300 milliwatts to over 4000 watts.

These units can be driven by virtually any signal source. They're completely broadband and untuned, amplifying inputs of AM, FM, TV, SSB, and pulse modulations with minimum distortion. Their unconditional stability and fail-safe design make them impervious to severe mismatch conditions, and capable of delivering rated power to any load impedance from an open to a closed circuit.

The design excellence of ENI amplifiers is symbolized by the perfect geometry of the design elements we use with our logo. For our latest catalog, please contact us at any of the offices listed below.

ENI

The advanced design line of RF power amplifiers

UNITED STATES HEADQUARTERS: ENI, INC., 100 Highpower Road, Rochester, NY 14623-3498 USA, Tel (716) 427-8300, Tlx 671 1542 ENI UW, Telfax 716-4277839
WEST COAST: ENI, INC., 2318C Walsh Avenue, Santa Clara, CA 95051, Tel (408) 727-0993, Telfax 4087271352
EUROPE: ENI EUROPE LTD., Mundells Court, Welwyn Garden City, Hertfordshire AL7 1EN England, Tel (0707) 371558, Tlx 24849 ENI UK G, Telfax 707339286
JAPAN: ENI-JAPAN, 10-20, Shibasaki-cho 3 Chome Tachikawa City, Tokyo, Tel (81) 0425 229011, Fax (81) 0425 222636

INFO/CARD 28

See us at RF Expo/East, Booth #322.

Envelope Detection and A.M. Noise Figure Measurement

The Envelope Detector is Used to Discuss Weak Signal Reception

By William Sabin
Collins Divisions of Rockwell International Corp.

This paper discusses the weak-signal reception of a double sideband plus carrier (AM) signal using the envelope detector, which is assumed to be piecewise linear and lossless. These points are considered: (a) the determination of receiver noise figure, based on an AM sensitivity measurement, (b) the effects of a wideband IF followed by a narrowband audio, and (c) the effect of synthesizer phase noise on ultimate signal-to-noise ratio. One purpose of this article is to discuss the behavior of the envelope detector in an AM (double sideband) receiver, as it affects the measurement and calculation of the signal and noise levels of the RF, detector and audio (or baseband). Another goal is to determine the noise figure of an AM receiver from a sensitivity measurement.

This discussion is restricted by assuming that the detector is piecewise linear as shown in Figure 1. Op-amp detectors closely approximate this result and semiconductor diodes come close at the high input levels found in high gain, high quality receivers. There are advantages to this kind of detector in many applications. The IF signal bandwidth (assumed to be rectangular and have linear phase) is at least twice the audio bandwidth so that both sidebands are detected.

Considered in the frequency domain, this detector behaves like a mixer or product detector, with the AM carrier taking on the role of a local oscillator. That is, the commutating or switching action of the carrier translates the RF signal to baseband. When this happens the lower sideband modulation folds around the zero frequency axis and combines with the upper sideband. At RF, the sidebands are phase conjugates with respect to the carrier. In the detector output they combine in phase to produce an AC output power which is four times greater (6 dB) than it would be if only one of the two sidebands were detected.

This means only that the full AC modulation power of the transmitted sidebands is recovered. It does not imply that a magnification of the input modulation power has somehow occurred. The maximum audio power recovered from the in-phase sum of the sidebands is exactly equal to the sum of the powers in the two sidebands. But if one sideband is removed, the audio (AC) output drops 6 dB, not 3 dB. This apparent discrepancy will be discussed.

At the input, the instantaneous noise vector (or phasor) may be thought of as the incoherent (random relative phase and amplitude) sum of lower and upper sideband noise vectors. Note that the variance (AC component) of the noise output of the detector may be less than the variance of the narrowband IF input noise.

An important property of this "translator" is that unless the transmission medium or the receiver phase linearity is disturbed, the carrier ("local oscillator") automatically bears the correct phase relationship to the two modulation sidebands to assure the maximum possible detector baseband signal output. If this relationship is lost, in transmission or reception, the output signal is reduced in amplitude and becomes distorted.

If the carrier is weak, the behavior is more complicated than the model discussed above. Also considered is the effect of low carrier-to-noise ratio on the detector performance, using computer simulations and the results (principally) of S.O. Rice (ref. 1).

Power and Voltage Relationships

Figure 2 shows a sine wave input to a full wave envelope detector. The circuitry is assumed to be lossless. The capacitor C is initially disconnected, as indicated. The transformer T can be

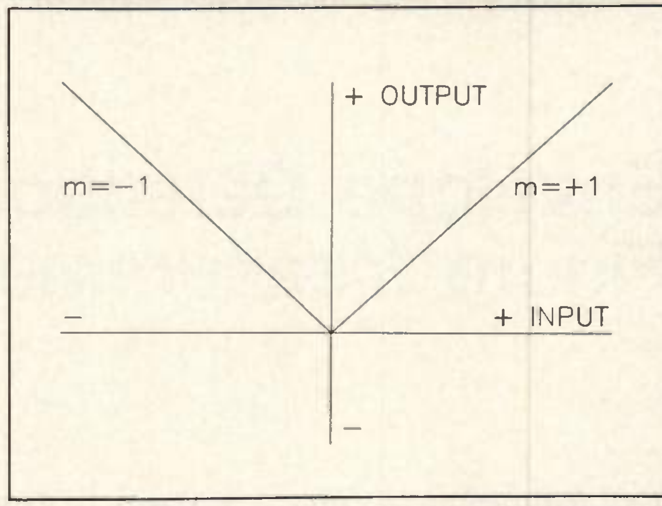

Figure 1. Ideal linear full wave envelope detector.

adjusted for impedance matching or for deliberate mismatching. When the impedance match is perfect the total power in the output loops is equal to:

$$P_{out} = \frac{1}{\pi R_L}\int_0^{\pi}\left[\frac{NE}{2}\,\mathrm{Sin}\,\theta\right]^2 d\theta = \frac{(NE)^2}{8R_L} = \frac{E^2}{8R_G}\,;\ R_L = N^2R_G$$

The power available from the generator is:

$$P_{avail} = \frac{1}{R_G}\left[\frac{E}{2\sqrt{2}}\right]^2 = \frac{E^2}{8R_G}$$

The two are equal.

The envelope of the output signal is a line joining the tips of the output loops, as shown in Figure 2. If capacitor C is now inserted (for impedance match, set $N^2 = R_L/(2R_G)$ (ref. 8)), Figure 2 also shows the resultant output voltage. The line indicated is not the envelope. The generator by itself cannot maintain the envelope level without an amplifier to provide the additional charge to C. This is the situation in a completely passive detector, where one tries to deliver maximum signal power to a load by impedance matching.

The DC voltage on C is not the "average" of the wave, since it also contains the harmonic energy. This means that the power under the envelope of the output signal is greater, by 3 dB, than the actual power in R_L. Therefore the unaided input signal cannot create this power level at the output without violating the law of conservation of energy. But if impedance matching is ignored and load resistor R_L is allowed to become large, the peak envelope voltage is closely approximated. In this case only signal and noise envelope voltage is considered, rather than power, and amplifiers are used to get the required output power; the power efficiency of the detector itself is not important. A constant can be used to relate available input power to detector output power.

In order to simplify the discussion, assume that the power output of the detector equals the available envelope power of the RF input. That is, the required amplification is included.

The AM Wave

Figure 3 shows the peak voltage values, the power spectrum and the envelope of the transmitted signal for a wave which is 30 percent modulated. The following relationships apply:

Carrier power = $(1.0)(0.707)^2/1.0 = 0.5$ W
Each sideband power = $(0.15)^2(0.707)^2/1.0 = 0.01125$ W
Total sideband power = $2(0.01125) = 0.0225$ W = $(m^2)/2(P(\text{carrier}))$
Envelope power = 1.045 W =
2(carrier power) + 2(sideband power)
(Integrate the square of the envelope over a full modulation cycle)
Envelope DC power = 1.0 W = 2.0(carrier power)
Envelope AC power = 0.045 W = 2.0(total sideband power)

For convenience, let the carrier frequency be an integer times the modulation frequency. The total average power in the wave is found by integrating the square of the AM wave as follows:

$$P_{avg} = \frac{1}{2\pi}\int_0^{2\pi} (1 + 0.3\,\text{Sin}\theta)^2\,\text{Sin}^2\omega_c t\,d\theta =$$

$.5 + .0225 = .5225$W

The sum of the powers in the spectrum of Figure 3 gives:

$$P_{avg} = \left(\frac{1}{\sqrt{2}}\right)^2 + \left(\frac{.15}{\sqrt{2}}\right)^2 + \left(\frac{.15}{\sqrt{2}}\right)^2 = 0.5225\text{W}$$

This illustrates Parseval's theorem, equating power in the time and frequency domains. In the envelope of the modulated wave an extra 3 dB shows up; 3 dB also shows up in the envelopes of the carrier and noise as well. Therefore, the relationships between carrier, sidebands and noise powers are preserved in the envelope of the incoming signal.

Figure 4 shows what happens to the baseband output signal if the two sidebands have different amplitudes and are not phased properly with respect to the carrier. The resultant vector R acquires a quadrature (Q) component and the in-phase (I) component is reduced. The audio output signal is the variations in length of the resultant vector, and these are now reduced, as the geometry shows. The tip of the resultant vector traces a line such as the example shown and distortion is generated in the audio output. A computer spectral analysis of the equation below shows that for 30 degrees phase shift between carrier C(=1.0) and sidebands A(=0.1) and A'(=0.4) the second harmonic is about 24 dB below the fundamental. The output envelope is given by the parametric equations:

$$I = 1.0 + m_2\text{Cos}(\omega_m t + \phi) + m_1\text{Cos}(\omega_m t - \phi)$$

$$Q = -m_2\text{Sin}(\omega_m t + \phi) + m_1\text{Sin}(\omega_m t - \phi)$$

where $m_1 = A/C$; $m_2 = A'/C$; $R = \sqrt{I \cdot I + Q \cdot Q}$;
ϕ is offset angle.

Carrier Only Plus Noise

Suppose that instead of modulation, only white narrowband noise and a carrier of constant envelope value are present. The lengths of vectors C and W (often called "phasors") in Figure 5 represent the magnitudes of the envelopes, at one instant, of the carrier and noise at the detector input. The phase angle of each at that instant with respect to some arbitrary reference is also shown. The following statements can be made regarding this input:

a) The noise vector W has a Rayleigh amplitude distribution and a uniform phase distribution from 0 to 2 π with respect to

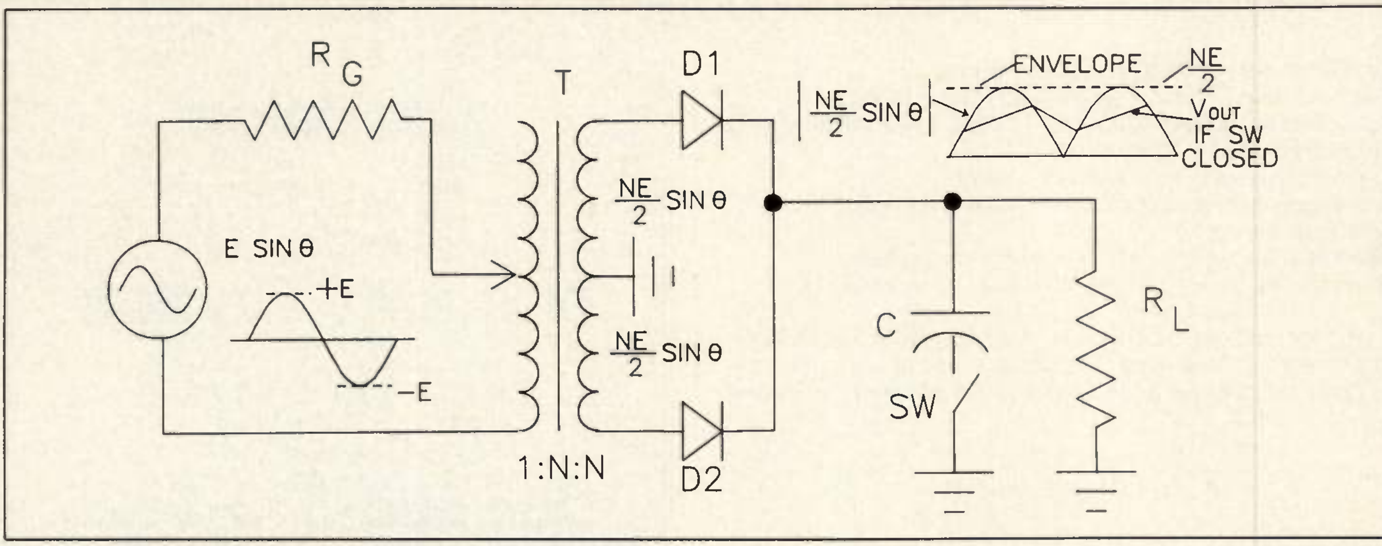

Figure 2. Full wave linear detector.

the phase of the carrier vector C.

b) W may be viewed as consisting of two components, the I component which is assumed to be in phase (0 or 180 deg) with the carrier C and the Q component which is in quadrature (±90 deg). The I and Q envelopes are statistically independent of each other.

c) The envelope of each of these components is Gaussian and has a second moment (also variance or AC component since there is not DC component) which is equal to one half the second moment of the envelope W. That is,

$$E(W)^2 = 2E(I^2) = 2E(Q^2) = 2VAR(I) = 2VAR(Q) = 2\sigma^2$$

where σ^2 is the incoming narrowband RF noise power, $2\sigma^2$ is the power in the noise envelope as previously discussed and E(*) is "expected value." That is, the total power in the envelope of W is equal to the power in the envelope of σ^2.

d) The variance of W is:

$$VAR(W) = (2 - \pi/2)\ \sigma^2 = 0.43\sigma^2 = 0.215(2\sigma^2)$$
(6.67 dB below $2\sigma^2$)

This would be the detector AC output noise if carrier C were not present. The DC power in W would then be:

$$DC^2 = (E(W))^2 = E(W^2) - VAR(W) = 2\sigma^2 - 0.43\sigma^2 = 1.57\sigma^2 = 0.785(2\sigma^2)$$
(1.05 dB below $2\sigma^2$)

e) The vector R in Figure 5 is the sum of noise vector W and carrier vector C. The instantaneous magnitude of R is the output of the envelope detector.

f) The magnitude of R has the Rician distribution and, from Figure 5, is equal to:

$$R^2 = (C + I)^2 + Q^2$$

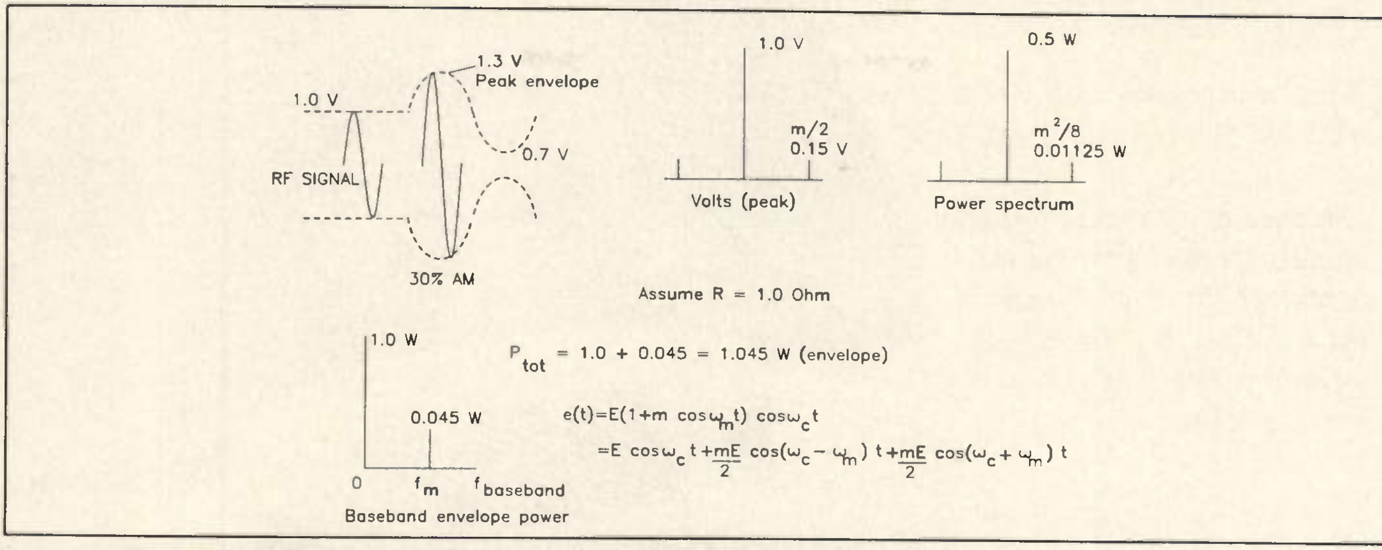

Figure 3. Time and frequency domain for a 30 percent modulated wave.

and,

$$dR = \left(\frac{C+I}{R}\right)dI + \left(\frac{Q}{R}\right)dQ$$

g) From these equations and Figure 5, the magnitude of R is much more sensitive to I than Q if C is large. For large C, the output noise is mostly the I component, and in the limit is 3 dB less than the input noise. However, the remainder of the quadrature noise does not just disappear; it shows up as an additional DC component. The sum of the noise and DC outputs due to quadrature noise is exactly equal to the quadrature input noise power.

h) Therefore, two quantities are of interest, the variance, or AC noise output of R which is involved with receiver sensitivity, and the DC component which may be used to operate the receiver AGC.

i) The Rician distribution is as follows:

$$f(R) = \frac{R}{\sigma^2} e^{-\left(\frac{R^2+C^2}{2\sigma^2}\right)} I_o\left(\frac{RC}{\sigma^2}\right)$$

The last term is a Bessel function:

$$I_o\left(\frac{RC}{\sigma^2}\right) = \frac{1}{2\pi}\int_o^{2\pi} e^{\left(\frac{RC}{\sigma^2}\cos\theta\right)} d\theta$$

j) The quantities of interest are the DC value and the variance, or AC noise output, of the detector. The variance is:

$$var(f(R)) = E[R^2 f(R)] - [E(Rf(R))]^2$$

which could be found by computer using numerical integration.

NOISE/COM

"NOISE IS OUR ONLY BUSINESS"

Broad Band Noise Sources

For Space, Military and Commercial Applications

DC-50 GHz

Broad Band Precision, Calibrated Waveguide

WR-22,-28,-42

TYPICAL STANDARD MODELS

NC 5100 Series	up to 50 GHz 15.5 dB ENR, noise figure meter compatible
NC 5200 Series	up to 50 GHz 21-25 dB ENR, high noise output
NC 5300 Series	up to 50 GHz 21-25 dB ENR, high noise output

For More Information And Quick Response Call:

GARY SIMONYAN at 201-488-4144

Broad Band Instruments

115V or 230V Standard
Bench Type or Rack Mounted

MANUALLY CONTROLLED
+ 10 dBM Output

TYPICAL STANDARD MODELS

NC 6101	up to 20 kHz
NC 6107	up to 100 MHz
NC 6108	up to 500 MHz
NC 6109	up to 1 GHz
NC 6110	up to 1.5 GHz
NC 6111	up to 2 GHz
NC 6218	up to 18 GHz

Other standard models available
MOST ARE IN STOCK

PROGRAMMABLE
IEEE-488 (GPIB), MATE (CIIL)
RS232, etc. + 10 dBM Output

TYPICAL STANDARD MODELS

NC 7101	up to 20 kHz
NC 7107	up to 100 MHz
NC 7108	up to 500 MHz
NC 7109	up to 1 GHz
NC 7110	up to 1.5 GHz
NC 7111	up to 2 GHz
NC 7218	up to 18 GHz

OPTIONAL: Remote variable filters, signal input combiner, 75 ohms output, marker input.
Other standard models available
MOST ARE IN STOCK

Custom & Hi Rel Products

HYBRID FOR SPACE QUALIFIED AMPLIFIED MODULES

10 Hz to 10 MHz, 7 GHz, 9 GHz, 14 GHz etc. Small size and weight

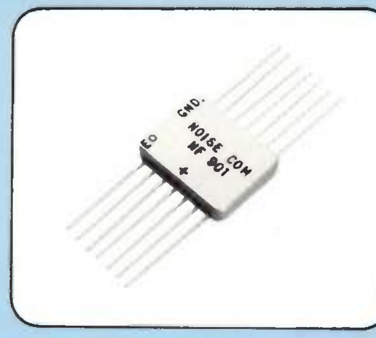

DC COUPLED AMPLIFIED MODULES

- 1 volt output into 50 ohms
- DC-100 kHz
- Low offset voltage
- Compact
- DC-4 MHz

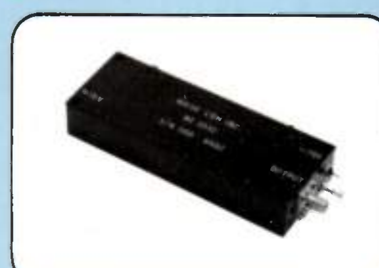

NOISE/COM

"NOISE IS OUR ONLY BUSINESS"

NOISE COM, INC.
E. 64 Midland Ave.
Paramus, NJ 07652
PHONE (201) 261-8797
FAX (201) 261-8339
TWX 910-380-8198

Instead, it proved better to use a statistical Pascal program which looked at 100 records, each with 1000 samples of R as described in Figure 5, and find the average variance for many different values of $C^2/2\sigma^2$, the ratio of carrier power to noise power.

The results of these calculations are shown in Figure 6, curves AC and DC. If the input noise power σ^2 is held constant and the carrier power $C^2/2$ is allowed to decrease, the output noise decreases. At the same time the average, or DC component, that is contributed by the noise, increases. In the limit, when the input becomes all noise, the Rayleigh situation (previously discussed) prevails.

So the total output power is always exactly equal to the input carrier-plus-noise power; nothing is lost. Some of the input noise is converted to DC, and this is why the output signal-to-noise is greater than the input signal-to-noise, if a coupling capacitor is used to remove the DC from the audio output; that is, if the DC is not considered part of the output signal. In a data detector the output, including the DC, is compared to a reference level to determine "on" or "off." The DC contributed by the quadrature noise is then important, although the variance (AC noise) is reduced in the detection process.

k) At low signal-to-noise ratios, influenced possibly by an IF noise bandwidth which is wider than necessary for the desired signal, the intermodulation of noise voltage with itself (N×N) produces a significant part of the output noise spectrum. About 75 percent of this occurs within the half-IF bandwidth (B/2) and the rest is at high frequencies which can be removed by lowpass filtering at the detector output. This is seen in Figure 7, which is similar to Figures 9 and 10 of reference 11.

Figure 7a shows the power spectrum of C×N, produced by noise intermodulating with the carrier, and also the power spectrum of N×N. The Fourier transform of the detector output autocorrelation of the N×N process (where the magnitude of N has the Rayleigh distribution) is the self-convolution of the IF narrowband noise power spectrum. The value of this self-convolution for each value of frequency shift is proportional to the output power spectral density; for a rectangular IF passband (nearly true in modern receivers) this is triangular in shape, as Figure 7a shows. For the linear detector the total N×N power is proportional to the IF bandwidth and the maximum value (2c) is proportional to the spectral density, n_o. The above topic is discussed in reference 9.

Figure 7b is Rice's method of showing the relative contributions of the C×N and the N×N processes, using the equations included in the Figure. σ^2 is constant and $C^2/2$ is variable. The C×N noise increases from zero to a constant value as $C^2/2$ increases. The N×N contribution appears to be indeterminate at very low $C^2/2\sigma^2$; that is, $C^2/2\sigma^2$ and h both approach zero. From previous discussion, note that the noise at zero carrier is the Rayleigh process; its spectrum is triangular in shape. At higher $C^2/2\sigma^2$ the N×N noise quickly drops to very small values.

When the IF bandwidth is much wider than the required audio width the N×N detector output noise can become large at low $C^2/2\sigma^2$. This output noise has the characteristic low frequency emphasis (verifiable by listening tests); at higher $C^2/2\sigma^2$, this spectrum flattens out.

The properties mentioned above are incorporated into Figure 6. At each value of $C^2/2\sigma^2$ the contributions of the C×N and the

N×N processes are shown. These values are calculated from Rice by modifying the dimensions to match the envelope values used in Figure 6. This is done by multiplying the vertical scale by π, which gives the desired value of parameter "a" (Figure 7b) at large $C^2/2\sigma^2$. (Rice's factor $1/\pi$ is based on an "averaging detector," rather than the true envelope detector used here). The C×N and N×N plots in Figure 6 should add up to the values in the AC plot (they do, approximately).

The shape of the AC curve in Figure 6 is correct only for a rectangular IF passband. For other shapes the amount of noise increase can be one or two dB greater, as discussed in reference 2.

Power Relationships in R, I and Q

If Figure 5 is considered to be a carrier C, length 1.0, and a fixed length modulation vector, W, which rotates around C with some frequency fm, a clear idea of the power relationships involved can be seen while avoiding the statistical approach used in the previous discussion of carrier-plus-noise. The total power in R, the vector sum of C and W is:

$$P_{tot} = \frac{1}{2\pi}\int_{0}^{2\pi} [(C + W\cos\theta)^2 + (W\sin\theta)^2]\, d\theta$$

The DC power is:

$$P_{dc} = \left[\frac{1}{2\pi}\int_{0}^{2\pi} \sqrt{[(C + W\cos\theta)^2 + (W\sin\theta)^2]}\, d\theta\right]^2$$

The total power contributed by W is P(tot) 1.0 and the DC power contributed by W is P(dc) 1.0. Table I lists the results for values of W from 0.0 to 1.0. P(ac) is the AC power contributed by W, and is equal to P(tot) − P(dc). Table I shows the following:

a) The total power in R is increased by exactly the amount of power in W.

b) As W gets larger in relation to C its contribution to the DC power increases faster than its contribution to the AC power.

c) At small values of W the contributions are almost equal and have the value $W^2/2$. At higher values the AC contribution is less than this.

This model also explains clearly why the AC output of the detector drops 6 dB, rather than 3 dB, when one sideband is removed. This question was raised at the beginning. At low modulation percentage, Table I shows that P(ac) is one half (-3 dB) of the modulation envelope power (W). The other half is converted to DC and is not available as useful AC output. At high modulation percentages the loss approaches 4.2 dB. (This is perhaps not generally recognized.) So if one sideband is filtered out of the AM input the AC output drops at least 6 dB. Moreover, as seen in Figure 4, the distortion becomes heavy at high values of m. This problem occurs in AME (amplitude modulation equivalent) mode, often used in SSB radios for AM operations. Again, note that all of the input power is accounted for; nothing is lost.

Weak Modulated Signals

A few interesting points should be mentioned regarding the linear detector behavior in the presence of a weak, modulated carrier in the presence of noise. At low signal levels the piecewise-linear detector exhibits a square-law behavior, as seen in the N×N process. It also has been observed (ref. 2 and 3) that the modulation of a weak signal is actually suppressed by noise;

the modulation is converted to noise. Reference 4 also points out that the presence of noise causes harmonic distortion of a weak signal, especially at high levels of modulation; a narrow audio tone-filter could respond to this harmonic.

A subject of study has been the relative merits of the square-law detector and the linear detector. Reference 5 finds that for diversity reception without any modulation the square-law detector is optimum. References 4 and 6 point out, however, that for amplitude-modulated diversity signals the linear detector has better signal-to-noise ratio, by about 2 dB, and contains much less second harmonic distortion. The linear detector is also believed to be better for FSK (frequency shift keyed) signals (ref. 7).

Pre- and Post-Detection Filtering

Figure 8 shows the usual situation in an AM receiver or spectrum analyzer. In some equipment the IF bandwidth is much wider than twice the desired audio (or video) bandwidth. After detection, the audio filter provides the desired signal and noise bandwidth. The spectral diagrams in Figure 8 illustrate that the noise output of the detector is confined mostly to one-half the IF bandwidth. The variance of this noise is at least 3 dB less than that of the input noise (on an envelope basis), as discussed previously.

The wide IF bandwidth causes a large DC output due to noise rectification. This output includes the N×N effect previously discussed, which enhances the DC level. If this voltage is used for AGC purposes there may be an excessive gain reduction caused by noise and also by adjacent channel signals. That is, the volume of a low-level desired signal may be reduced because noise dominates the AGC. As this signal increases, the audio level increases several dB until the signal is strong enough to dominate the AGC loop. An increase in atmospheric noise or broadband noise from a collocated transmitter can further reduce the volume (this could be desirable, perhaps). These effects have been observed in high-gain receivers which make AGC on internal noise plus received noise.

The ratio of audio output noise power to detector IF input noise power is given by:

$$\frac{N_{AF}}{N_{IF}}\ (\mathrm{dB}) = 10 \log\left(\frac{NB_{AF}}{NB_{IF}/2}\right) - 3.0 - K$$

where NB is noise bandwidth and K (a positive number) is the correction factor shown in Figure 6. For convenience, all references to "N" henceforth mean noise power, not voltage as in previous discussions.

Measuring Noise Voltage

A "true RMS" audio meter should be used to measure noise voltage, because peak-detecting rectifier meters respond differently to sine wave and noise signals. That is, the RMS value of the Rayleigh noise envelope is greater by the factor $20\log(2/\sqrt{\pi})$ (1.05 dB) than the value indicated on the peak-detecting meter which has been calibrated with the RMS value of a sine wave. The meter should have a crest factor rating (ratio of peak to RMS) of 5.0 or more.

Also, spectrum analyzers, especially those with logarithmic scales, respond differently to discrete and noise inputs. This difference should be determined for the instrument in use; it can be as much as 2.5 dB.

Measuring Sensitivity

The sensitivity is usually determined by observing the drop in audio output when the modulation (usually 30 percent at 1 kHz) is turned off while the carrier is left on. The carrier level

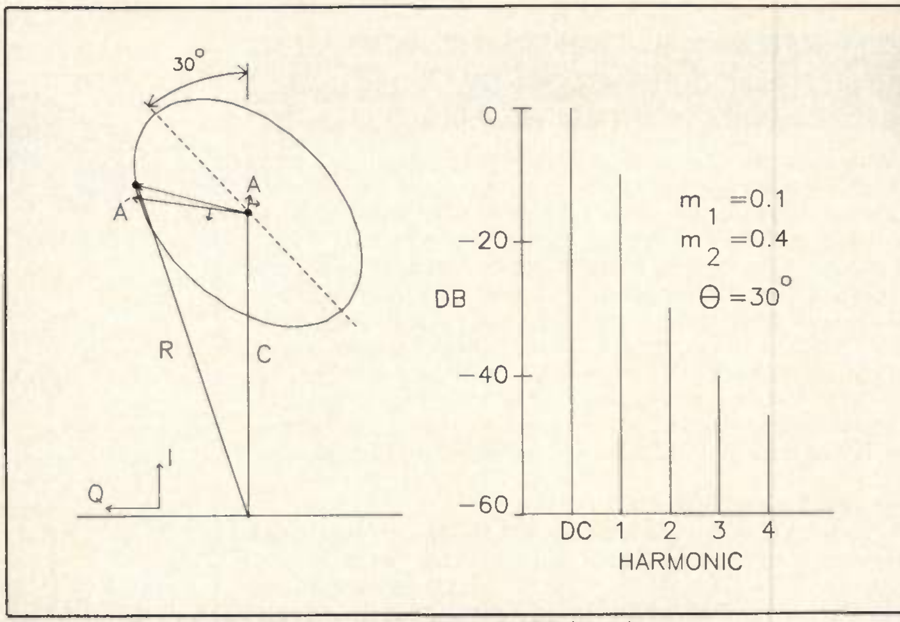

Figure 4. Results of improperly phased sidebands.

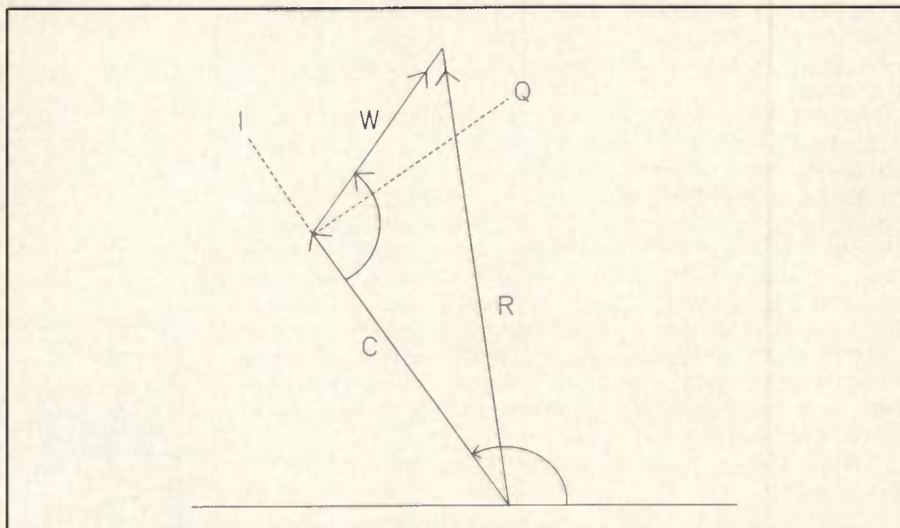

Figure 5. Detector input consisting of carrier and noise.

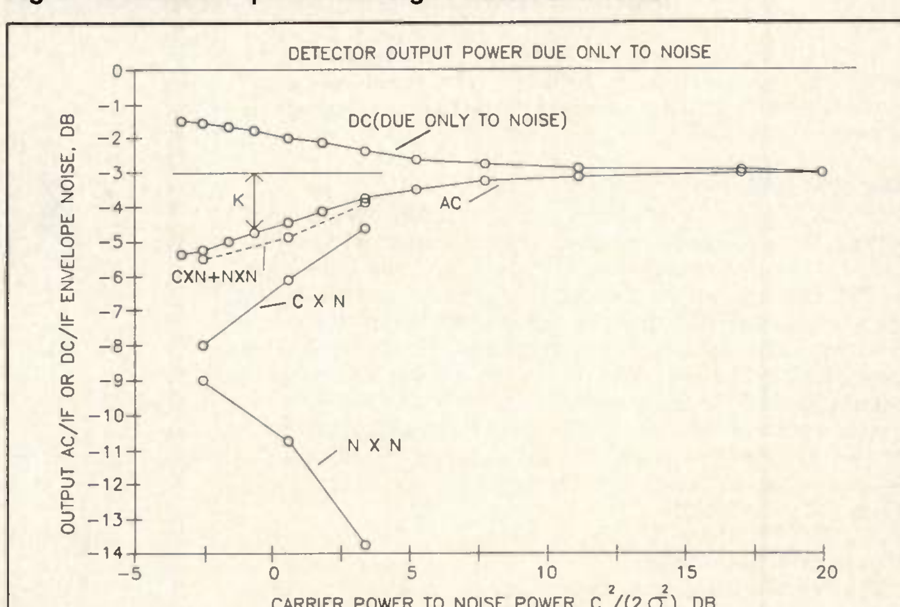

Figure 6. DC and variance of detector output.

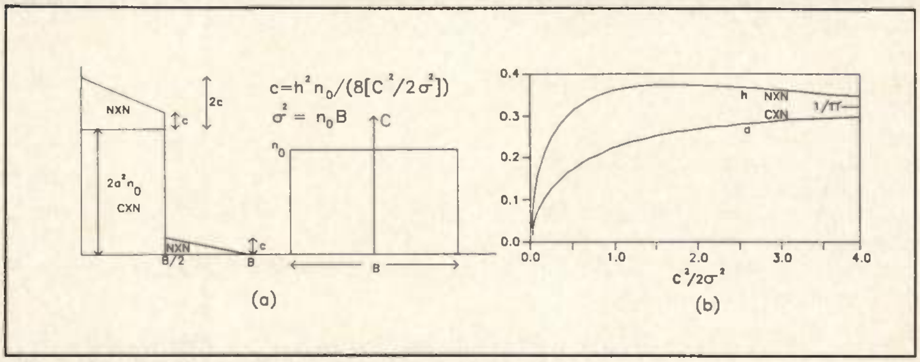

Figure 7. Rice's plots for C×N and N×N noise.

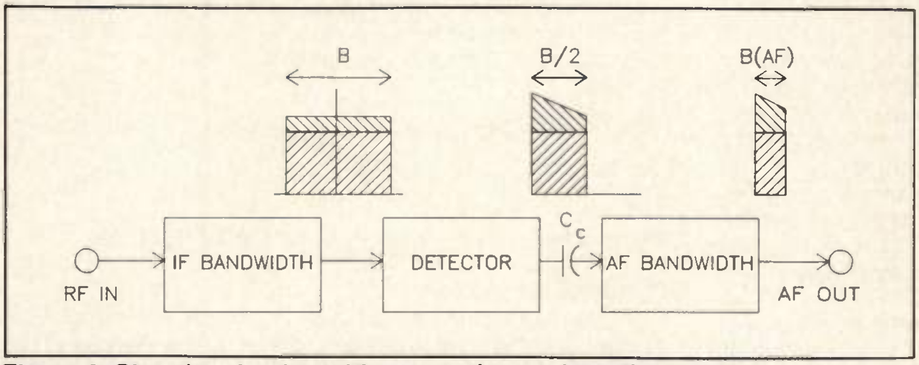

Figure 8. Signal and noise with pre- and post-detection system.

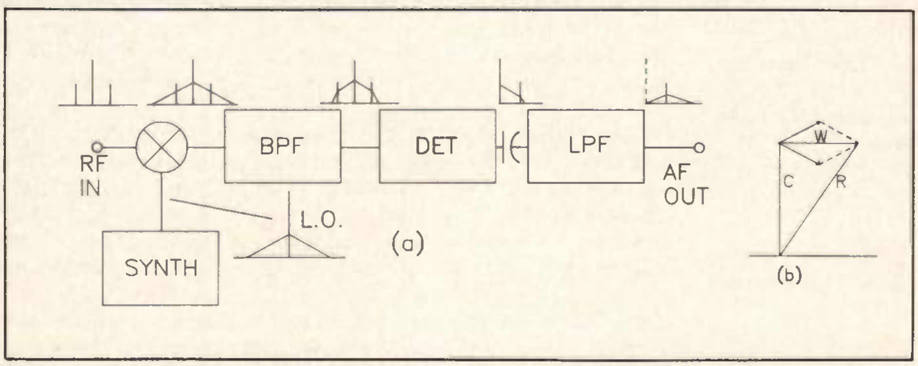

Figure 9. L.O. phase noise in an AM receiver with envelope detection.

W	W²	P(tot) − 1.0	P(dc) − 1.0	P(ac)
0.0	0.0000	0.0000	0.0000	0.0000
0.1	0.0100	0.0100	0.0050	0.0050
0.2	0.0400	0.0400	0.0201	0.0199
0.3	0.0900	0.0900	0.0457	0.0443
0.4	0.1600	0.1600	0.0824	0.0776
0.5	0.2500	0.2500	0.1310	0.1190
0.6	0.3600	0.3600	0.1929	0.1671
0.7	0.4900	0.4900	0.2697	0.2203
0.8	0.6400	0.6400	0.3638	0.2762
0.9	0.8100	0.8100	0.4787	0.3313
1.0	1.0000	1.0000	0.6210	0.3790

Table I. Power relationships in modulation vector W.

is adjusted until this drop is 10 dB. A significant error occurs if AGC is operating during this measurement because the AGC, and therefore the receiver gain, changes when the modulation is turned on and off.

If the AGC cannot be easily turned off, another method is to use a notch filter to remove the modulation tone from the audio output; then the AGC is not affected. The signal-to-noise ratio is affected slightly by the loss of noise within the notch bandwidth, but this can be calibrated out. This method is often called the SINAD method. For either method, one should be sure that discrete residual outputs such as hum and distortion are well below the noise level; use an audio spectrum analyzer for verification.

Calculation of AM Receiver Noise Figure

Formulas for calculating the noise figure of an AM receiver, based on a 10 dB (S + N)/N sensitivity measurement can now be derived. The method takes into account the special behavior of the audio noise which occurs with envelope detection. The block diagram of Figure 8 will be used. In one case the AF bandwidth is equal to or less than one-half the IF bandwidth; in the second case the AF bandwidth is equal or greater.

In order to simplify the discussion, and without any error being introduced, assume that the receiver gain for the desired carrier and modulation, from antenna to audio output, is exactly unity (0.0 dB). Then receiver gain values need not create unnecessary complications. Only the noise level changes.

If the audio (S + N)/N = 10 dB then, S/N = 9.54 dB where S is audio power and N is noise power. The audio noise output is:

$$N_{audio}\ \text{dBm} = S - 9.54 = P_{SB} - 9.54$$

where the audio and the sideband signal power have the same value.

The detector output noise will be greater than this if the half-IF bandwidth is greater than the audio bandwidth.

$$N_{detector}\ \text{dBm} = N_{audio} + 10 \log \frac{B_{IF}}{2B_{audio}}$$

The IF noise level is greater than this by 3 dB plus the correction factor K (a positive number).

$$N_{IF}\ \text{dBm} = N_{detector} + 3.0 + K$$

where K remains to be determined from Figure 6 (which implies a rectangular IF band). To find K, the IF value of $C^2/2N$ is needed; $C^2/2$ (the signal generator carrier power in dBm) is known and the first estimate for $C^2/2N$ is:

$$\frac{C^2}{2N_{IF}}\ \text{dB} = \frac{C^2}{2} N_{detector} - 3.0$$

From Figure 6, find K for this $C^2/2N$. Then get a new $C^2/2N$

$$\frac{C^2}{2N_{IF}}\ \text{(second estimate)} = \frac{C^2}{2N_{IF}}\ \text{(first estimate)} - K$$

At this new value of $C^2/2N$, get a new value for K. Use the first estimate of $C^2/2N$ and the new K to get an improved value for the second estimate of $C^2/2N$.

The value of IF noise is known, using the equation above. Knowing the IF noise bandwidth, the IF noise density is:

$$N_D\ \text{dBm/Hz} = N_{IF} - 10 \log (B_{IF})$$

At room temperature the thermal noise density is –174 dBm/Hz. The receiver noise figure is then defined to be:

$$\text{NF dB} = 174\ \text{dBm} + N_D\ \text{dBm} = 174 + N_{AF}\ 10 \log B_{AF} + 3.0 + K$$
$$N_{AF} = C^2/2 - 9.54 + 10 \log (m^2/2)$$

These are combined to get the formula:

$$\text{NF dB} = 164.46 + C^2/2 + 10 \log (m^2/2) + 10 \log (B) + K$$

where B is the dominant noise bandwidth and is chosen as follows:

a) If the AF bandwidth is narrower than IF/2 then $B = B_{AF}$

b) If the IF/2 bandwidth is narrower than AF then $B = 0.5\ B_{IF}$

c) If the AF bandwidth is nearly equal to 0.5×IF bandwidth then B is the effective noise bandwidth for the combination.

For example, for option b) above, if

$$\frac{C^2}{2} = -103\ \text{dBm},\ B_{IF} = 6000\ \text{Hz},\ m = 0.3,\ \text{then}\ K = 0.3\ \text{dB}$$

(Figure 6) and,

$$\text{NF} = 164.46 - 103 - 13.47 - 34.77 + 0.3 = 13.52\ \text{dB}$$

Synthesizer Noise

A measurement of interest in an AM receiver is the ultimate ratio of signal to noise. As the signal increases the noise level eventually becomes a constant number of dB below the desired audio. The audio is usually due to a 30 percent modulation of the signal generator. This noise limit may be determined by local oscillator phase noise which becomes attached by intermodulation to the carrier of the RF test signal. Figure 9a shows the circuit path situation.

The synthesizer L.O. output contains almost no amplitude fluctuations. The loop noise sources tend to phase modulate the VCO, and if it is "pure" phase modulation there is no amplitude change. For this to happen, the entire set of phase modulation sidebands for each Fourier frequency ±fm (with respect to the carrier frequency) must be present in the right amplitude and phase. Also, at any instant the upper and lower noise-sideband pairs must have equal amplitudes and be phase conjugates with respect to the 90 degree "Q" axis (odd harmonics) or the carrier "I" axis (even harmonics). This must be so, if there is no amplitude variation of the resultant vector R. If these relationships are disturbed, amplitude variations appear, as shown in Figure 9b for example, where only one pair of sidebands is shown.

When this noise is modulated onto the RF test carrier by a perfect mixer, the phase relationships are maintained with respect to the RF carrier. That is, the RF carrier is phase modulated by the L.O. noise sidebands and the variance of the resultant carrier vector (R in Figure 9b) can be potentially zero. The result is that the envelope detector tends to reject the phase noise. The ultimate signal-to-noise ratio can therefore be much larger than one would encounter in an FM receiver (or in an SSB receiver).

The phase noise from the L.O. does not add any additional power to the detector input. The case previously considered was "additive" noise from an independent noise source; the carrier power and noise power added in the receiver IF. In the case of phase modulation of the signal carrier by the L.O. phase noise, the power in the noise sidebands is matched by an equivalent reduction of power in carrier C. The values of the carrier amplitude C' and the first and second sidebands are given approximately (see Figure 9b) by:

$$\frac{C'}{C} = 1 - \frac{(W/C)^2}{4}$$

$$\frac{S(1)}{C} = \frac{W/C}{2}$$

$$\frac{S(2)}{C} = \frac{(W/C)^2}{8}$$

The result in the ideal case is that resultant vector R contains no variations which can affect an envelope detector.

But if the AM receiver signal path has poor differential delay with respect to the carrier (say at the edges of an IF filter) the quadrature phase relationship between noise and carrier can be changed and substantial amplitude changes can occur. The detector then produces appreciable noise output. It can be difficult to predict exactly what noise output level will be experienced. A computer program might use the filter delay and frequency response properties, the synthesizer phase noise spectrum (amplitude and phase) and the audio frequency response to get the audio noise spectrum and its RMS value; this might be a rather ambitious exercise, possibly of dubious value.

It is also found that quadrature noise which produces changes in R causes a frequency doubling effect in the detector. That is, input sideband frequency fm into the detector produces frequency 2fm in the output. Figure 9b shows how this effect can occur. rf

References

1. S.O. Rice, "Mathematical Analysis of Random Noise, Part 4," *Bell System Technical Journal,* January, 1945.
2. E.G. Fubini and D.C. Johnson, "Signal-to-Noise Ratio in AM Receivers," *Proceedings of IRE,* Dec., 1948, pp. 1461-1466.
3. M. Schwartz, *Information Transmission, Modulation and Noise,* Second Edition, New York, McGraw-Hill, p. 463.
4. W.R. Bennett, "Envelope Detection of a Unit-Index Amplitude-Modulated Carrier Accompanied by Noise," *IEEE Trans. Inf. Th.,* Nov. 1974, pp. 723-728.
5. H.T. Friis and C.B. Feldman, "A Multiple Unit Steerable Antenna for Short-wave Reception," *Bell System Tech. J.,* Vol. 16, pp. 337-419, July, 1937.
6. W.R. Bennett and S.O. Rice, "Envelope Detection of an Amplitude Modulated Carrier Accompanied by Noise," *IRE Trans. Inf. Th.,* July, 1977, pp. 526-529.
7. M. Schwartz, W.R. Bennett and S. Stein, *Communication Systems and Techniques,* New York, McGraw-Hill, 1966, pp. 104-105, 521.
8. S. Seely, *Radio Electronics,* McGraw-Hill, New York, 1956, p. 257.
9. W.B. Davenport and W.L. Root, *Random Signals and Noise,* McGraw-Hill, New York, 1958, chapters 12 and 13.

About the Author

William E. Sabin is a design engineer in the Advanced Technology Dept., of Rockwell-Collins. He holds an MSEE degree from the University of Iowa and is widely experienced in HF receiver and exciter design, synthesizer design, power supplies, spread spectrum techniques and digital design. He can be reached at Collins Divisions of Rockwell International Corp., Mail Station 107-140, Cedar Rapids, IA 52498. Tel: (319) 395-8391.

RF Testing with Complex Waveforms

Digital Synthesizers Simulate Complex Modulation

By Greg Lowitz and Chris Pedersen
Hewlett-Packard Company

Designers of modern radar, EW and communications systems continue to exploit complex modulation formats to enhance system accuracy and achieve new standards in performance. In radar, for example, there is growing interest in waveform adaptive radars (WARs) to optimize sub-clutter visibility for a given target scenario. In addition, many new systems use waveform predistortion to neutralize effects of amplitude and phase errors caused by high-power transmitters and component nonlinearities (1,2,3). In cases where low time sidelobes are critical and an unweighted pulse must be transmitted, nonlinear-FM (NLFM) chirps can enhance target imaging and probability of detection, without compromising signal-to-noise ratio. The intent of this article, however, is to familiarize the design and test engineer with new tools that can improve the product development and test process. In particular, a special focus on radar and communications receiver test illustrates many of the powerful benefits of digital-synthesis-based signal simulation.

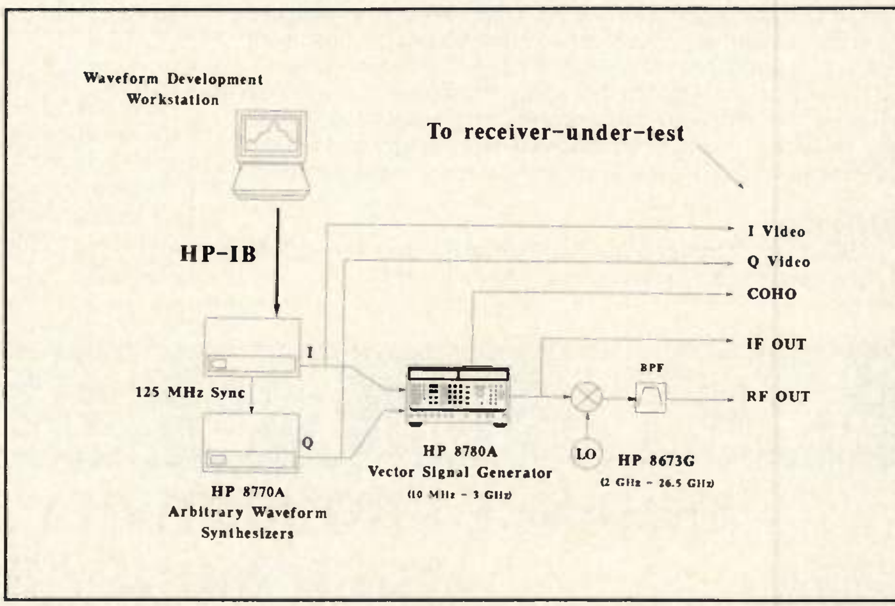

Figure 1. General signal simulator (Vector Arbitrary Waveform Synthesis).

Many current and soon-to-be-deployed radars already use frequency agility (6), multiphase coding and chirp FM to achieve different objectives, including defense against jamming or other electronic countermeasures (ECM). With escalating costs of flight tests, a benchtop simulation alternative becomes essential if an EW receiver design is to remain on schedule and have a high probability of success (7).

Similarly, pressure to increase channel efficiency and reduce bit-error rates is leading to a number of spread-spectrum transmission techniques for advanced communication systems and satellite links. Digital modulation schemes such as BPSK, QPSK, 8PSK, 256 QAM, FSK and MSK are increasingly common, not to mention other more exotic modulation formats now under development. Testing receiver susceptibility to multipath fading, phase noise and AM-PM conversion are just a few examples of advanced tests that designers want to make in the lab.

This surge in complex modulation requirements has created a growing demand for advanced test and measurement equipment, including complex signal simulators that overcome the limitations of conventional function and RF signal generators. For test applications requiring complex real-world signals, basic sine and square waves are no longer sufficient to thoroughly calibrate and characterize a system's performance. Furthermore, as designers race to lead the competition, new testing techniques become necessary to fully stress product susceptibility and reaction to imperfect environments. All too often, products are developed and tested under ideal conditions, resulting unwittingly in designs that are less robust than were otherwise possible.

As engineers and managers seek more efficient design and test techniques, a new generation of flexible, reconfigurable signal simulators is working its way onto designers' benchtops. Based on powerful digital synthesis techniques, these new simulators combine the best attributes of analog and digital technology into one powerful combination. High-speed multiplexed memories, digital phase accumulators, fast multipliers and radio-frequency DACs make possible this growing revolution in testing technology. In comparison to other waveform synthesis, a well-engineered digital synthesizer offers the following benefits (8):

1. Virtually unlimited modulation formats
2. Stable and repeatable signals with digital precision
3. Software reconfigurability
4. Phase-continuous frequency switching
5. Amplitude, phase and frequency agility
6. Low noise and distortion with careful design
7. Very wide modulation bandwidth
8. Potential for size reduction through integration
9. Reasonable cost

System Selection

Choosing the right digital synthesis system is no trivial task. Selection depends on many factors including

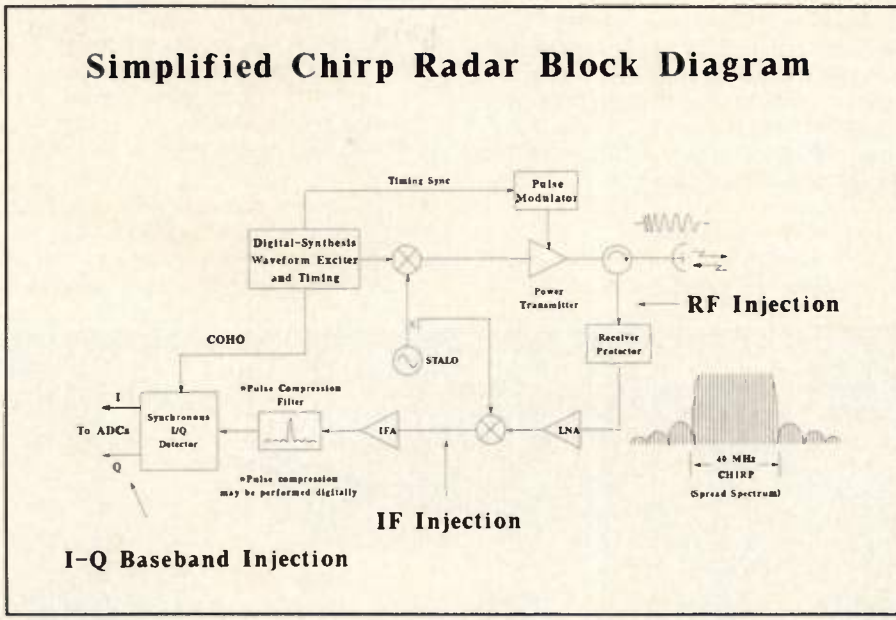

Figure 2. Simplified chirp radar block diagram.

modulation bandwidth, frequency coverage, spectral purity, need for coherence, cost and supportability. However, for many receiver test applications in radar and communications, the general purpose signal simulator should have the following characteristics:

1. Flexible modulation
2. Availability of RF, IF, I/Q baseband signals for direct injection (15)
3. Coherent reference (for synchronous detection schemes)
4. Low phase noise and spurious distortion (application dependent)
5. Reliable performance
6. Intuitive operation

With these requirements in mind, Figure 1 illustrates one possible implementation of an advanced signal simulator that provides the necessary stimulus for direct signal injection into a receiver's RF, IF, or baseband I and Q inputs. The heart of this I/Q modulation configuration — known as Vector Arbitrary Waveform Synthesis — is two digital synthesizers (HP 8770A) that modulate the I and Q inputs of a Vector Signal Generator (HP 8780A) (16,17), providing 100 MHz of complex modulation anywhere from 10 MHz to 3 GHz (7,8). A fallout of I/Q modulation is the handy coherent reference useful for driving the COHO input of the synchronous detector in the radar or communication receiver. The addition of a local oscillator together with an external mixer/filter combination permits further upconversion to any microwave or millimeter-wave frequency. By taking advantage of a novel compensation algorithm, this system can be completely self-calibrated to achieve image rejection and carrier suppression of -60 dBc (18,19). Absolute flatness of 0.1 dB across the band is also achieved. Designers of I/Q modulators recognize the difficulty in achieving this level of performance (20).

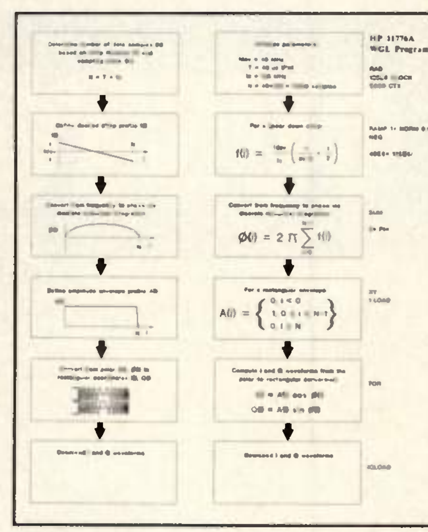

Figure 3. Flowchart for generating radar chirps.

Of course, many variations of this configuration are possible. For example, the I and Q inputs of the HP 8780A Vector Signal Generator are specified for modulation bandwidths up to 350 MHz/channel, for a combined 700 MHz signal bandwidth. In conjunction with digital synthesizers of comparable bandwidth, it becomes possible to generate coherent chirps in excess of 500 MHz. Alternatively, the HP 8780A offers direct digital inputs to simplify the generation of quadrature-amplitude-modulated (QAM) waveforms with up to 64 states. External scalar and FM inputs allow further simulation flexibility. In some systems, it's not uncommon to use any or all of the available modulation inputs to provide the right combination of test signals.

Applications in Radar Test (21)

Consider the operational requirements of a modern radar system. It must transmit, receive and process waveforms to estimate target type, range, velocity, altitude and direction of travel. Often the radar has multiple modes of operation, each optimized to a given measurement requirement. Examples include low-, medium-, and high-PRF modes, as well as stagger and agility to avoid range ambiguities and complicate detection by hostile radar warning receivers. The most advanced systems exploit polarization scattering to enhance target recognition. This generally implies a high-resolution radar with sufficient bandwidth for the imaging requirement at hand. For example, a 100 MHz bandwidth provides better than 6 ft range resolution, excluding degradations due to system errors. This would be adequate for identifying large ships or strategic buildings, but inadequate for distinguishing an American tank from a Soviet counterpart. In practice, however, the signal processing requirements for unfailing reliability are staggering — if not statistically impossible. For this reason, supplemental data gathered by secondary confirmation means (such as visual identification, IFF transponders and electronic intelligence) generally form an important part of the target detection/identification process.

In the case of a simple pulse-Doppler radar where no intrapulse modulation is present, conventional RF signal generators have been used to simulate simple target returns for calibrating Doppler filters and range accuracy on the radar PPI display. However, these methods fall short when the radar is chirped or phase-coded as is common today. Even for the simple pulsed-RF case, complex target scenarios comprised of multiple moving targets have been difficult to produce without the expense of a large target simulation system. Furthermore, these systems have limited access and are generally unavailable to the radar designer on a continuous basis.

With these demanding requirements in mind, Table 1 provides an abridged list of radar tests that could benefit from off-the-shelf signal-simulation hardware (22, 23). That's because the benchtop signal simulator is capable of generating highly complex radar signals, including effects of system nonlinearities. These signals can be used in lieu of the transmitter to simulate linear and nonlinear chirps, amplitude weighing, Barker, polyphase, m-sequences, TWT distortions, and so forth (18,22). With this capability, it is possible to define coherent pulse bursts containing multiple scatterers of different ranges, Dopplers, directions and radar cross sections. This is useful for testing range-Doppler bins, in addition to two-target resolving ability and range-sidelobe suppression. Further uses include simulation of clutter and ECM signals such as noise jamming, or range- and velocity-gate stealing. While this benchtop approach must not be viewed as a total substitute for more thorough testing on larger systems, it provides a more cost-effective solution to ensure on-going design and process integrity in the lab and on the production floor.

Armed with the power of I/Q modulation techniques, test the range accuracy and resolution of the chirp radar receiver of Figure 2. The properties of the transmitted waveform are:

Waveform Type: Linear FM Chirp, Flat Amplitude
Chirp deviation: 40 MHz
Chirp duration: 40 us
Chirp rate: 1 MHz/us
Chirp direction: down

By following the flowchart in Figure 3, these parameters can be translated into I and Q signals via simple mathematical manipulations. The HP 11776A Waveform Generation Software facilitates this process; however, any suitable computer could be used to generate the waveform data samples. Once defined, the signals are downloaded to the signal simulator for subsequent injection into the desired point in the radar system. To ensure complete coherence and accurate triggering, the signal simulator must be phase-locked to the radar, either through its COHO or 10 MHz reference. By taking advantage of the simulator's memory sequencer, calibration targets can be programmed to fall in specified range bins, corresponding to a fixed time delay from each PRF trigger. Furthermore, alternating returns can have a 180 degree phase shift, often called "optimum" Doppler. To verify the output of the signal simulator, an HP 8566B spectrum analyzer reveals the familiar LFM spectrum centered about a 60 MHz IF (Figure 4a), while the HP 5371A Frequency and Time Interval Analyzer verifies the chirp profile (Figure 4b, top graph). Quadratic phase-fitting using Chu's algorithm (24) reveals a ±2

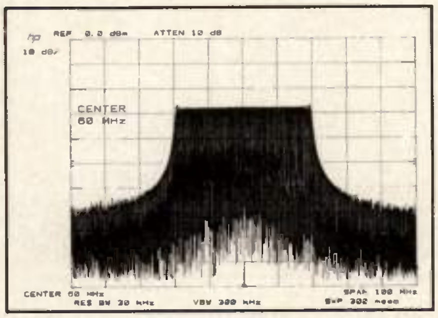

Figure 4a. Spectrum of a 40 MHz chirp at 60 MHz IF.

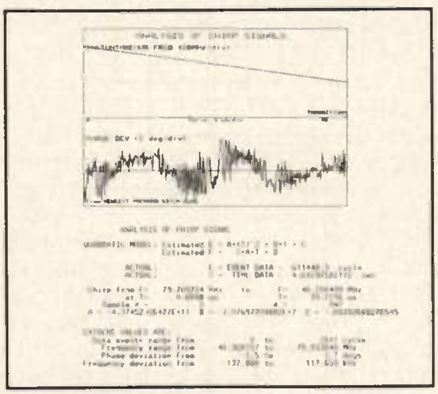

Figure 4b. Chirp signal analysis.

degree RMS phase ripple across the 40 MHz span (Figure 4b, bottom graph). Theoretically, this phase error could be largely eliminated by predistorting the chirp, thus ensuring nearly ideal range sidelobe performance (2).

From here, multiple signals can be superimposed to test radar functionality as described earlier. Figure 5 shows the magnitude of the compressed response of two targets of equal cross section separated by 100 feet. At 6 dB per division, peak sidelobes are down approximately 30 dB, which correlates well to the theoretical 31.5 dB for Hanning weighting (raised cosine with no pedestal). To simulate the nonideal effects of a pulsed TWT, Figure 6 compares an

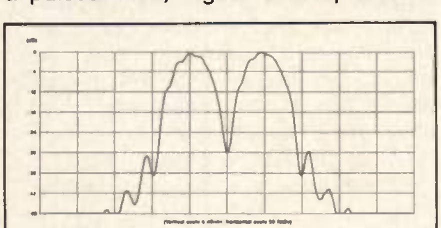

Figure 5. Two targets spaced 100 feet apart test radar ability to resolve closely spaced objects.

ideal target return to one whose transmitted signal contains 20 percent linear pulse droop and 3 cycles of 20 degree p-p chirp nonlinearity. Notice the slight spreading of the mainlobe and the nearly 10 dB degradation of peak sidelobes. The paired-echo theory more fully describes the sensitivity between phase error and sidelobe levels. As Figure 6 illustrates, these errors could potentially mask a small target in the presence of a larger one.

Because of the modulation flexibility of digital synthesizers, it is also possible to create noisy signals (25,26) to simulate jammers as spot, barrage, swept and selective (8,22). This is particularly useful for testing the radar's ability to operate under adverse conditions. In addition, it can be used to test adaptive array radars for nulling in the presence of sidelobe jammers. The process requires defining the desired amplitude and phase spectrum of the signal (versus frequency) and performing a complex inverse FFT to obtain the I and Q channel data. Figures 7a and 7b show some examples of noise spectra useful for this type of application.

Applications in Digital Communications (18,27)

Like many radar systems, modern digital microwave radios (DMRs) also employ complex modulation but for different objectives: to transmit and process digital data (information) and voice. Compared to traditional analog

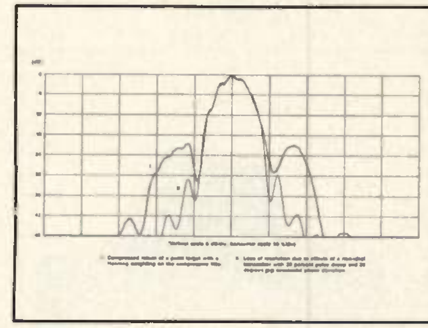

Figure 6. Comparison of signal return.

transmissions, digital techniques offer several advantages, including improved noise immunity, mixed data and voice, and reduced complexity in some aspects of modem design. Common formats for digital communication transceivers include 16 and 64 QAM (quadrature amplitude modulation). However, as manufacturers strive to improve spectral efficiency and overall transmission capacity, 256 QAM and experimental 1024 QAM system are emerging. This heightened modulation complexity greatly narrows the available performance margins for a given bit error rate (BER). More than ever, designers must contend with effects of noise, high-power amplifier nonlinearities, modem errors and multipath fade. If not properly corrected, the multipath fade can have the most dramatic effect on transmission integrity.

Not surprisingly, considerable interest is mounting for accurate multipath fade simulations, and products are becoming available for simulating its effect on 70 MHz DMR IF signals. Generally, these products mimic a two or three fade whereby the channel simulation comprises multiple transmission paths, each with a specified delay, amplitude and phase. This allows fades to be modeled in terms of their depth, notch width and position within the channel. In some cases, however, the elegant simplicity of this approach means less sophistication, particularly when testing adaptive equalizers. First, the two-path model provides relatively simple fades — unlike actual fades which generally exhibit a more complex structure (multiple reflective paths). Second, although the two-port approach offers some dynamic control over the fade, most are limited to sinusoidal variation.

When highly sophisticated fades are necessary in conjunction with controlled degradations, the digital synthesis system described earlier provides a possible alternative. With this new approach, it is possible to simulate the dynamic effects of multipath fading, including "n" number of primary paths, in addition to arbitrary control of the fade's dynamics. Furthermore, no additional hardware is necessary to simultaneously add controlled impairments, such as AM-AM or AM-PM conversion, phase noise and cross-talk.

Understanding Multipath Fading

Before one can simulate multipath fade, it is useful to understand exactly what it is. Multipath fade is the net result of multiple transmission paths of varying length through a transmission medium as viewed by the receiver (Figure 8). For digital microwave radios, multipath fading results from two phenomena: refraction and reflection. To minimize the potential for multipath interference, the transmission signal path, usually between two antenna towers bounded by the beamwidth of the antennas, avoids reflectors (trees, buildings, ground). Furthermore, antenna beamwidths are as narrow as is practical. Regardless of the care taken in path selection, however, only reflective fades can be effectively eliminated. Refractive fades occur because of the variable nature of air as a transmission medium. Refractive distortion has been studied in considerable depth and can be modeled as the sum of several different transmission paths of variable lengths and attenuations.

Multipath fading is often described as "notches" in the complex frequency spectrum. These notches, resulting from the constructive and destructive addition of multiple delayed signals, clearly influence the integrity of the received data. Notch depth varies as the ratio of delayed to undelayed signals, while spacing between notches is the reciprocal of the time delay between signals. This is the well-known "comb" filter effect.

In practice, only single notches are observed over the transmission path and band. However, the fades may

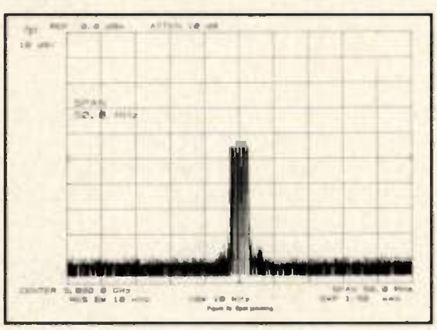

Figure 7a. Spot jamming.

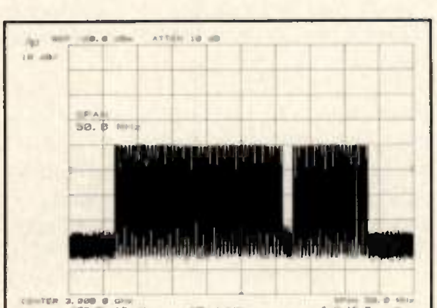

Figure 7b. Selective Jamming.

occur quickly and are constantly changing over time. This dynamic nature is what makes effective compensating equalizers so difficult to design, particularly when the transmitter or receiver is in motion. Since the fading phenomenon is so easily described in the frequency domain (where time delay is just a phase slope), programs can be written to model the effects of any number of fades. A complex inverse Fourier transform converts the result into time-domain I and Q signals, which are subsequently downloaded to the signal simulator.

Using the process outlined in (18), a dynamic multipath fade was simulated. The sequence of photographs of Figure 9 shows the frequency spectrum and constellation diagram from the HP 8981 Vector Modulation Analyzer. For this case, a two-path fade was simulated with varying degrees of notch depth while the position of the notch was varied across the channel band. The dramatic smearing of the data states illustrates how disruptive multipath fading can be.

Conclusion

Modern systems in radar/EW and communications increasingly rely on complex modulation. The demand for versatile test equipment capable of supplying a broad range of modulation and impairments is leading to new developments in digital-synthesis-based signal simulators. Combining two digital synthesizers in an I/Q modulation configuration results in a powerful, general purpose signal simulator suitable for advanced system design and test. Finally, a brief look at two common digital synthesis architectures, coupled with a treatment of technical consideration, help the newcomer to better understand the relative advantages and tradeoffs of this rapidly emerging technology.

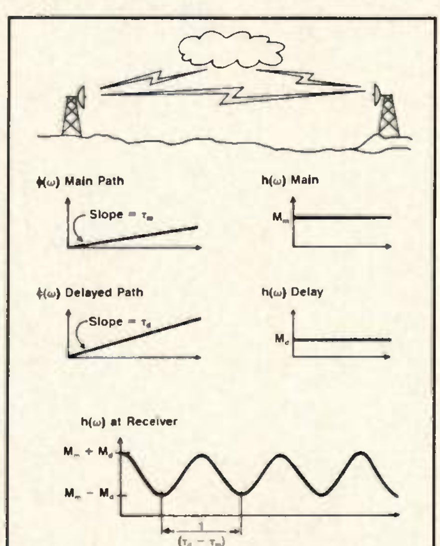

Figure 8. Multiple reflective paths.

The authors wish to thank David Chu, Eric Munro and Bryan Hovey of Hewlett-Packard for their contributions of software necessary to generate and display many of the waveforms presented.

References

1. S.J. Rabinowitz, E. Brookner, C.E. Muehe and C.M. Johnson, "Applications of Digital Technology to Radar," *IEEE Proceedings,* Vol. 73, No. 2, February 1985.
2. W.D. Gallaway, K.F. Luckscheiter, E.H. Cowen and J.W. Wilhelm, "A Direct Digitally Synthesized Exciter Achieving Near Theoretical Performance for an Operational SAR System," *IEEE 1988 National Radar Conference Proceedings*, pp. 22-26.
3. G. Lowitz and R. Armitano, "Predistortion Improves Digital Synthesizer Accuracy," *Electronic Design*, March 31, 1988.
4. J.F. Michaels, "Application of Electromagnetic Environment Simulation to Radar Performance Testing, Operability Assessment and Training," *IEEE National Radar Conference,* 1985, pp. 125-129.
5. "Simulation — The Requirement," *International Countermeasures Handbook*, June 1977, pp. 527-529.
6. J.A.H. Wall, "A Target Simulator for Frequency Agile Radars," *Proceedings of the 11th European Microwave Conference*, 1981, pp. 251-256.
7. R. Hassun, D. Kreitter and J. Minck, "Benchtop Signal Simulation Becomes a Reality," *Defense Electronics,* November 1987, pp. 129-143.
8. G. Lowitz, "Digital RF Synthesis: Theory and Application of a Booming Technology," *RF Expo '88 Proceedings,* Anaheim, CA, 1988, pp. 103-113.
9. G. Lowitz, "HP 8770S Signal Simulator System," *Hewlett-Packard lit.* 5954-8890, July 1987.
10. H. Eisenson, "Digital Techniques Hatch High-Speed Direct Synthesizer," *Microwaves and RF,* October 1987, pp. 165-170.
11. E.W. McCune, "Numbers Modulate Frequency and Phase of Digital Oscillator," *Microwaves & RF,* June 1987, pp. 201-203.

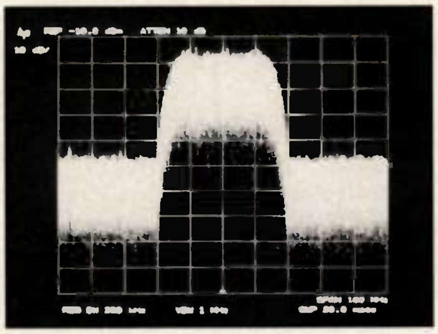

Figure 9a. Spectrum of unfaded simulated 16 QAM digital microwave radio signal.

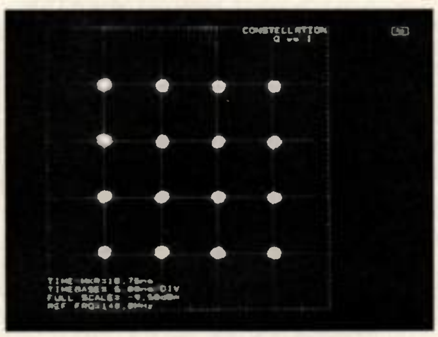

Figure 9b. Constellation of unfaded simulated signal.

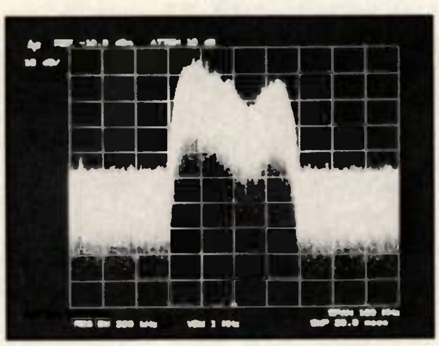

Figure 9c. Spectrum of simulated in-band notch (td-10ns) with 20 dB notch depth.

Figure 9d. Constellation of same in-band notch without equalization.

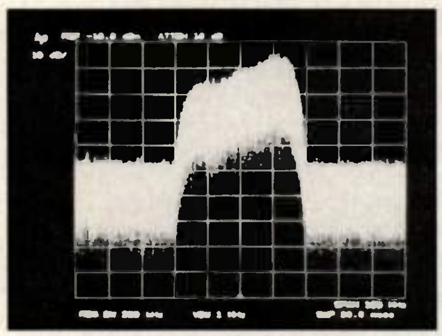

Figure 9e. Spectrum of simulated out-of-band notch (td-6.3ns) with 20 dB notch depth.

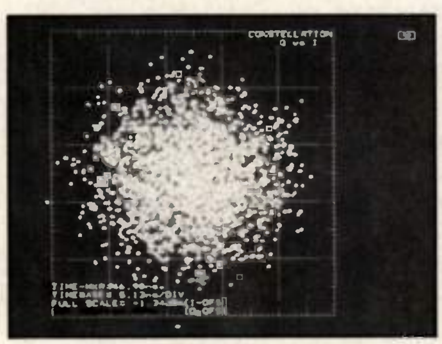

Figure 9f. Constellation of same out-of-band notch without equalization.

Two-tone intermodulation distortion	MTI cancellation
Gain/phase channel matching	Doppler estimation
Minimum detectable signal (MDS)	Probability of detection/false alarm
Dynamic range	Effects of non-ideal components (unintentional modulation)
Range accuracy	Influence of Doppler shift on detectability of phase-coded waveforms
Two-target resolving ability	Automatic gain control (AGC)
Range sidelobe levels	Sensitivity time control (STC)
Compressed pulsewidth (3, 4, 6 dB points)	Susceptibility to jamming and other countermeasures
Multiple-target tracking	Analog-to-digital converter (ADC) linearity
Synchronous-detector quadrature error and gain imbalance	Robustness of signal processing algorithms
Target recognition (radar cross section simulation)	
Subclutter visibility	

Table 1. Radar receiver/signal processor tests that benefit from signal simulation.

12. W. Sagun, F. Ives, G. Baldwin and T. Hornak, "A 125 MHz 12-Bit Digital-to-Analog Converter System," *Hewlett-Packard Journal*, April 1988.
13. R. Hassun and A. Kovalick, "An Arbitrary Waveform Synthesizer for DC to 125 MHz," *Hewlett-Packard Journal*, April 1988.
14. K. Hsieh, T. Knotts, G. Baldwin and T. Hornak, "A 12-bit 1-Gword/s GaAs Digital-to-Analog Converter System," *IEEE Journal of Solid-State Circuits*, Vol. sc-22, No. 6, December 1987.
15. D.B. Leeson and W.K. Saunders, "Test Equipment for Coherent Radar," *EASCON Proceedings*, 1974, pp. 221-228.
16. E.D. McHenry, "A Wideband FM Subsystem for a Low-Noise Synthesizer Module," *Hewlett-Packard Journal*, December 1987, pp. 45-58.
17. D.R. Gildea and D.R. Chambers, "Vector Modulation in a Signal Generator," *Hewlett-Packard Journal*, December 1987, pp. 25-29.
18. J. Grau, "A Calibrated Signal Simulation System Utilizing I/Q Modulation Techniques," *RF & Microwave Measurements Symposium*, Hewlett-Packard lit. 5951-6943, April 1988.
19. J.Grau, "Calibrated Microwave System for Complex Arbitrary Signal Simulation Using HP 8780A Vector Signal Generator and HP 8770A Arbitrary Wave-

form Synthesizers," *Hewlett-Packard Application Note* 343-5, July 1988.
20. M. Tuckman, "I-Q Vector Modulator -- The Ideal Control Component?" *MSN & CT*, May 1988, pp. 105-115.
21. A. Kovalick and R. Hassun, "Arbitrary Waveform Synthesizer Applications in Magnetic Recording and Radar," *Hewlett-Packard Journal*, April 1988.
22. Hewlett-Packard, "Analysis and Simulation Techniques for Modern Radar," Seminar Handouts, May 1988.
23. Hewlett-Packard, "Coherent Pulsed Tests of Radar and Communications Systems," HP Application Note 343-3.
24. D. Chu, "Phase Digitizing Sharpens Timing Measurements," *IEEE Spectrum*, July 1988, pp. 28-32.
25. P. Thysell, "Effective Use of the HP 8770S Signal Simulator System," Hewlett-Packard Product Note (PN 8770S-2), 1987.
26. K. Kafadar, "Digital Signal-Synthesis Tools Model Real-World Environments," *EDN*, November 12, 1987, pp. 239-248.
27. A.H. Naegeli and E.D. McHenry, "Simulation and Analysis of I/Q Vector Modulation for Testing of Modern Microwave Systems," *RF & Microwave Measurements Symposium*, April 1988, Hewlett-Packard lit. 5951-7095.
28. W. Sagun, "After the DAC: Optimum Processing of Analog Signals," Publication pending in Electronic Design (1988).
29. R. Hassun, A. Kovalick and W. Sagun, "The Theory of RF/Analog Waveform Synthesis by Digital Means," RF & Microwaves Symposium, April 1987.
30. D.D. Caviglia, A. DeGloria, G. Donzellini, G. Parodi and D. Ponta, "Design and Construction of an Arbitrary Waveform Generator," *IEEE Transactions on Instrumentation and Measurement*, Vol. IM-32, No. 3, September 1983, pp. 398-403.
31. R.J. Zavrel, Jr., "Digital Modulation Using the NCMO," *RF Design*, March 1988, pp. 27-32.
32. A. Kovalick and R. Hassun, "Digital Phase Domain Amplitude Modulation Method and Apparatus," U.S. Patent 4,331,941, May 25, 1982.
33. R. Hassun and A. Kovalick, "Waveform Synthesis Using Multiplexed Parallel Synthesizers," U.S. Patent 4,454,486, June 12, 1984.
34. B.H. Hutchinson, "Contemporary Frequency Synthesis Techniques," *Frequency Synthesis and Applications*, IEEE Press, New York, 1975.
35. D. Sunderland, R.A. Strauch, S.S. Wharfield, H.T. Peterson and C.R. Cole, "CMOS/SOS Frequency Synthesizer LSI Circuit for Spread Spectrum Communications," *IEEE Journal of Solid State Circuits SC-19*, No.4, 1984.
36. A. Kovalick, "Apparatus and Method of Phase-to-Amplitude Conversion in a Sine Function Generator," U.S. Patent 4,482,974, November 13, 1984.

About the Authors

Greg Lowitz and Chris Pedersen can be reached at Hewlett-Packard Co., 1501 Page Mill Road, Palo Alto, CA 94304; Tel: (415) 857-2096.

System Noise Analysis Using Spreadsheets

By John H. Bordelon and
Dr. David R. Hertling
Georgia Institute of Technology

Computer spreadsheets are increasingly being recognized as useful tools for the RF engineer, and not just for preparing budget estimates. Spreadsheets have been found useful for radar system parameterization, pulse transformer design, switch mode power supply design, and other applications. This article describes the use of computer spreadsheets for noise analysis of a system of cascaded two-ports. System noise temperatures, gain/temperature ratios, and other data are calculated from the gain and noise figure or noise temperature data of the individual system blocks. A review of system noise concepts and equations is presented, followed by an actual application for which a particular spreadsheet construction was recently found useful.

The work presented here was done on an Apple Macintosh Plus, using Microsoft Excel. However, any computer system and spreadsheet program which has log functions can be used. It is not expected that the spreadsheet application presented here will be sufficiently powerful or general to satisfy every potential user. A significant advantage of a spreadsheet for such calculations is that it can be easily modified or expanded to satisfy the needs of different users.

Before describing the spreadsheet and how it is applied to two-port systems, a brief tutorial on noise characterization of two-port networks is given. This tutorial will serve to inform the reader who needs a refresher in two-port noise theory, and to establish a common base of terminology with those familiar with the subject.

Noise Characterization of Two-Ports

Consider the block diagram of Figure 1 for a noisy two-port. S_i, S_o, N_i, and N_o are available signal and noise input and output powers respectively, G is the available gain, and B is the noise bandwidth in hertz.

If the gain of the two-port is known,

$$S_o = GS_i \tag{1}$$

But,

$$N_o \neq GN_i$$

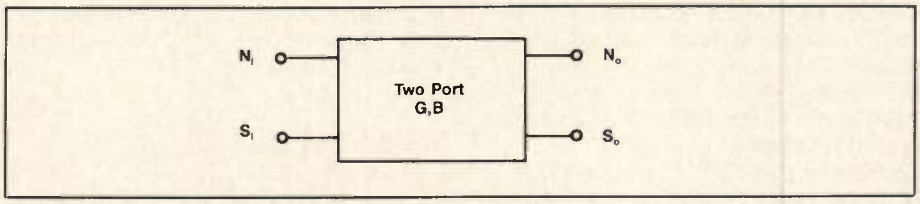

Figure 1. Block diagram for a noisy two-port.

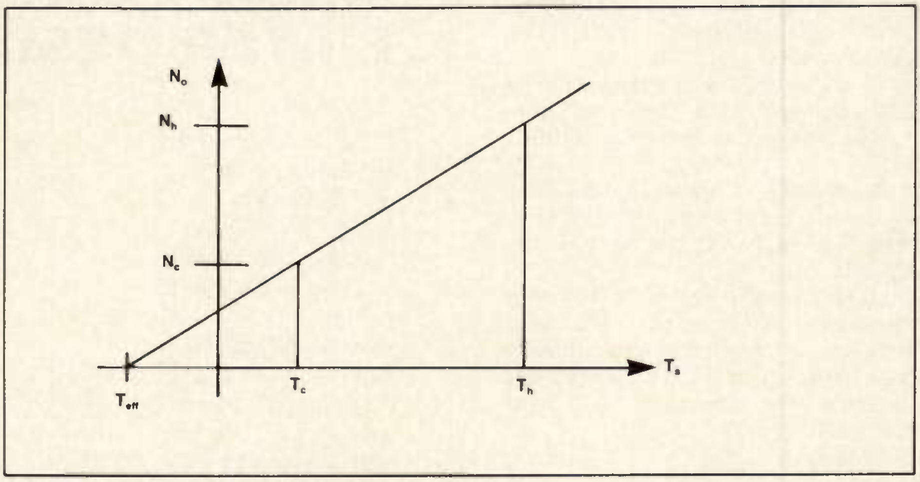

Figure 2. N_o vs. T_s for a noisy two-port.

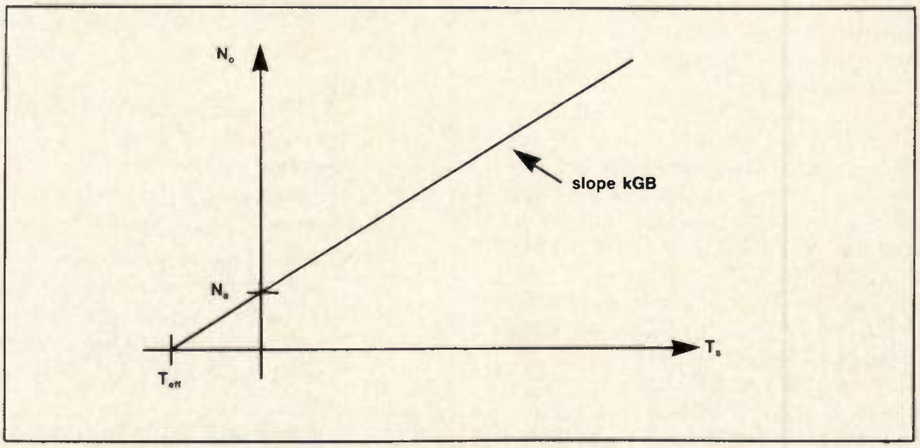

Figure 3. Hot and cold source determination of T_{eff}.

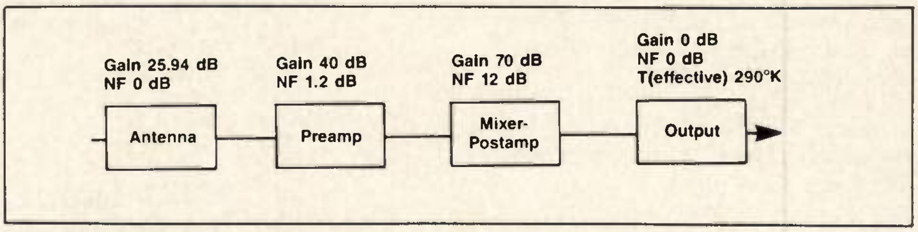

Figure 4. Example S-band telemetry system.

This is because the output noise is due to both the input noise and the internal noise of the two-port. The concept of noise figure allows the user to quantitatively compare the noise performance of two-port networks. Noise figure is defined as follows:

$$F = \frac{S_i/N_i}{S_o/N_o} \tag{2}$$

Noise figure can also be expressed in decibels.

$$F = 10 \log_{10}(F) \text{ (dB)} \tag{3}$$

Note that the term noise factor is sometimes used to designate the dimensionless quantity, with noise figure being used to designate this quantity expressed in dB.

Most engineers and textbooks, however, use the term noise figure universally. In this article only the term noise figure is used. If the quantity is in dB, it is labeled explicitly.

The available input noise figure is supplied by a matched termination at the input of the two-port. A matched resistive termination at room temperature has an available noise power,

$$P_{av} = kT_oB \tag{4}$$

where k is Boltzmann's constant, T_o is 290 degrees Kelvin, and B is the bandwidth in hertz. The noise figure can then be expressed as:

$$F = \frac{N_o}{GkT_oB} \tag{5}$$

Note that if the available noise output power can be measured, then the noise figure can be calculated directly from (5). The available output noise power, N_o, can be measured directly. However, a single accurate measurement at such a low power level is difficult to make.

The next question which might arise is how does one physically interpret the noise figure? If the input to the two-port has a matched termination at room temperature, the noise figure simply expresses the degradation of the signal-to-noise ratio. Two-ports, however, are not always operated with a matched termination at their input port. Assume the noise figure of a two-port is known and consider the following:

$$N_o = FGkT_oB \tag{6}$$

$$N_o = G[kT_oB + (F\text{-}1)kT_oB] \tag{7}$$

By doing a few algebraic manipulations, output noise has been expressed in a form convenient for physical interpretation. The first term in the square brackets is simply the available noise at the input provided by the matched termination. The second term can be interpreted as the internal noise of the two-port "referred to its input." In any two-port consisting of many components, the total noise of the two-port is distributed throughout its circuitry. Noise generated by a component nearer its input port contributes to the total output noise differently than an identical component nearer its output port. This is because the noise powers generated by these two noise sources need to be multiplied by different gains to calculate their respective contributions to the output noise. By referring all noise sources to the input, the designer can see the total effect of internal noise sources on the signal-to-noise ratio. The total noise of the two-port could equally as well be referred to the output; however, this is usually not done. After the noise has been referred to the input, the two-port can now be considered noiseless with the same gain, G.

A noiseless two-port network has the same signal-to-noise ratio at the input and output, and thus a noise figure equal to unity. By separating the internal noise of the two-port from the input noise, the designer can consider the effects of other noise sources, such as the one which will actually be used in the system being designed or analyzed. The matched termination at the input port is merely used to facilitate measuring the noise figure. If the temperature of the noise source is greater than 290 degrees K, then the signal-to-noise ratio of the two-port is degraded by a factor less than the noise figure. If the temperature of the noise source is less than 290 degrees K then the signal-to-noise ratio of the two-port is degraded by a factor greater than the noise figure. For consistency, unless stated otherwise, published noise figure data measurements are always defined with a matched termination at room temperature (290 degrees K) at the input of the two-port. The IEEE standard definition of noise figure specifies a source temperature of 290 degrees K.

Effective Noise Temperature

Another way of expressing the noise performance of a two-port is by specifying its effective noise temperature. This is a fictitious temperature which is nothing more than a different way of expressing the noise figure of a two-port. A two-port has a certain internal noise. In the pre-

Stage N		1	2	3	
Two-port data:	Gain (dB)	25.94	40	70	0
	NF (dB)	0	1.2	12	0
	NF	1	1.31826	15.84893	1
	T(effective)	0	92.2945	4306.19	290
Two-port name:		Antenna	PAM	Mixer-AIL	Output

Gain(cum., dB)		25.94	65.94	135.94
T(input)	40	40	1322945	1.33E+13
T(eff., sys.)		92.72507	4306.19	290
T(sys.)	40	132.7251	1327251	1.33E+13
T(sys., dB)	16.0205999	21.22953	61.22953	131.2295
G/T(dB/K)	-16.0206	4.71047	4.71047	4.71047
T(hot)	141.62	141.62	2339145	2.34E+13
T(cold)	40	40	1322945	1.33E+13
Y(dB)	5.49064599	5.490646	2.475154	2.469029
Signal (dBm)	-138	-112.06	-72.06	-2.06
Noise BW(kHz)	3000	3000	3000	3000
S/N(dB)	-20.190603	5.749397	0.55458	0.540467

Figure 5. S-band telemetry system, expected results.

ceding section the reader could refer all the internal noise of a two-port to its input port and then consider it to be noiseless. Alternatively a resistor (whose temperature is the effective noise temperature of the two-port) could be placed at the input of a noiseless two-port with the same gain. Note that this system would have the same available noise output power as the original noisy two-port and would therefore be equivalent in noise performance. The principal advantage of equivalent noise temperature is that noise calculations are typically easier. In order to find the relationship between effective noise temperature and noise figure, equate the available noise power of a resistor at T_{eff} to the internal noise of a two-port referred to its input.

$$kT_{eff}B = (F\text{-}1)kT_oB \tag{8}$$

$$T_{eff} = T_o(F\text{-}1) \tag{9}$$

$$F = 1 + \frac{T_{eff}}{T_o} \tag{10}$$

Note that T_{eff} is not a physical temperature. It is not unusual to have effective noise temperatures which are thousands of degrees Kelvin.

Cascaded Two-Port Systems

Most systems are composed of cascaded two-ports. In order to calculate overall noise figure of a system, the noise figure of a cascade of two-ports has to be calculated. The formula for the overall figure of cascaded two-ports is:

$$F_{ov} = F_1 + \frac{F_2 - 1}{G_1} + \frac{F_3 - 1}{G_1G_2} + \cdots + \frac{F_n - 1}{G_1G_2 \cdots G_n} \tag{11}$$

$F_1, \cdots, F_N$ are the noise figures; and $G_1, \cdots, G_n$ are the available gains of the n stages.

In terms of effective temperatures the formula is:

$$T_{eff} = T_1 + \frac{T_2}{G_1} + \frac{T_3}{G_1G_2} + \cdots + \frac{T_n}{G_1G_2 \cdots G_{n-1}} \tag{12}$$

$T_1, \cdots, T_n$ are the effective temperatures of the n stages.

From examination of these formulas it is apparent that the noise performance of the system is dominated by the stages near the input if their gain is high.

Stage N		1	2	3	
Two-port data:	Gain (dB)	25.94	40	70	0
	NF (dB)	0	1.2	12	0
	NF	1	1.31826	15.84893	1
	T(effective)	0	92.2945	4306.19	290
Two-port name:		Antenna	PAM	Mixer-AIL	Output
Gain(cum., dB)			25.94	65.94	135.94
T(input)		61	61	1532945	1.54E+13
T(eff., sys.)			92.72507	4306.19	290
T(sys.)		61	153.7251	1537251	1.54E+13
T(sys., dB)		17.8532984	21.86745	61.86745	131.8674
G/T(dB/K)		-17.853298	4.072553	4.072553	4.072553
T(hot)		162.62	162.62	2549145	2.55E+13
T(cold)		61	61	1532945	1.54E+13
Y(dB)		4.25844122	4.258441	2.20868	2.203828
Signal (dBm)		-138	-112.06	-72.06	-2.06
Noise BW(kHz)		3000	3000	3000	3000
S/N(dB)		-22.023302	3.916698	-0.08527	-0.09745

Figure 6. S-band telemetry system, corrected results.

Measurement of Noise Figure

As previously mentioned, total available noise output power of a two-port is usually a very small quantity. It is very difficult to make a single accurate measurement of such a quantity. A very common method of measuring noise figure can be understood by considering Figure 2 which is a plot of the available noise output power, N_o, versus the source temperature, T_s.

Note that the power output versus source temperature is a straight line with a slope of kGB which intersects the vertical axis at a point greater than zero. This point is often called N_a for "added noise." The effective temperature can be found from this straight line by extrapolating past the vertical-axis intercept until the line intersects the horizontal axis. This point is the effective noise temperature of the two-port. This straight line therefore is a complete representation of the noise performance of the two-port. Since two points determine a straight line, the line can be drawn by finding two points. This is done by driving the input of the two-port with a noise source which has two well-known noise temperatures and measuring the available noise output powers, N_c and N_h, for respective "cold" and "hot" temperatures, T_c and T_h. This procedure is illustrated in Figure 3. The cold noise temperature is often the physical temperature of the noise source. The hot temperature can be, for example, the effective temperature of a diode in avalanche breakdown. Any two temperatures for which the output noise of the source is accurately known can be used. This method results in calculated noise figure which depends upon the ratio of measured quantities and not their absolute values.

Once these two points have been found, the straight line can be drawn and the noise figure and effective temperature can be found graphically or algebraically. Modern noise figure meters use microprocessors to do these calculations automatically and to display the noise figure digitally.

Often the ratio of N_h to N_c is called the Y factor. The noise figure can be expressed in terms of the Y factor as follows:

$$kGB = \frac{N_h - N_c}{T_h - T_c} \qquad (13)$$

$$T_{eff} = \frac{T_h - YT_c}{Y - 1} \qquad (14)$$

$$F = 1 + \frac{T_{eff}}{T_o} \qquad (15)$$

	1	2	3		4	5	6	7
1		Appendix - Spreadsheet Formulas		1				
2	Stage N		1	2		2		3
3	Two-port data:	Gain (dB)		3				
4		NF (dB)		4				
5		NF	=10^(R[-1]C/10)	5	REPEATS>>>>>>>			
6		T(effective)	=290*(R[-1]C-1)	6	REPEATS>>>>>>>			
7				7				
8	Two-port name:		Antenna	8		Two-Port #1		Two-Port #2
9				9				
10	Gain(cum., dB)			10	=R[-7]C[-1]		=RC[-2]+R[-7]C[-1]	REPEATS>>>
11	T(input)	40		11	=RC[-2]		=(RC[-2]+R[-5]C[-1])*10^(R[-8]C[-1]/10)	REPEATS>>>
12	T(eff., sys.)			12	=R[-6]C[1]+RC[2]/(10^(R[-9]C[1]/10))	REPEATS>>>		
13	T(sys.)	40		13	=R[-1]C+R[-2]C	REPEATS>>>		
14	T(sys., dB)	=10*LOG10(R[-1]C)	REPEATS>>>>>>>	14				
15	G/T(dB/K)	=R[-5]C-R[-1]C	REPEATS>>>>>>>	15				
16	T(hot)	141.62		16	=RC[-2]		=(RC[-2]+R[-10]C[-1])*10^(R[-13]C[-1]/10)	REPEATS>>>
17	T(cold)	40		17	=RC[-2]		=(RC[-2]+R[-11]C[-1])*10^(R[-14]C[-1]/10)	REPEATS>>>
18	Y(dB)	=10*LOG10(R[-2]C/R[-1]C)	REPEATS>>>>>>>	18				
19	Signal (dBm)	-138		19	=RC[-2]+R[-16]C[-1]	REPEATS>>>		
20	Noise BW(kHz)	3000		20	3000		3000	
21	S/N(dB)	=R[-2]C-10*LOG10(1.38E-23*R[-10]C*R[-1]C*1000)-30	REPEATS>>>>>>>	21				

Appendix 1. Spreadsheet formulas.

The G/T Figure of Merit

Many receiving system designers use the G/T figure of merit. The signal power at the terminals of a receiving antenna can be expressed as:

$$P_R = P_T G_T G_R (\lambda/4\pi R)^2 \tag{16}$$

P_R is the received power in watts; P_T is the power the transmitter delivers to the transmitting antenna; G_T and G_R are the transmitting and receiving antenna gains, respectively; λ is the wavelength; and R is the distance between the transmitting and receiving antennas.

The noise power applied to the input of the receiver by the antenna is:

$$P_N = kT_{ant}B \tag{17}$$

where T_{ant} is the antenna effective temperature.

The signal-to-noise ratio at the input of the receiver can then be expressed as:

$$\frac{S}{N} = \frac{P_R}{P_N} =$$

$$\left(\frac{G_R}{T_{ant}}\right)\left(\frac{P_T G_T}{kB}\right)\left(\frac{\lambda}{4\pi R}\right)^2 \tag{18}$$

Typically the receiving system designer only has control over the G_R and T_{ant}. The ratio of these two quantities is the familiar G/T ratio which the designer tries to maximize. It is also useful to note that in a system of cascaded two-port networks, the G/T ratio remains constant throughout the system.

Description of the Spreadsheet

RF engineers who work mostly with very low noise systems usually prefer the noise temperature concept. Noise figure is usually preferred by those working with the systems in the HF and VHF range. There is no fundamental difficulty with using either approach for an application; however, calculations are generally made easier by using noise temperatures. The spreadsheet described here uses the noise temperature concept, although noise figures may be entered for the two-port devices making up the system. One problem that someone accustomed to noise figure may encounter is simply the difficulty of relating to values of noise temperature.

The spreadsheet is laid out so that the names of the various two-ports and their parameters are alternated with the calculated interstage data. As a further aid to clarity, the Border option under the Format menu in Excel is used to create the block diagram of the system on the spreadsheet. The program requires that the user enter gain and noise figure values. For purely passive devices, the noise figure in dB is simply the loss of the stage in dB. The spreadsheet then calculates the noise figure (in dimensionless units) and the equivalent input noise temperature. For this calculation a T_0 of 290 degrees K is assumed. Other data that must be entered by the user are T(input), T(hot), T(cold), Signal (dBm), and Noise BW (kHz).

The notation used in the spreadsheet for the various temperatures is somewhat different from that used in the preceding tutorial. Table 1 defines the temperatures as named in the spreadsheet. The spreadsheet begins by calculating noise figure as a dimensionless quantity and equivalent input noise temperature for each two-port as described above. Next, cumulative gain and T(input) are calculated. T(input) is the apparent temperature seen at the input of any given stage and is a function of T(input), T(effective), and gain of the preceding stage. T(input) is given by:

$$\underbrace{T(\text{input})}_{\text{Nth stage}} = \underbrace{(T(\text{input}) + T(\text{eff}))G}_{(N-1)\text{th stage}} \qquad (19)$$

where G is dimensionless.

The spreadsheet next calculates T(eff,sys). This calculation proceeds from the far right of the spreadsheet to the left. T(eff,sys) is the effective input noise temperature of the cascade of two-ports to the right of the point being specified. To begin calculating T(eff,sys) at the input to each stage, assume a temperature for the output load terminating the cascade of two-ports. This is ordinarily assumed to be 290 degrees K. It has little effect upon T(eff,sys) at the input to the system. Starting at the input to the last stage, T(eff,sys) at the input to the last stage is calculated as the T(eff) of that stage plus the quantity T(eff,sys) at the output divided by the gain.

$$\underbrace{T(\text{eff,sys})}_{\substack{\text{Nth}\\ \text{stage}}} = \underbrace{T(\text{eff})}_{\substack{\text{Nth}\\ \text{stage}}} + \underbrace{T(\text{eff,sys})}_{\substack{(N-1)\text{th}\\ \text{stage}}}/\underbrace{G}_{\substack{\text{Nth}\\ \text{stage}}} \qquad (20)$$

Next, the spreadsheet calculates T(sys) for each point in the cascade of two-ports. This is simply the sum of T(input) and T(eff,sys) at each point in the system.

The next calculation is the value in dB, referenced to 1 degree K, of T(sys). This is followed by the value of G/T(dB/K) which is the difference in gain(cum.,dB) and T(sys,dB). It is important to notice, as was explained in an earlier section, that the value G/T remains constant throughout the system.

The rest of the values calculated by the spreadsheet are ones the authors found useful. The values of T(hot), T(cold), and Y(dB) can be used to show how the noise level at any point in the system varies for two different input temperatures. The different temperatures can be those of hot-cold noise source or, in the example described in the next section, the sun used as a noise source. As would be expected, the relative levels of noise, as expressed by Y(dB), show a decreasing ratio between the two noise levels as the observer moves from the input to the output of the cascade of two-ports. In this respect, this spreadsheet is a useful teaching tool. The calculations used for these two temperatures are exactly the same as those used to calculate T(input). The remaining three rows of data allow the user to calculate signal-to-noise ratio through the system for any arbitrarily selected signal level and any bandwidth at any point in the system.

An Example Application

The application driving the design of this spreadsheet was gain/temperature (G/T) measurements of an S-band telemetry system. Figure 4 is a block diagram of this system.

It should be noted in passing that the noise figure of the antenna is quoted as 0 dB, since the antenna has no loss and no active elements. The so-called antenna temperature is considered an attribute of the antenna's environment. The question was whether the sun could be used as a noise source to measure G/T with the equipment available, and what Y factor would be expected. Obviously, if the Y factor was too small or large, a reasonable measurement was impossible. Figure 5 shows the resulting spreadsheet giving the expected results. The cold sky temperature was assumed to be 40 degrees K. The parameters of the various two-ports were known, and a telephone call to the National Bureau of Standards gave the solar flux for the time period during which the measurements were made. From this equivalent T(hot) was computed at the frequency of interest. It is worthwhile to digress for a moment and fill in the details of this computation.

Solar flux is measured daily at a number of discrete frequencies by the NBS. In this case, the flux at 2685 MHz was used, being closest to the frequency of interest. Between 1500 and 3000 MHz, the quoted value may be corrected for the frequency of interest by the empirical relation:

$$\phi = \phi_o(f_t/f_o)^{1/2} \qquad (21)$$

ϕ is the corrected value for the frequency of interest; ϕ_o is the value quoted by NBS; f_t is the frequency of interest; f_o is the NBS measurement frequency; and one solar flux unit is equal to 10^{-22} watt/m^{2}Hz.

The solar flux was quoted as 57, and the correction equation yielded a value of 52.76 at the frequency of interest, 2300 MHz. T_{hot} was then computed from:

$$T_{hot} = \frac{\phi\lambda^2 G}{8\pi kL} + T_{cold} \qquad (22)$$

λ is the wavelength; G is the antenna gain in dimensionless units; k is Boltzmann's constant; L is a correction factor for the angular extent of the sun relative to the antenna beamwidth; and T_{cold} is the assumed value for the "cold" sky.

The correction factor L compensates for the angular extent of the sun disk, 0.5 degrees, relative to the azimuth and elevation beamwidths of the antenna under test. It is given by:

$$L = 1 + 0.38(\theta_d/\theta_{AZ}\theta_{EL})^2 \qquad (23)$$

θ_d is the angular extent of the solar disk in degrees; and θ_{AZ} and θ_{EL} are the azimuth and elevation 3 dB bandwidths of the antenna in degrees.

The value of T_{hot} was calculated to be 141.62 degrees K. This value is very dependent on antenna gain, so antenna gain should be accurately known beforehand.

As can be seen, the spreadsheet predicted a Y factor that was very reasonable, 2.47 dB. On making the measurement, however, a 2.2 dB Y factor was observed, yielding a G/T of 4.06 dB, instead of the expected value of 4.71 dB. The value of G/T was computed from the Y factor using the equation:

$$\frac{G}{T} = \frac{8\pi kL\,(Y-1)}{\phi\lambda^2} \qquad (24)$$

where the factors in the equation are the same as those defined above, with the exception that the Y factor should be a dimensionless quantity.

The G/T ratio of a system is a function of the antenna temperature. This is not the physical temperature of the antenna itself, but the apparent temperature of the sky toward which the antenna is pointed. In truth, this temperature is the result of an integration over the entire antenna pattern, and so may include not only "cold" sky in the antenna main lobe but also various hotter backgrounds in sidelobes. There was reason to suspect that T(cold) was higher than the 40 degrees K postulated. The measurement was performed on a hot asphalt parking lot, with many surrounding objects, including a brick building, that were also quite warm. All of these objects would, of course, be visible to the sidelobes of the antenna, and would raise the apparent sky temperature above that of the cold sky itself. As shown in Figure 6, the value of T(cold) was adjusted on the spreadsheet until the observed results were duplicated and, indeed, the value of T(cold) thus calculated was a quite reasonable 61 degrees K. It should be noted that T(hot) is also a function of T(cold), so the value of T(hot) in the revised spreadsheet shows an increase. The spreadsheet program in this case provided confidence in the measurements.

Another application for such a program is to help the designer determine design tradeoffs quickly. A particular component gain may increase system dynamic range without seriously compromising T(sys). A good engineering balance between sensitivity and dynamic range usually involves careful gain distribution throughout a receiver, rather than the sledgehammer expedient of fixing the noise figure with a high-gain low-noise preamp at the front end. The spreadsheet is a very useful tool for determining the optimum configuration.

Conclusions

An interesting application of a computer spreadsheet has been presented. Spreadsheets are powerful tools which can be applied to a variety of engineering problems. This particular spreadsheet is very useful for designing or analyzing the noise performance of a system of cascaded two-ports. An application example with actual data using the spreadsheet was also given. Implementation of this spreadsheet on any computer with a spreadsheet capable of log functions should be straightforward.

The authors wish to thank Dr. E.B. Joy of the Georgia Tech School of Electrical Engineering and Dr. Lee Edwards of the Georgia Tech Research Institute for their helpful suggestions, comments, and careful proofreading of this manuscript. rf

References

1. Fundamentals of RF and Microwave Noise Figure Measurements, Hewlett-Packard Application Note 57-1.

About the Authors

John E. Bordelon is senior research engineer at the Electronic Support Measures Division of Georgia Tech Research Institute. He can be reached at (404) 894-7137. Dr. David R. Hertling is associate professor at the school of electrical engineering, Georgia Institute of Technology, Atlanta, GA 30332. Tel: (404) 894-2932.

The following temperatures are defined at the input of their respective stages as shown on the spreadsheet.

T(input)	the effective temperature of the input noise to the stage.
T(eff)	the effective temperature of the stage only.
T(eff,sys)	the effective temperature of the stage and the successive cascaded stages.
T(sys)	for a given stage, equals T(eff,sys) + T(input).
T(hot)	the effective temperature of the input noise to the stage with a noise source at its hot temperature at the input to the system.
T(cold)	the effective temperature of the input noise to the stage with a noise source at its cold temperature at the input to the system.

Table 1. Temperature definitions.

Model 3115 Double Ridge Guide
1–18 GHz
Model 3116 Double Ridge Guide
18–40 GHz

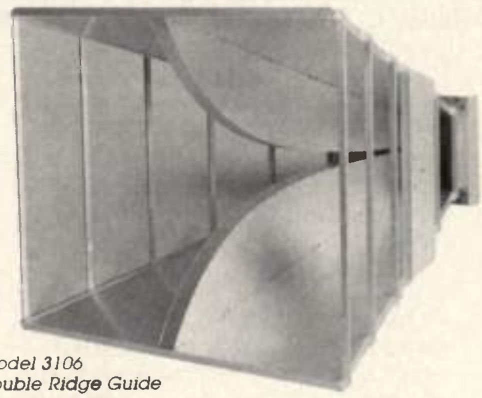

Model 3106
Double Ridge Guide
200 MHz–2 GHz

Model TR3 Non-Metallic Tripod
22.68 kg capacity

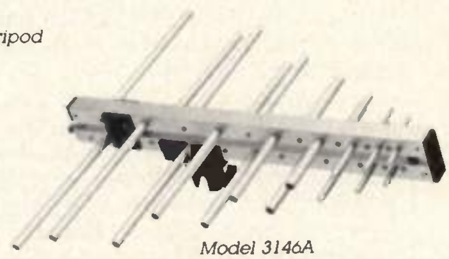

Model 3146A
Log Periodic
300 MHz–1 GHz
four other models available

Model 1060 Turntable
with controller and IEEE-488 bus option
1–7.6 meter diameter available

Model 6502
Active Loop Antenna
10 kHz–30 MHz

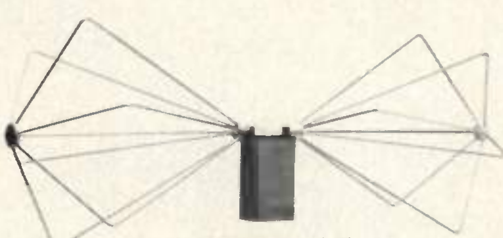

Model 3109 Biconical
20–200 MHz
three other models available

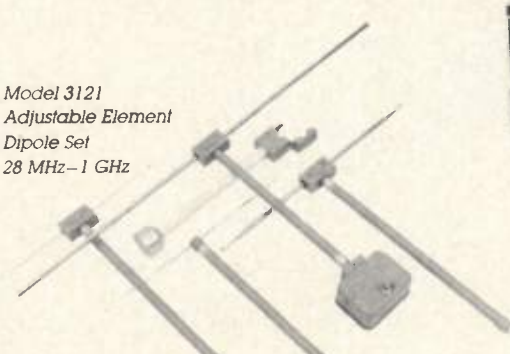

Model 3121
Adjustable Element
Dipole Set
28 MHz–1 GHz

Model 3925 PLISN
2 kHz–1 GHz
five other models available

TEST WITH CONFIDENCE.

ENGINEERED TO PERFORM

If compliance testing is your primary responsibility, you need top-of-the-line products you can count on. Like EMCO antennas, designed for repeatable FCC/VDE testing. Manufactured for the stringent requirements of MIL-STD testing. With high sensitivity for TEMPEST testing. Most have VSWR ratios of less than 2:1. And all exhibit exceptional dynamic range and linearity.

CALIBRATED INDIVIDUALLY

Every EMCO antenna is individually calibrated using both C63.4 and ARP 958 standards, then shipped to you with a signed Certificate of Compliance—a claim no other manufacturer of test antennas can make.

MANUFACTURED WITH CARE

We choose only the best and most durable materials for EMCO products. Then we pay close attention to details—machined tolerances are often less than one one-thousandth of an inch. And while we've automated for efficiency, we still take the time to hand-assemble and inspect each one of our products.

TWO-YEAR WARRANTY, SERVICE WORLD-WIDE

Because we know how well every EMCO product is engineered and built, we can back each one with a two-year warranty—twice the industry standard. And EMCO has more than 30 representatives worldwide to help you—wherever you are. Call our 800 number for more information and the name of your EMCO representative. Ask for your free catalog of EMCO products, too!

FIRST IN QUALITY
FIRST IN PERFORMANCE.
1-800-253-3761

EMCO
The Electro-Mechanics Company

Call toll-free between 7:30 A.M. and 4:30 P.M. (CST)
In Texas, call 512-835-4684 International Telex 797627
P.O. Box 1546, Austin, Texas 78767

INFO/CARD 64

Electrostatic Discharge as an EMI Issue

By Daryl Gerke
Kimmel Gerke and Associates, Inc.

This article addresses electrostatic discharge (ESD) as an electromagnetic interference (EMI) problem. Most ESD programs are aimed at preventing ESD and subsequent damage to components during manufacturing. Discussed is the need to address ESD occurrences and their effect on systems and equipment during the design phase. In order to explore ESD as an EMI problem, this article follows the general EMI model of source, coupling path, and victim.

The damaging effects of electrostatic discharge (ESD) upon electronic components and printed circuit boards are a major concern in manufacturing. An entire industry has been developed to serve those needs, whose primary strategy is the prevention of static buildup and the resulting discharge.

For equipment in the field, however, this strategy of prevention is not enough. Sooner or later, a discharge will occur. At that time, ESD becomes an EMI (electromagnetic interference) problem. Any equipment designer responsible for EMI control must also consider the effects of an ESD event upon his or her design.

These ESD problems have become increasingly acute in recent years, as electronic devices have decreased in size and increased in speed. The result is damage or upset at lower energy levels than in the past.

The problems are particularly vexing with systems incorporating microprocessors and other digital logic. As the speed of digital systems has increased, the bandwidths have increased to beyond the ESD bandwidth, thus fully opening the "window of susceptibility" to ESD upset.

ESD as an EMI Source

Figure 1 shows a representative ESD waveform, from a typical human ESD event. Peak human ESD voltages can reach 20,000 to 30,000 volts, and peak currents can easily reach 5 to 10 amps. ESD rise times are typically in the 1 to 3 nanosecond range.

In the manufacturing arena, the key ESD parameters of concern are the peak voltage and the energy in the ESD event. This is because the failure modes are usually either voltage breakdown or overheating due to too much energy.

In the EMI area the key parameters of

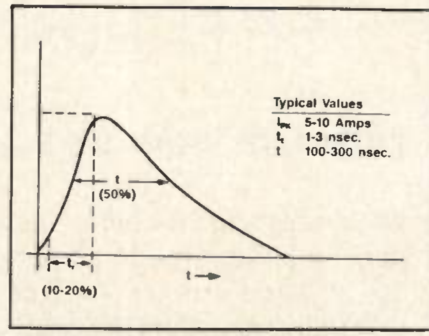

Figure 1. Typical ESD current waveform.

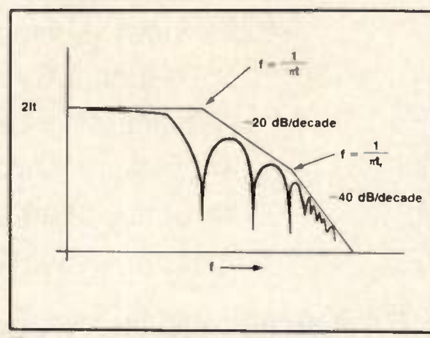

Figure 2. Typical ESD frequency spectra.

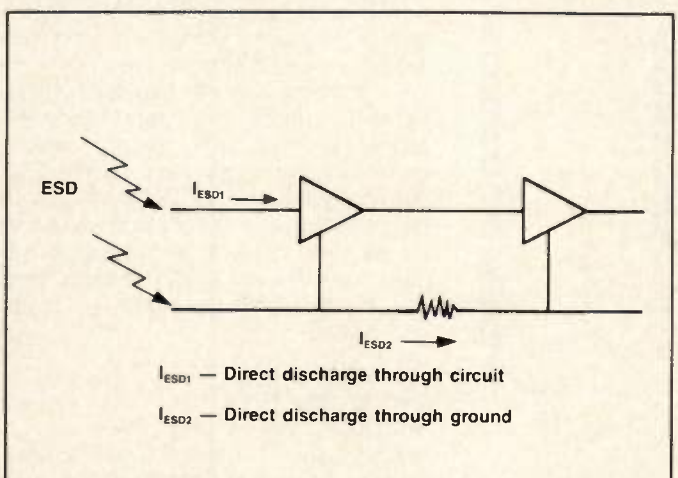

Figure 3. Direct discharge ESD currents.

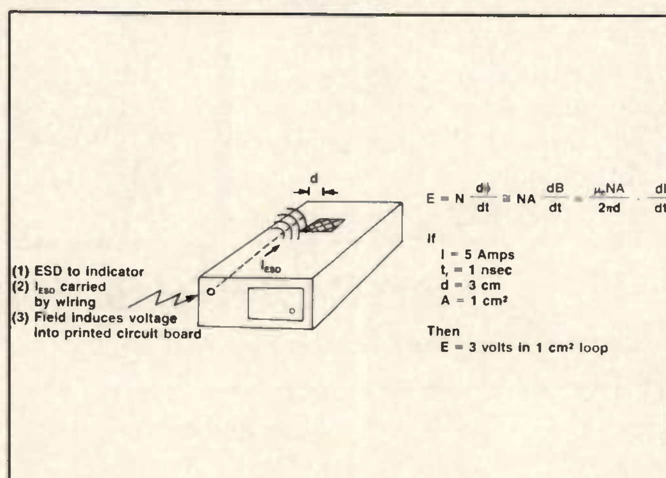

Figure 4. Indirect discharge ESD.

concern are usually peak currents and rise time. This is because the failure modes (and the solutions) are frequency and impedance related.

ESD is a relatively fast transient, with rise times in the 1 to 3 nanosecond range. In the frequency domain, this means significant energy is present well into the VHF range, as shown in Figure 2. Using the Fourier transform and a "bandwidth" definition of $1/(\pi \times \text{rise time})$, a 1 nanosecond rise time translates to over 300 MHz. This means that 300 MHz design rules must be applied for ESD shielding, grounding, and filtering.

In an effort to standardize ESD testing, several models have been developed. The most popular is the "human body model," which attempts to characterize the discharge from a human being. Several variations exist, but essentially humans look like 100 to 300 pF of capacitance discharging through 1 to 3 kohms of resistance.

Additional work is still being done in this area. One of the more interesting recent revelations is a "precursor," or a fast discharge followed by a slower discharge. This is believed to be due to a discharge from the hand and arm, followed by a discharge from the entire body. This phenomena is dependent upon the rate at which the body approaches the equipment, and is one of the problems with repeatability in ESD testing.

The standards for ESD sources continue to evolve as new research is done in this area. In addition to the human body model, additional models for furniture and other sources are under investigation.

ESD Coupling Paths

There are several ESD coupling paths into a system. There is the direct discharge through a device, which often results in damage, plus the direct discharge through the circuit grounding system, which often results in upset due to "ground bounce." Finally, there is indirect discharge, or the coupling of ESD energy via an electromagnetic field.

Direct Discharge

Much has been written about direct discharge through circuits and the resulting damage. This is the primary concern during manufacturing, when devices are exposed and extremely vulnerable. Incidentally, devices are no less susceptible to damage just because they are mounted on a circuit board, so manufacturing precautions (static pads, wrist straps) are necessary during servicing and repair. Also, the system must be designed so that no ESD currents flow into vulnerable circuits during normal system operation.

A second direct discharge path is common impedance coupling in the system ground, as shown in Figure 3. This path is a bit more subtle, and is often overlooked. A common example is to terminate input/output decoupling capacitors to the power return plane in a circuit board, rather than the chassis. In this case, ESD currents are forced to flow in the circuit return paths, often upsetting them. A better solution here is to terminate the I/O capacitors directly to the chassis, thus steering the currents away from the power return path.

Indirect Discharge

It is this latter case, the indirect discharge, that is often the cause of mysterious ESD failures. Maxwell's equations say that any time-varying current (continuous or transient) creates a corresponding electromagnetic field. Due to

A Dynamic Range of 120dB puts High and Low Level Signals on Screen Simultaneously

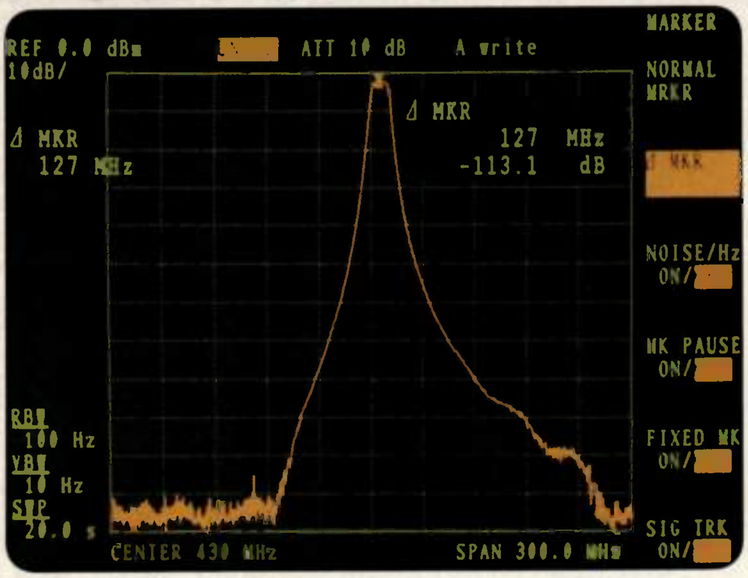

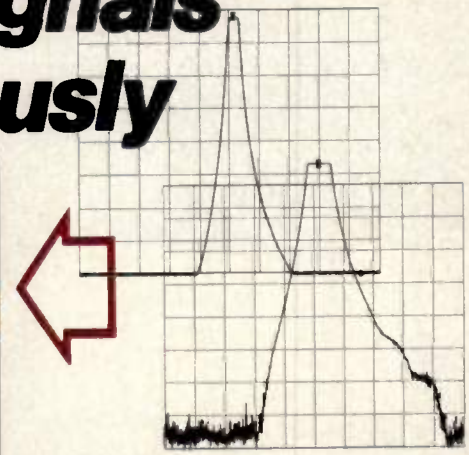

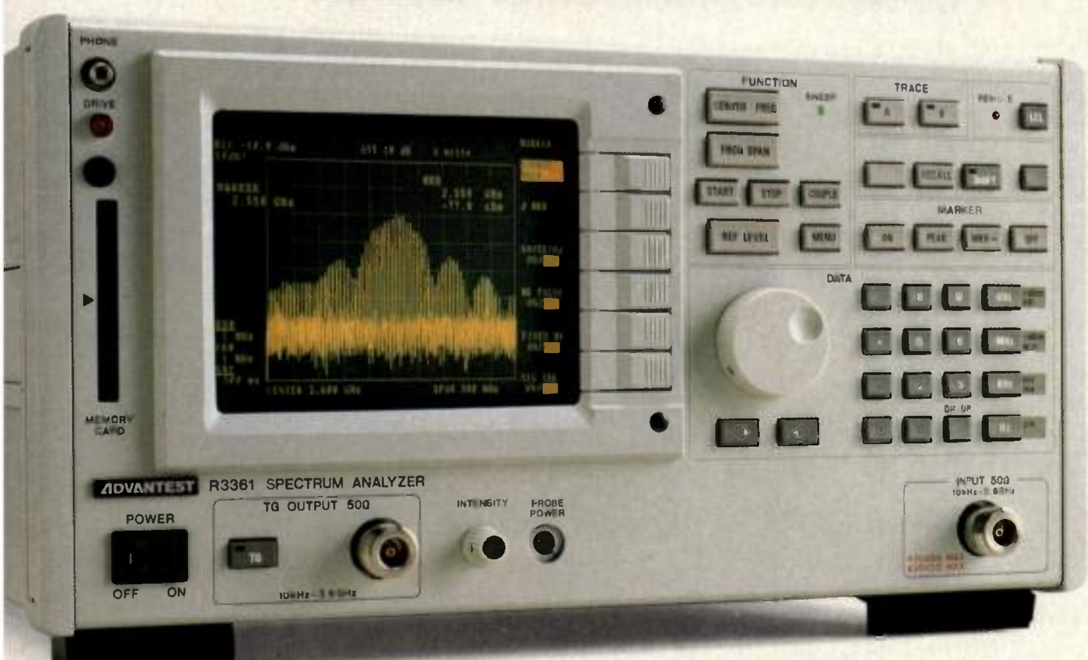

The R3261/3361 series synthesized spectrum analyzers are compact, lightweight, synthesized analyzers covering the frequency ranges of 9kHz to 2.4GHz (R3261A/3361A) and 9kHz to 3.6GHz (R3261B/3361B). They represent the combination of ADVANTEST's many years of experience in RF circuit technology with the latest in software calibration technology. The bottom line for the user is a guaranteed overall level accuracy of 1dB. In addition, these analyzers feature: stop, start, and center frequency resolution to 1Hz, together with a built-in frequency counter, also with 1Hz resolution. The result is a truly powerful analyzer in an amazingly compact package.

New R3261/3361 Series Spectrum Analyzer

- Frequency range···9kHz to 3.6GHz (R3261B/3361B)
  9kHz to 2.4GHz (R3261A/3361A)
- Built-in tracking generator (R3361A/3361B)
- Overall level accuracy of 1dB
- 120dB displayable dynamic range
- Synthesis technique used for 1Hz-resolution setting and measurements
- High performance and portability
- Quasi-peak measurements 70dB dynamic range
- Memory card and GP-IB provided as standard
- Built-in control function (option)
- User definable soft keys

ADVANTEST®

Advantest America, Inc. 300 Knightsbridge Parkway, Lincolnshire, IL 60069, U.S.A. Phone:(312)634-2552 Facsimile:(312)634-2872

Advantest UK Limited CI Tower, St. Georges Square, High Street, New Malden, Surrey, KT3 4HH, U.K. Phone:(01)336-1606 Facsimile:(01)336-1657

INFO/CARD 67 See us at Wescon/88, Booth #3155.

the speed and current levels associated with an ESD event, these resulting fields can easily upset nearby electronic equipment.

This manifestation of ESD has become a significant problem with digital systems since the late 1970s. Prior to that time, most digital systems were too slow, relative to ESD, so the electromagnetic field was effectively ignored. Since ESD has a typical rise time of 1 to 3 nanoseconds, this was much faster than the logic of the 70s. Today, however, logic can easily respond to edge rates of 1 nanosecond or less. Thus, these faster edge rates have opened fully the "window of susceptibility" to ESD.

As a simple example, Figure 4 shows the coupling of an ESD current-induced field into an adjacent circuit board. This simple calculation predicts an induced voltage of 3 volts, which is more than enough to cause an upset in a digital circuit.

Incidentally, this problem revealed itself in a vivid fashion with the early electronic cash registers. Since ESD was a concern, the cash registers were carefully designed with plastic cases and switches to eliminate any direct discharge. Unfortunately, no shielding was used, and the indirect discharge from customers touching metal counters was often enough to completely disable the cash registers.

ESD Victims

As modern electronic components have increased in speed and decreased in size, their vulnerability to ESD has dramatically increased as well. Upset thresholds have decreased, as digital circuits with 1 to 3 nanosecond edge rates no longer ignore ESD transients, but accept them as valid data. Furthermore, devices that rely on stored charges (such as memories) are smaller, and thus become susceptible to upsets at much lower energy levels.

Damage thresholds have also decreased. Many modern circuits suffer damage at voltage levels as low as 100 volts. Since the human threshold of feeling for ESD is around 2000 volts, it is quite possible that damage has occurred with no warning or indication. Even more insidious, devices may not be destroyed, but only weakened, and become the "walking wounded" that result in increased field failures at a later time.

Interface circuits, such as input/output or probes, are particularly vulnerable as ESD victims. Special precautions are often needed to prevent ESD damage to differential oscilloscope probes, spectrum analyzer inputs, and computer input/output interfaces.

Designing and Testing for ESD

While most electronic companies today have an active ESD program for manufacturing, many still ignore ESD when designing new products. This is unfortunate, since, as stated earlier, today's technology is more vulnerable than ever to ESD effects. The author is personally familiar with product recalls that were directly related to ESD.

A primary design goal should be to make a system less vulnerable to both damage and upset from an ESD event. One must assume that eventually an event will occur, and that it must be dealt with. This is unlike manufacturing where the goal is to prevent ESD events (in manufacturing, if the ESD event occurs, it is usually too late.)

ESD-tolerant design should begin with component selection, and continue through the board and system design.

Particular attention is needed with cables, connectors, and shielding, due to the electromagnetic field effects of the indirect discharge. In microprocessor systems, even software should be designed to accommodate ESD-induced errors. In short, it is not enough to simply design a system to work; it must also be designed not to fail in the presence of ESD.

Testing electronic systems for ESD vulnerability is strongly recommended. The testing is relatively simple and inexpensive, and can quickly reveal any design shortcomings. Tests are usually done with an "ESD gun," a device that closely simulates the discharge voltages and currents from a human being. Two types of tests are used. In the first case, the simulated ESD is discharged directly into the equipment. All exposed metal surfaces (including keyboards, connectors, switches, and indicators) should be able to withstand at least 7,500 to 10,000 volts. For systems with plastic enclosures, an additional set of tests are conducted, discharging the ESD into a nearby metallic plate to simulate the electromagnetic field effects of ESD. For a small system, a full set of tests can typically be done in a day or less.

Sub-system ESD testing can also be performed. It is becoming more and more popular to test printed circuit boards for indirect discharge ESD effects early in the prototype stage. At this point, it is relatively easy to identify specific weak points, and harden them at minimum expense. An ounce of prevention at design time is worth many pounds of cure in field service time and customer satisfaction.

Summary

Electrostatic discharge is a serious threat to today's electronic systems. And while manufacturing personnel are usually well aware of ESD and have implemented strong ESD prevention programs, design personnel may not be as concerned with ESD. Nevertheless, with the increasing speed and decreasing size of today's electronic devices, ignoring ESD is poor engineering.

ESD is a very real EMI problem, and systems must be designed to tolerate ESD, just as they must be designed to tolerate other effects of the modern electromagnetic environment.

References

1. Michel Mardiguian, *Electronic Discharge — Understand, Simulate and Fix ESD Problems,* Interference Control Technologies, 1986.
2. *Electronic Discharge Protection Test Handbook,* KeyTek Instrument Corporation, 1983.
3. Michel Mardiguian, "Indirect ESD Testing," *EMC EXPO 88 Symposium Record,* August 1988.
4. Daryl Gerke, "ESD Miniature Lightning," *The Inside Line,* Toma Publishing, September 1988 (Vol. 1, No. 6).
5. Daryl Gerke, "Designing Microcomputer Systems to Tolerate Noise," *Society of Automotive Engineers #870787,* April 1987.

About the Author

Daryl Gerke, P.E., is a principal at the consulting firm of Kimmel Gerke Associates, Ltd., which specializes in electromagnetic interference and compatibility (EMI/EMC) engineering. This includes electrostatic discharge (ESD), EMC compliance (FCC, VDE, MIL-STD), electromagnetic pulse (EMP) and related issues. Mr. Gerke can be reached 1544 N. Pascal, St. Paul, MN 55108. Tel:(612) 330-3728 or (612) 646-7715.

Circulator Improves Notch Filter Selectivity

By Gary Thomas
General Electric Mobile Communications

Reflective notch filters operate by presenting a short circuit across a transmission line at the tuned frequency of the notch. By adding a circulator and an adjustable stub tuner to the basic circuit a much narrower absorptive notch filter can be produced. Although similar to a prize-winning contest entry published in the July 1988 issue of RF Design, *this article (submitted prior to the contest) offers a different perspective on the concept.*

Band reject or notch filters are used extensively at RF frequencies to eliminate undesired signals. Typical applications include improving intermod rejection in communications receivers by eliminating signals on specific off-channel frequencies and increasing the dynamic range of a spectrum analyzer. This is done by reducing the level of a strong input signal component to avoid overloading the instrument's input circuits while measurements on weaker spectral components are being made.

The required width (selectivity), depth (rejection), and tuning range of the stopband along with the maximum permissible insertion loss in the passband determine the usefulness of a particular notch filter in a given application. In addition, the power handling and temperature stability of the filter may be important considerations in some cases.

Series Tuned Trap

The most common form of the notch filter discussed above is the series tuned trap shown in Figure 1a. In this configuration one or both of the reactive components can be made variable to allow tuning of the notch frequency. The resistive component shown represents the dissipative loss of the filter and determines its unloaded Q (usually every effort is made to keep this resistive component as low as possible). In turn the unloaded Q sets the limit for selectivity and rejection of the filter. Practical filters can be implemented using discrete components as shown in Figure 1a, a half-wave short circuit stub as shown in Figure 1b, or a selective cavity (quarter-wave open stub) as shown in Figure 1c.

These three implementations of the notch filter are electrically similar and operate in principle by presenting a short circuit across the transmission line at resonance causing total reflection of the input signal at that frequency. Since the resonant structure appears as an open circuit at frequencies off resonance, all other spectral components pass the boundary unimpeded. In practice, due to resistive losses and finite reactances the resonant circuit is neither a perfect short at resonance nor a perfect open off resonance. As a result there is never complete reflection of the tuned frequencies nor transmission of the off tuned frequencies. In addition there may be a gradual transition between these two regions.

Figure 2 shows the measured response of a typical series tuned trap notch filter. Measurements were done using a Wiltron 560 Scalar Network Analyzer with a 610D/61084D sweep generator. This filter consists of a 0 to 40 pF air variable capacitor in series with a lumped inductor made from 3 cm of 14 Ga. copper wire formed in a single loop. The entire assembly is housed in a cylindrical metal enclosure approximately 5 cm in diameter and 7.5 cm long. Connection to the trap is made through a BNC connector. The resulting one port is placed across the transmission line using a standard "T" connector.

In spite of its simple construction, this notch filter is very useful for measuring the second harmonic of a UHF transmitter. As seen in Figure 2, if the filter is placed between the transmitter and spectrum analyzer the transmitter fundamental output at 450 MHz will be reduced by 35 dB while the second harmonic component at 900 MHz will suffer less than 1 dB attenuation. Thus the filter can be used to increase the dynamic range of the test setup by as much as 35 dB.

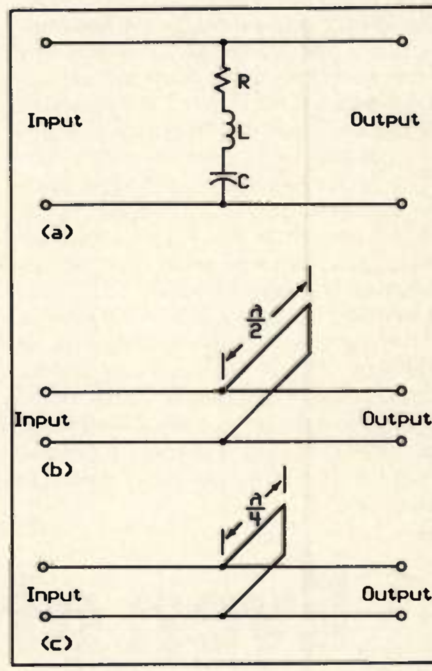

Figure 1. Various reflective notch filters.

Unfortunately, due to the width of the notch this simple filter is not useful for measurements close to the tuned frequency. This is easily seen in Figure 3 which shows the filter response on an expanded scale. In general, measurements close to the frequency being

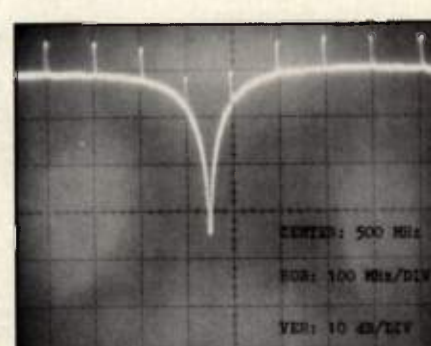

Figure 2. Measured response of series tuned trap.

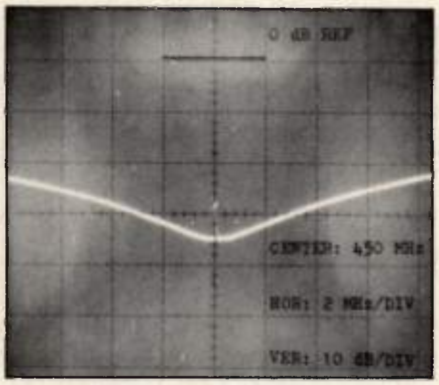

Figure 3. Measured response of series tuned trap (expanded scale).

notched require a different, more selective filter. This usually means a larger, more expensive filter which may not be readily available.

Improved Filter

The selectivity of the simple notch filter can be improved significantly by the addition of a circulator and tuning stub (Figure 4). The response of this combination is shown in Figure 5. The improvement obtained is seen by comparing Figure 5 and Figure 3 (both photos were taken with the same analyzer settings).

Although the addition of a circulator and tuning stub to the simple notch filter seems innocuous enough, in fact it completely changes the way in which the transmission null is achieved. To see this, refer to Figure 4 and note that in order to have zero transmission between port 1 and port 3 of the circulator the network attached to port 2 must appear to be a perfect 50 ohm termination. In other words, the simple notch filter must absorb all of the incident power at the notch frequency. The fact that it does this is difficult to accept because, as pointed out earlier, every effort is usually made to minimize the dissipative loss of the reflective notch filter when it is made. In fact if the tuning stub were not present, very little of the power emerging from port 2 would be absorbed in the reactive load of the trap and virtually all power would be reflected and appear at port 3. There would be essentially no notch at all. However, when the sliding stub tuner is included in the circuit and adjusted properly, it acts as an ideal transformer stepping up the small resistive loss of the cavity to 50 ohms. The fact that the extremely high transformation ratio required tends to make the matching section very narrowband is a benefit rather than a drawback since the application is for a narrow notch filter in the first place. Similarly the circulator used for the filter does not have to be particularly broadband as long as it is tuned to the desired notch frequency.

Applications

As mentioned above, the improved notch filter operates by absorbing the power at the notch frequency rather than reflecting it back to the source. In fact if the termination at port 3 is a good broadband load, then the source connected to port 1 of the circulator sees a low VSWR at all frequencies. This can be very useful when testing transmitters which might become unstable while working into a high VSWR or an amplifier which incorporates a reverse power detection circuit which shuts down the

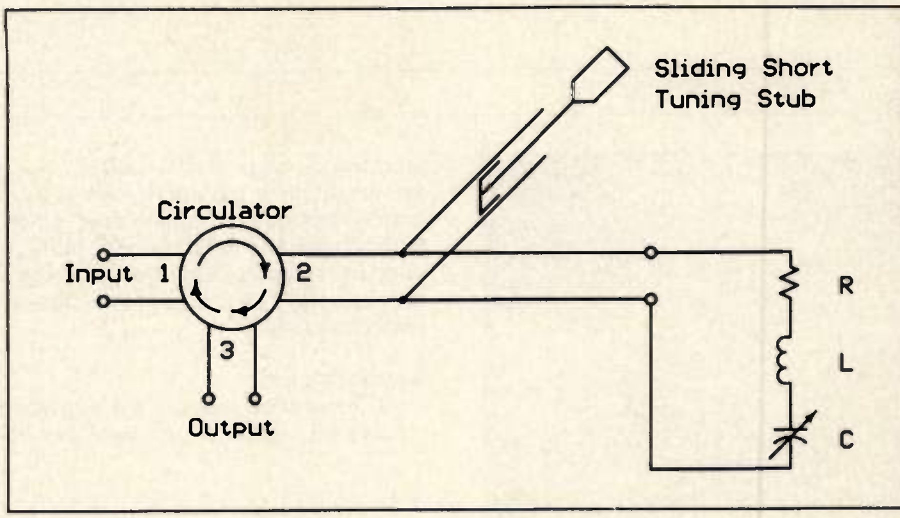

Figure 4. Improved notch filter.

transmitter output to prevent damage to the final PA stages due to a short or open circuit at the antenna port.

One disadvantage of the absorptive filter is that when it is tuned to the output of a high power device the trap absorbs virtually all of the output power and can get very hot. This can cause it to detune as it warms up or may destroy it if it cannot dissipate the power absorbed.

In practice the absorptive filter is more difficult to tune than the simple series tuned trap since the two tuning adjustments (the trap and the stretch line) are interactive. Nonetheless, this technique has been used successfully to extend the performance of a large selective cavity for such critical applications as measuring 25 kHz spurious FM sidebands 110 dB down from a 150 MHz carrier.

Since the absorptive filter operates by using the signal separation properties of the circulator, any directive device such as a hybrid splitter or return loss bridge can be used in its place. The

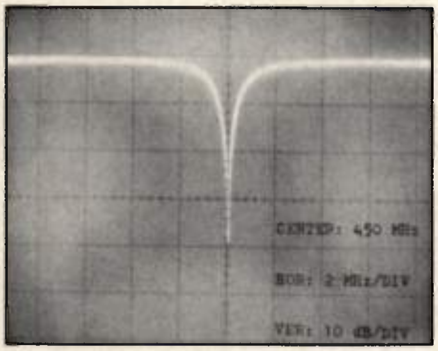

Figure 5. Measured response of improved filter (same scale as Fig. 3).

main disadvantage of using these devices is that they have much larger insertion loss and worse return loss at frequencies away from the notch.

Finally it should be noted that although you would expect the notch depth to be limited by the ultimate isolation of the circulator, in practice the leakage around the device is partially cancelled by the small reflected signal from the cavity. The correct phasing of these two signals results automatically when the two adjustments are tuned for the deepest notch.

Conclusion

A technique to increase the selectivity of narrow bandstop filters has been presented. The method can be used to improve the performance of small inexpensive notch filters or to achieve exceptional performance from larger, more expensive units. It offers the additional benefit that the resultant filter is absorptive and protects the source under test from large reflections.

References

1. Robert E. Collin, *Foundations of Microwave Engineering,* McGraw-Hill, 1966
2. Milton S. Kiver, *Introduction to UHF Circuits and Components,* Van Nostrand, 1955
3. *About Selective Cavities,* Decibel Products Inc., 1964

About The Author

Gary Thomas is a senior staff engineer with General Electric Mobile Communications, Mountainview Road, Lynchburg, VA 24502. Tel: (804) 948-6019.

STATEMENT OF OWNERSHIP, MANAGEMENT AND CIRCULATION (Required by 39 U.S.C. 3685)

1. Title of Publication: RF DESIGN
1B. Publication No.: 453490
2. Date of Filing: Oct. 3, 1988
3. Frequency of Issue: Monthly plus one extra issue
3A. No. of issues published annually: 13
3B. Annual Subscription Price: $33.00
4. Complete Mailing Address of Known Office of Publication: 6300 South Syracuse Way, Ste. 650, Englewood, Colorado 80111
5. Complete Mailing Address of the Headquarters of General Business Offices of the Publisher: 6300 South Syracuse Way, Ste. 650, Englewood, Colorado 80111
6. Full Names and Complete Mailing Address of Publisher, Editor and Managing Editor: Publisher: Robert A. Searle, 6300 S. Syracuse Way, Ste. 650, Englewood, Colorado 80111 Editor: Gary A. Breed, 6300 S. Syracuse Way, Ste. 650, Englewood, Colorado 80111
7. Owner (if owned by a corporation, its name and address must be stated and also immediately thereunder the names and addresses of stockholders owning or holding 1 percent or more of total amount of stock. If not owned by a corporation, the names and addresses of the individual owners must be given. If owned by a partnership or other unincorporated firm, its name and address, as well as that of each individual must be given. If the publication is published by a nonprofit organization, its name and address must be stated.) (item must be completed): Cardiff Publishing Company, a subsidiary of Argus Press Holdings Inc., 6255 Barfield Road, Atlanta, GA 30328-4369, Argus Holdings Inc., 6255 Barfield Road, Atlanta, GA 30328-4369
8. Known bondholders, mortgagees, and other security holders owning or holding 1 percent or more of total amount of bonds, mortgages or other securities (if there are none, so state): None

9. Extent and nature of circulation	Average No. copies each issue during preceding 12 months	Actual No. copies of single issue published nearest to filing date
A. Total No. Copies (Net Press Run)	37,668	40,876
B. Paid and/or requested circulation		
1. Sales through dealers and carriers, street vendors and counter sales	None	None
2. Mail subscription (Paid and/or requested)	34,811	36,391
C. Total paid and/or requested circulation (Sum of 10B1 and 10B2)	34,811	36,391
D. Free distribution by mail, carrier or other means (samples, complimentary and other free copies)	1,478	1,085
E. Total Distribution (Sum of C and D)	36,289	37,476
F. Copies not distributed		
1. Office use, left over, unaccounted, spoiled after printing	1,379	3,400
2. Return from News Agents	None	None
G. TOTAL (Sum of E, F1 and 2 — should equal net press run shown in A)	37,668	40,876

10. I certify that the statements made by me above are correct and complete. (Signed) Robert A. Searle, President/Publisher

New Products Featured at RF Expo East

Dozens of Companies Choose Philadelphia to Unveil New Products

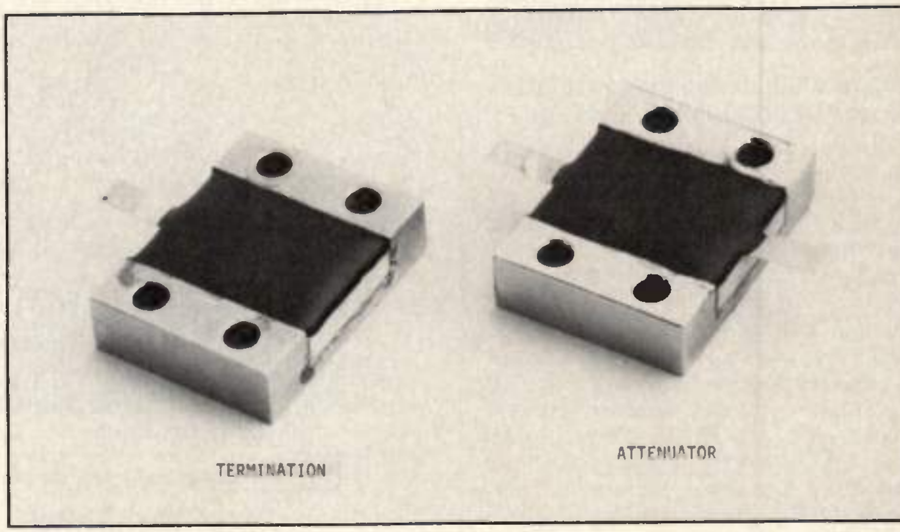

Stripline Attenuators JFW Industries

These attenuators use beryllium oxide ceramic substrates and thick film resistor inks to achieve transfer of heat from the film area through the substrate to the heat sink. When mounted to an appropriate sink the temperature rise is approximately 0.6 degrees C/W. Typical TCR is 125 PPM/degree C. 50 ohms is standard, but, other impedances are available. The range provided is DC through 3 GHz with maximum VSWR of 1.15:1 from DC to 1 GHz. Power rating for the A-210 Series is 125 watts average and 1000 watts peak.

The T-290 Series of terminations have a frequency range of DC to 1 GHz with VSWR from DC to 0.1 GHz of 1.05:1. Power rating is 250 watts average and 1000 watts peak. **JFW Industries, Inc., Indianapolis, IN. INFO/CARD #230**

Stripline Power Divider Merrimac

The PDM-02S-4G represents a range of stripline dividers covering multi-octaves with tight phase and amplitude balance. This low frequency example has an amplitude balance of 0.2 dB max., phase balance of 2 degrees and insertion loss of 0.9 dB. Output port isolation exceeds 17 dB over the 0.5 to 7.5 GHz range. Price is $995.

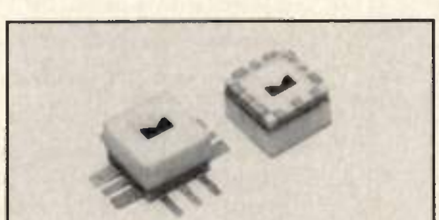

The 0.25" square surface mount package from Merrimac is designed for 50 ohm coplanar systems. The Kovar input leads are designed to suit various mounting configurations. Price starts at $95. **Merrimac Industries, Inc., West Caldwell, NJ. INFO/CARD #229**

FM IF Source Signetics

MC3361 is a low-power FM IF second source that operates down to 2 V and consumes 4.2 mA. NE/SA615 is a low-power mixer FM IF system with input frequencies up to 500 MHz and 25 MHz IF bandwidths. **Signetics, Sunnyvale, CA. INFO/CARD #228.**

Custom SAW Devices
McCoy Electronics

McCoy is offering to design, fabricate and test (both electrically and environmentally) custom surface acoustic wave (SAW) device requirements over the following product areas: delay lines from 20 to 1200 MHz and up to 20 us, bandpass filters from 20 to 400 MHz with fractional bandwidths to 50 percent and hybrid oscillators from 100 to 1200 MHz. **McCoy Electronics, Mt. Holly Springs, PA. INFO/CARD #227.**

Oscillator Design Software
Circuit Busters

Oscillator designs 16 different L-C, transmission line, SAW and quartz crystal oscillators. It computes bias and RF component values based on user responses to program prompts. The program then writes a Superstar file which is used to analyze the open loop Bode response and to optimize the design parameters. Application frequency range is audio to approximately 2 GHz. The software runs on IBM PC/XT/AT/PS2 and compatible computers. Price is $495. **Circuit Busters, Inc., Stone Mountain, GA. INFO/CARD #226.**

Calibration Unit
S.T. Research

Model 8400A is designed to facilitate the maintenance and calibration of noise figure meters. The unit provides a

two-level IF signal which simulates the Noise On/Noise Off ratio emanating from a typical receiver IF output. The ratio and output are variable. **S.T. Research Corp., Newington, VA. Please circle INFO/CARD #225.**

Voltage-Controlled SAW Oscillators
RF Monolithics

RFM will unveil a line of voltage-controlled SAW oscillators (VCSO). Typical SSB phase noise is -115 dBc/Hz at 1 kHz for a 500 MHz VCSO. The devices are available up to 1 GHz. **RF Monolithics, Inc., Dallas, TX. Please circle INFO/CARD #224.**

MOSFET Devices
SGS-Thomson

SGS-Thomson introduces a line of MOSFET devices with power levels from 5 to 300 watts at 28 and 50 V at 250 MHz. Also available are devices with power from 5 to 50 watts at 28 V and 500 MHz.

Also being introduced is a 150 watt transistor which operates from 470 to 860 MHz. The SD 1492 is optimized for 28 volt operation with more than 7 dB gain. **SGS-Thomson Microelectronics, Montgomeryville, PA. Please circle INFO/CARD #223.**

Oscillation Transistor
California Eastern Labs

The NE64700 oscillation transistor has a gain of 22 dB at 2 GHz with an F_T of 11 GHz. Typical specifications include

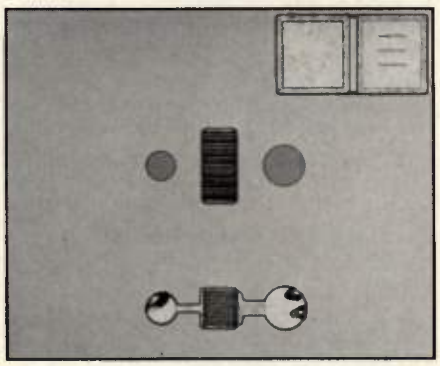

V_{CBO} of 30 V, V_{CEO} of 11 V and V_{EBO} of 2.5 V. **California Eastern Laboratories, Inc., Santa Clara, CA. Please circle INFO/CARD #222.**

SMT SAW Devices
Sawtek

Sawtek unveils a line of hermetic surface mount packages for SAW devices. The small size maximizes the integration potential of SAW frequency control elements. **Sawtek Inc., Orlando, FL. INFO/CARD #221.**

Class A Amplifier
Amplifier Research

Model 100HB is a Class A power amplifier with 100 watt minimum output from 400 to 1000 MHz. An integral leveling preamplifier and front-panel metering of forward and reflected power

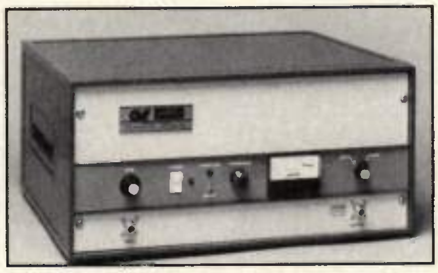

are featured. **Amplifier Research, Souderton, PA. INFO/CARD #220.**

Class AB Linear Amplifier
Power System Technology

PST's Model BHE 5819-500, 500-1000 MHz, 500 watt amplifier features a 500 MHz bandwidth and minimum gain of 57 dB. AM distortion at 85 percent depth of modulation is 10 percent maximum and two-tone intermod is -20 dBc referenced to 500 watts PEP. **Power Systems Technology, Inc., Happauge, NY. INFO/CARD #219.**

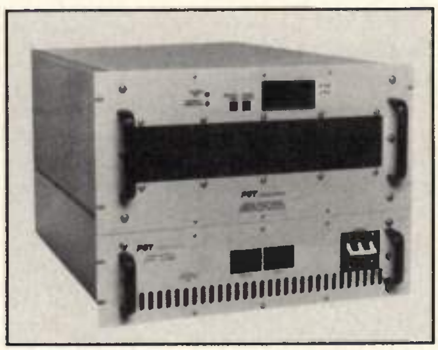

Digital Wattmeter
Coaxial Dynamics

Coaxial Dynamics will unveil the Model 83550A peak/CW digital wattmeter along with the Model 7510P peak/CW frequency/RF wattmeter. **Coaxial Dynamics, Inc., Cleveland, OH. Please circle INFO/CARD #218.**

Integrated Microwave Subsystems
AEL Defense Corp.

Integrated microwave subsystems together with shop replaceable assemblies will be introduced. **AEL Defense Corp., Lansdale, PA. Please circle INFO/CARD #217.**

SMB and SMC Connectors
Applied Engineering Products

AEP has added 44 SMB and SMC connectors to their QPL line bringing their total to 100 SMB and SMC connectors qualified to MIL-C-39012. **Applied Engineering Products, New Haven, CT. INFO/CARD #216.**

SAW Spectrum Analyzer
Phonon Corp.

The AS160-6-50 is a 50 percent POI real-time spectrum analyzer based on SAW technology. It is capable of processing signals of 6 MHz bandwidth with 30 kHz resolution. Time sidelobes are suppressed greater than 25 dB. **Phonon Corp., Simsbury, CT. Please circle INFO/CARD #215.**

TWT Amplifiers
Keltec Florida

The R640 Series of pulse TWT amplifiers features power up to 10 kW.

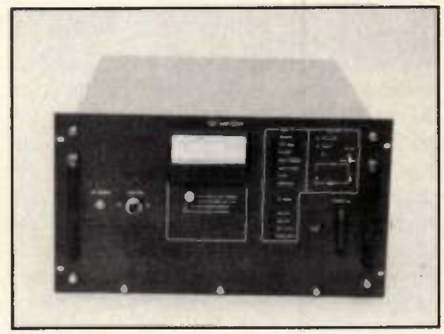

Applications include EMI/EMC test standards and radar threat simulators. **Keltec Florida, Inc., Fort Walton Beach, FL. INFO/CARD #214.**

Microwave Counter
XL Microwave

This 10 Hz to 20 GHz microwave counter features high sensitivity, fast data acquisition, GPIB and power meter as standard. It costs $3,900. **XL Microwave, Inc., Oakland, CA. Please circle INFO/CARD #213.**

Capacitor Kit
ATC

The ATC "Capacitor Pick List Kits" feature five different kits from $19.95 to $99.95. **American Technical Ceramics, Huntington Station, NY. Please circle INFO/CARD #212.**

Bipolar MMIC
Avantek

Model #INA-02170 is a low-noise, cascadable silicon MMIC which features 1.9 dB noise figure, 31 dB gain and 11 dBm P_{1dB} at 0.5 GHz. It is housed in a 70 mil hermetic gold ceramic surface mount package. Applications included IF and RF amplification at frequencies

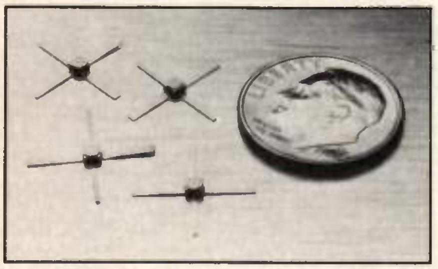

up to 2 GHz. **Avantek, Inc., Santa Clara, CA. INFO/CARD #211.**

Board Level DDS
Digital RF Solutions

The DX-2070 is a board level direct digital synthesizer based on the NCMO™ system. Numeric phase or frequency modulation is included with clock speed up to 20 MHz and power consumption of less than 2 watts. **Digital RF Solutions Corp., Santa Clara, CA. Please circle INFO/CARD #210.**

Flexible Cable Assemblies
Micro-Coax Components

Micro-Coax unveils the UTiFLEX flexible microwave cable assemblies featuring low insertion loss and low VSWR up to 26.5 GHz. Also available are SMA male and female connectors with 25 ohm characteristic impedance for use with 25 ohm semi-rigid cable. **Micro-Coax Components, Inc., Collegeville, PA. INFO/CARD #209.**

Combination Receiver/ Network/Spectrum Analyzer
Rohde & Schwarz

The FSAC combines the functions of a spectrum analyzer, network analyzer and calibrated receiver with noise less than -157 dBm (6 Hz bandwidth) and SSB phase noise less than -114 dBc at 1 kHz offset. Model FSAC is priced at $69,500. **Rohde & Schwarz, Lanham, MD. INFO/CARD #208.**

Extended Capability For Analyzer System
Hewlett-Packard

HP introduces new products and options to extend the capability of the HP 8702A lightwave-component-ana-

lyzer system. The system can now characterize 1,300 nm components up to a 6 GHz modulation bandwidth and 1,550 nm components up to a 3 GHz modulation bandwidth. **Hewlett-Packard Company, Palo Alto, CA. INFO/CARD #207.**

INFO/CARD 30

INFO/CARD 78

Air-Powered Tools for EMI/RFI Testing from EMCO

An air-powered antenna mast and metal- topped turntable for EMI and RFI testing is available. The mast and turntable eliminate a potential source of transient noise from the test environment using pneumatics instead of electric motors for positioning movements. They are suited for use in areas sensitive to transient noise such as automated test sites and anechoic chambers. Model 1053 is the mast while Model 1064 is the turntable.

Both devices are powered from any source of dry air which can be supplied at 90 psi at 40 cfm. Variable rates of speed for ascent (mast) and rotation (turntable) are adjustable. Each unit comes with a digital readout controller that includes an IEEE-488 bus and 10 meters of cable. Options such as shielded room kits, pneumatic po- larization (mast) and mercury slip rings (turntable) are available.

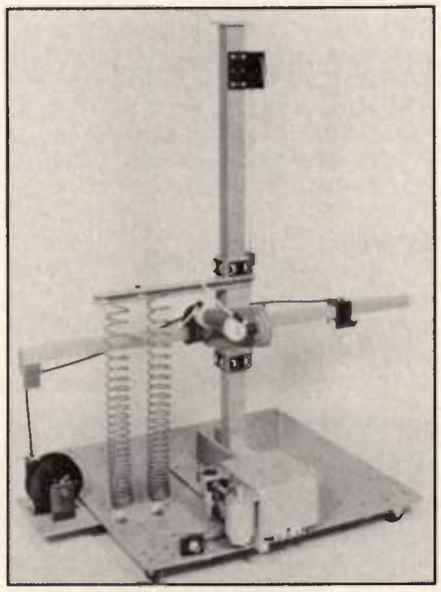

The cost of the mast with controller and IEEE bus is $11,995, and the turntable with IEEE bus is $10,800. **Electro-Mechanics Company, Austin, TX. INFO/CARD #207**

Quartz Crystals

Fundamental mode 40 MHz quartz crystals for use with Texas Instruments' TMS320 digital signal processors are available from Innovative Frequency. These chemically milled resonators offer low power consumption, small size and high stability.

Also available are inverted mesa quartz wafers from 35 MHz to 500 MHz for application in hybrid oscillators. Fundamental frequency is 350 MHz and overtone is at 500 MHz. **Innovative Frequency Control Products, Inc., Plainfield, PA. INFO/CARD #206**

Slag Free/Laser Machined Substrates

A slag removal process eliminates virtually all circuit-interrupting slag from

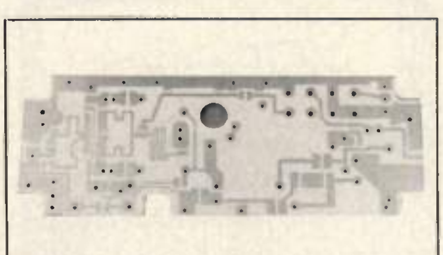

holes and edges of 99.6 percent Al_2O_3 Superstrate^R substrates after custom machining has been performed. By removing slag such as alumina, glass particles and silicates on the walls of holes, this process offers improved adhesion of metallization and longer mask life. It also eliminates the need for substrate scraping. Superstrates are available in customized configurations that include contouring, drilling and scribing with positioning accuracies of ±0.001 inch. Metallized, etched and pattern-plated versions may be specified in a selection of metals including chromium, gold, copper, titanium tungsten, tantalum nitride, nichrome and nickel. **MRC Hybrid Products, Pearl River, NY. INFO/CARD #205**

RF Pulse Amplifier

Model 3200 covers 6 MHz to 220 MHz at 1000 watts of linear peak pulse or 100 watts of CW power. An integrating detector limits maximum pulse and CW power, pulse width and duty cycle. The standard system will supply up to 20 ms pulses at 10 percent duty cycle. Pulse droop is less than two percent, amplitude linearity is ±1 dB from linear with less than ±5 percent of phase change with output power. Blanking time is less than 2 us. A front panel meter is also included. Price is $17,900. **American Microwave Technology, Inc., Fullerton, CA. INFO/CARD #204**

GPIB Switch Bank

Trilithic introduces the Interlink line of addressable switch banks for laboratory, systems and production line ATE applications. Interchangeable control cards

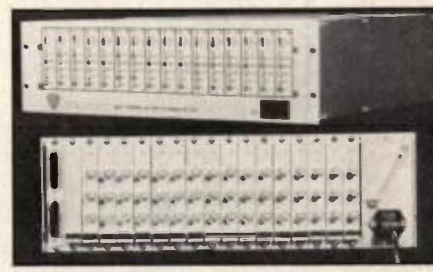

are available for GPIB, RS-232C and other interfaces. SPDT switch cards are available covering DC to 1, 4, 8, 12.4, 18.5, 26.5 and 40 GHz. Because the internal bus is accessible, a single primary system address can control up to 1020 channels. The utility cards include SPDT and SP4T switches and up to 8 cell programmable attenuators. A manual control front panel with LED status indicators is optional. **Trilithic, Indianapolis, IN. INFO/CARD #203**

VHF and Microwave Synthesizers

The synthesizer is available as a stand-alone VHF synthesizer or as part of a microwave frequency synthesizer which utilizes frequency agile phase-locked signal sources to multiply the VHF signal to frequencies up to 23 GHz.

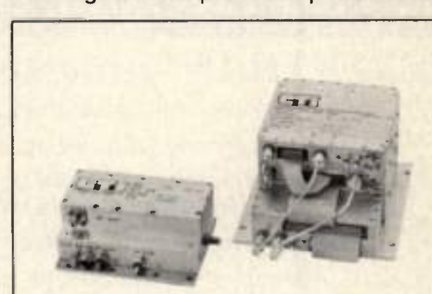

The VHF synthesizer is available from less than 30 MHz to greater than 500 MHz and the microwave synthesizer is available from 500 MHz to 23 GHz. Phase noise for offset frequencies of less than 100 Hz is determined principally by external references. **Communication Techniques, Inc., Whippany, NJ. INFO/CARD #202**

Fast Filter Structure

The fast filter structure (FFS) from Monolithic Instruments implements a lowpass filter, highpass filter or Hilbert transform with a circuit complexity of 3 to 5 percent of conventional circuits. A prototype of the FFS uses 12 additional operations to implement a 64 point finite impulse response (FIR) structure. It is based on a 16-bit 2901-type processor which executes 12 computational cycles at a clock period of 100 ns, accommodating a 1200 ns sampling interval. Dynamic range of approximately 80 dB is achievable. **Monolithic Instruments, Inc., Florissant, MO. INFO/CARD #201**

Multi-Loop Frequency Synthesizer

The Luff Research Model MLS synthesizer covers octave bands to 1000 MHz and 500 MHz bands to 2 GHz with 1 kHz resolution. When purchased in quantities of 1 to 4, price is $2750. **Luff Research, Jackson Heights, NY. Please circle INFO/CARD #200**

Dielectric Resonator Tuners

The Dyna-Trim tuners allow for flexibility in design and achieve a tuning range up to two percent with minimum Q degradation. These devices feature high resolution tuning and a self-locking torque mechanism.

Also available is the CR8500 Series of coaxial resonators designed for operation between 800 MHz and 3.5 GHz. The resonators behave like Hi-Q parallel resonant circuits with a high resonant impedance. The low loss silver plating improves circuit Q while minimizing the environmental effects on frequency. **Alpha Industries, Inc., Woburn, MA. INFO/CARD #199.**

SMT Oscillator Package

GE Ceramics introduces a surface-mountable ceramic oscillator package which measures 0.35 by 0.45 in. and has 4 leads. All alumina monolithic ceramic construction is featured. **GE Ceramics, Chattanooga, TN. Please circle INFO/CARD #198.**

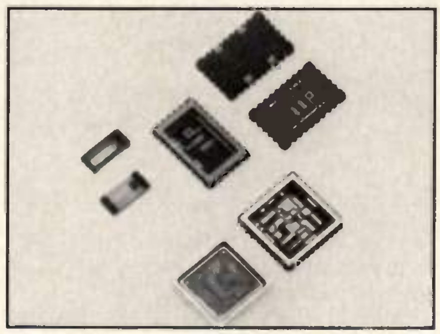

Optocoupler for Video Applications

The HCPL-4562 optocoupler is designed for video-isolation circuits. It has a 20 MHz bandwidth and typical phase variation of 9 degrees between 3 and 4 MHz. The device is priced at $2.06 when purchased between quantities of 2,500 to 4,999. Option 100, the surface mount version, is an additional $0.25. **Hewlett-Packard Company, Palo Alto, CA. INFO/CARD #197.**

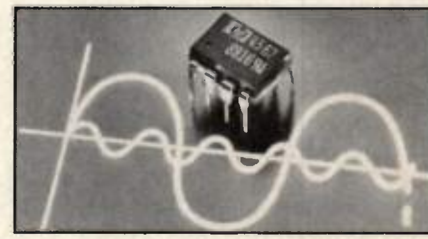

Thick Metal Cladding for Laminates

Ultralam™ woven glass microwave circuit laminate is available with a thick-metal backing laminated to one side and copper foil on the other. The metal cladding is typically 0.010 in. to 0.500 in. thick, is flat and parallel to ±0.002 in. and serves as a ground plane for stripline and microstrip circuit boards. Common thick-metal options include aluminum, brass and copper, although other materials such as Invar or a copper/Invar/copper composite can be specified. Typical applications include discrete microwave device packages such as filters, couplers and switches. **Rogers Corp., Rogers, CT. Please circle INFO/CARD #196.**

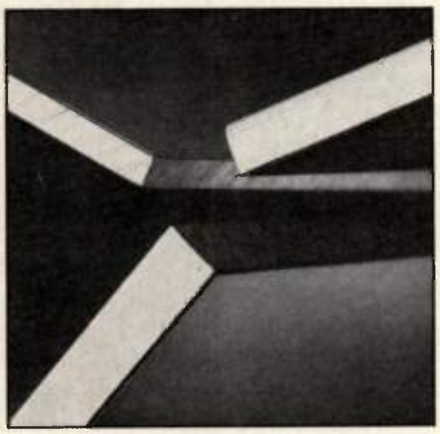

Filters Provide EMP Protection

Sage introduces the Model FF4182-1 Series of filters which will withstand a 1270 volt DC pulse without damage.

FF4182-1 operates over a 1025 to 1095 MHz range with less than 1.25:1 VSWR, less than 0.5 dB insertion loss and phase tracking between units within 4 degrees peak to peak. It will handle 2 kW peak and 200 watts average RF signals. Rejection is greater than 53 dB from DC to 100 MHz and greater than 40 dB from DC to 600 MHz.

Model FF4182-2 has a passband from 2.7 to 2.9 GHz with 1.35:1 maximum VSWR and 0.5 dB insertion loss. The unit provides 60 dB minimum rejection from DC to 100 MHz and greater than 40 dB from DC to 200 MHz. **Sage Laboratories, Inc., Natick, MA. Please circle INFO/CARD #195**

10 MHz Digitizer

The ADC-00110 analog-to-digital and track/hold hybrid is a 12-bit 10 MHz unit. It contains a T/H, A/D converter, data

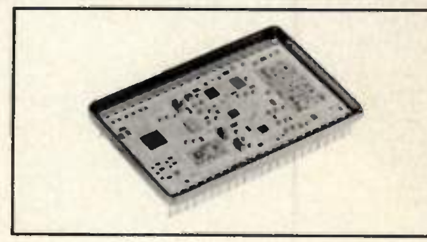

registers, tri-state output buffer and timing circuits in a 46-pin plug-in package. The signal to noise ratio is 66 dB and linearity is specified at 0.025 percent. Typical applications include radar and sonar digitizing. **ILC Data Device Corp., Bohemia, NY. Please circle INFO/CARD #194.**

Linear Amplifier

The 230A is a continuous-duty linear amplifier covering the 1.8, 3.5, 7.0, 14, 21, 24 and 28 MHz bands (24 and 28 MHz bands are for export). It consists of a microcontroller for metering and control and an RF/power supply deck

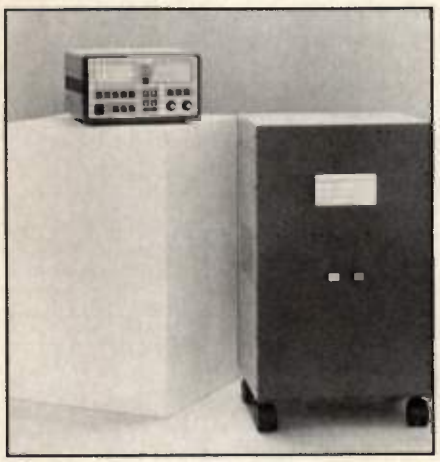

which may be remotely located. Features include LCD displays, drive power of 50 to 70 watts and RS-232C interface. Output power is 1500 W PEP and input impedance is 50 ohms unbalanced. VSWR is less than 1.5:1 and harmonic suppression is -45 dB min. **Advanced Radio Devices, Sterling, VA. Please circle INFO/CARD #193.**

Analog Switches

While the DG540 and DG541 provide the same SPST function, the DG540 includes extra ground lines between the

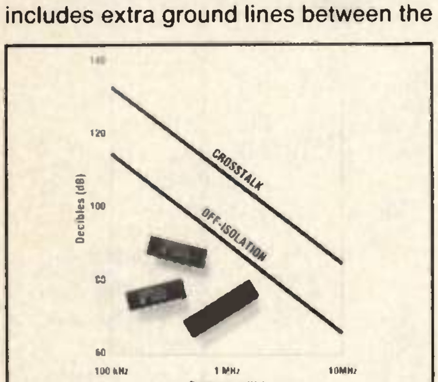

analog signal pins to improve off-isolation and reduce crosstalk. The 20-pin DG540 offers higher off-isolation than the DG541 (-80 dB versus -58 dB at 5 MHz) while the 16-pin DG541 offers a lower-priced, more compact alternative. The DG542 has four analog switches configured as two SPDT functions. Each SPDT switch may be used as a selector between two channels, allowing the DG542 to handle two sets of wideband/video signals simultaneously. All three switches are rated for ESD protection to ±4000 volts on all pins. The 540 is available in 20-pin plastic and sidebrazed DIPs and in PLCC surface mount packages. Packaging for the 541 and 542 includes

16-pin plastic, sidebrazed and small outline options. Price ranges from $3.93 to $15.83 in 100-piece quantities. **Siliconix, Inc., Santa Clara, CA. INFO/CARD #192**

Lightning Pulse Simulator

The NSG 587 is a dual-wave surge generator that can deliver a 1.2/50 microsecond open circuit voltage pulse up to 12 kV or an 8/20 microsecond short circuit pulse of up to 5,000 A. The dual-wave capability is in conformance with the requirements of ANSI/IEEE C62.41 - 1980 (IEEE 587) Category B. The generator is $14,950. **Schaffner EMC, Inc., Union, NJ. INFO/CARD #191**

Ferrite SMT Beads

Fair-Rite introduces two types of ferrite beads that provide impedances of 45 and 90 ohms at 100 MHz. Dimensions are 0.12 x 0.10 x 0.160 in. and 0.12 x 0.10 x 0.335 in., respectively. Both are available reeled at 3,000 per 13 inch carrier and prices range from

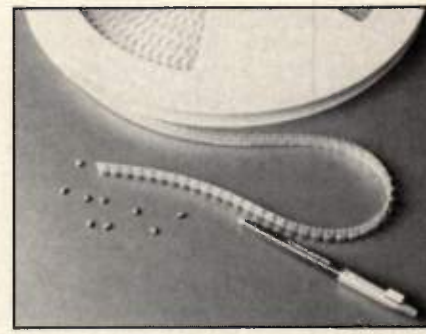

$63 to $73 per thousand for production quantities. **Fair-Rite Products Corp., Wallkill, NY. INFO/CARD #191**

Flexible 50-ohm Coax Cable

Cablewave Systems introduces the HCC 7/8-inch Flexwell, air dielectric 50-ohm coaxial cable with a tubular center conductor. It has a maximum operating frequency of 5 GHz and impedance characteristic of 50 ohms. Peak handling capability is 76.7 kW. **Cablewave System Div., North Haven, CT. INFO/CARD #190**

Test and Characterization Software

The MicroCAT software family provides an environment in which testing and characterizing solutions can be accomplished and in which users can design custom automated testing routines or do manual testing on microwave integrated circuits. Features include: a modular format which allows the user to employ existing applications or create custom ones; a macro utility to create test routines from menu selections; a database of test results and conditions; a database that can be transferred to Touchstone, Lotus, etc.; plotting of RF device characteristics in polar, Smith or rectangular with or without automatic scaling; and the ability to calculate and display statistical characteristics of equivalent circuits. Also available is a Model Extraction module that derives circuit elements of passive and active devices such as FETs and diodes. The MicroCAT Test Executive software package is $6,000 and the module is $8,000. **Cascade Microtech, Inc., Beaverton, OR. INFO/CARD #182.**

Thermal Analysis Package

Visionics Corp. introduces a PC-based, three-dimensional thermal analysis package which will interface to their EE Designer III CAE/CAD integrated electronic design software. Using the thermal package, circuit board designs can be checked for potential thermal problems. It models component conduction, convection and radiation characteristics which enable the user to predict thermal distribution and locate problems in designs after component placement. Environmental parameters such as temperature, pressure, humidity and natural or forced air velocity can be specified for inclusion in the analysis. This program is an option to the EE Designer III and is priced at $1,000. It runs on IBM PC/XT/AT/PS2 and compatibles with 640K, color graphics, hard drive and mouse. **Visionics Corp., Sunnyvale, CA. INFO/CARD #181.**

Transfer Software

This package is capable of transferring data from an HP 8510, HP 8720 or HP 8753 network analyzer to an AT-compatible computer and can also store data in a file format compatible with EEsof's Touchstone. The transfer routines can be integrated into user-written test programs. Floating point transfer times are less than 0.5 seconds for a 201 point trace. The software is available for either QuickBASIC or BASICA and works with either the NationalInstruments PCIIA or IOTech Personal 488 GP-IB interface. **Innovative Measurement Solutions, Atlanta, GA. Please circle INFO/CARD #105.**

Database for Test Engineers

Test Quality has announced an enhancement to TekBase, a database management data found in test facilities, engineering departments, and R&D environments. It is now available for the HP9000 Series 300 and 800 Unix workstations. The database accepts information over LAN, IEE-488, serial and GP-IO interfaces, enabling engineers to send data directly from test instruments and data acquisition devices and perform mathematical functions on the data. **Test Quality Company, Santa Clara, CA. INFO/CARD #104.**

EMI Filter Catalog

This catalog lists more than 230 standard EMI filter designs available from Aerovox. It includes specifications and ordering information for general purpose, high performance, dual mode suppression and medical EMI filter designs and configurations. **Aerovox Inc., New Bedford, MA. INFO/CARD #195.**

Notes on RF Relays

ITT Components has announced the availability of application notes on RF relays from Takamisawa Electric Company of Tokyo. Information contained includes characteristics, construction, measurement methodology, mounting and applications. **ITT Components - North America, Irvine, CA. Please circle INFO/CARD #194.**

DRO Brochure

This brochure entitled "Dielectric Resonator Oscillators" features information on free running DROs and phase-locked fixed frequency DROs. Electrical characteristics together with ordering information and outline drawings are featured. Photos, performance graphs and functional block diagrams are also included. **Miteq, Hauppauge, NY. Please circle INFO/CARD #193.**

Short Form Catalog

ILC Data Device Corp. has released a catalog that describes over 100 hybrid and discrete data conversion and MIL-STD-1553 products. Specifications and technical data for MIL-STD-1553 data bus products, analog-to-digital, digital-to-analog, synchro-to-digital and digital-to-synchro converters are also included. **ILC Data Device Corp., Bohemia, NY. Please circle INFO/CARD #192.**

Image Reject Mixer Handbook

This handbook from Locus provides information on image reject mixers with quadrature hybrids and group delay equalizers. Sections highlight broadband quadrature hybrids, image reject mixers, group/envelop delay equalization, and application information. Also included are tables which provide specifications on broadband quadrature hybrids, image reject downconverters, image reject upconverters (single-sideband modulators), group delay equalizers, and radio frequency converters. **Locus, Inc., State College, PA. Please circle INFO/CARD #191.**

Automated RF Measurement

Mirage Systems introduces a brochure on the automated RF measurement system. It makes I/Q RF measurements of pulsed and CW signals. **Mirage Systems, Sunnyvale, CA. Please circle INFO/CARD #189.**

Software Data Sheet
This data sheet describes the time domain measurement software option for Wiltron's Model 360 vector network analyzer. Option 02 allows the conversion of transmission or reflection measurement data from the frequency domain to the time domain or the distance domain. The data sheet also describes modes of operation, windowing functions, gating functions and available displays. **Wiltron Company, Morgan Hill, CA. INFO/CARD #188.**

Lowpass Filter Catalog
Bulletin 05 from Microwave Filter Company describes custom high power lowpass filters which suppress harmonic emissions, add minimum loss and match the reliability of respective operating systems. It describes power, loss and rejection of medium power lowpass filters with passbands ranging from 10 to 450 MHz and high power lowpass filters with passbands from 1 to 400 MHz. It also briefly explains transmitter systems and how filters will solve requirements. Also covered is information on how to minimize the cost of lowpass filters in transmitter systems. **Microwave Filter Company, East Syracuse, NY. INFO/CARD #187.**

Frequency Product Guide
This product guide is designed to introduce the reader to a temperature-compensated family of frequency dividers, prescalars and fractional frequency multipliers. Specification together with performance graphs, package styles and sizes are shown. A list of technical and application notes is shown. **Telemus Electronic System Inc., Nepean, Ontario, Canada. INFO/CARD #186.**

Product and Applications Catalog
Tachonic Plastics introduces its revised TFE-glass product and applications brochure. It highlights the company's PTFE and silicone-coated fiberglass fabrics, tapes and belts. Also described are typical industrial applications. Specifications are offered and special constructions, treatments and capabilities are described. **Tachonic Plastics, Ltd., Petersburg, NY. INFO/CARD #185.**

Fables Booklet
This publication from EEsof contains various software-related articles and industry news. A section on upcoming events and available literature is included. **EEsof, Inc., Westlake Village, CA. INFO/CARD #184.**

Catalog on Used Equipment
Listed in this catalog are used test and measurement equipment available for sale. Over 750 items from more than 60 manufacturers are featured. Also shown are the terms and conditions of sales and a list of U.S. sales offices and inventory resource centers. **Continental Resources, Inc., Bedford, MA. Please circle INFO/CARD #183.**

Advertiser Index


D
MRF154
8509

SIEMENS

GaAs transistors, GaAs MMICs

Giga speed in large numbers

Giga: from VHF to Ku band
Speed: ex stock
Numbers: on tape & reel, for cost-saving SMD assembly, in CERamic EConomy (CEREC) packages

Product families:	
0.5 μm FETs:	CFY 18-xx
1 μm FETs:	CFY 19-xx
dual-gate FETs:	CFY 20, CFY 22
GaAs MMICs:	CGY 40

For your applications in the SHF range, an outstanding combination in performance: cascadable – low-noise – linear – reliable.

All GaAs components are offered in HiRel/MIL versions as well.

By the way, we are experts in silicon microwave devices, too.

If you'd like to hear more, just write Siemens AG, Infoservice 12/Z069e, Postfach 23 48, D-8510 Fürth, quoting "GaAs microwave devices".

In USA:
Siemens Components Inc.
Special Products Division
186 Wood Ave. South
Iselin, NJ 08830

TopTech Components: Siemens

electronica '88
Munich

8.–12.11.88
Siemens, Hall 23, Position A4

12/Z069e

INFO/CARD 100